

# DEVELOPMENT OF A TWO DIMENSIONAL HYDRODYNAMIC NUMERICAL MODEL FOR USE IN A SHALLOW, WELL-MIXED ESTUARY

G. F. MCHUGH

CIRCULATING COPY  
Sea Grant Depository

# DEVELOPMENT OF A TWO- DIMENSIONAL HYDRODYNAMIC NUMERICAL MODEL FOR A SHALLOW, WELL-MIXED ESTUARY

G. F. MCHUGH

CENTER FOR WETLAND RESOURCES  
LOUISIANA STATE UNIVERSITY  
BATON ROUGE, LA 70803



Sea Grant Publication  
No. LSU-T-76-008

NATIONAL SEA GRANT PROGRAM  
FEDERAL BUREAU OF INVESTIGATION  
URI, JARVIS VILLAGE, PO BOX 3800  
NARRAGANSETT, RI 02882

This work is a result of research sponsored by the Louisiana Sea Grant Program, a part of the National Sea Grant Program maintained by the National Oceanic and Atmospheric Administration of the U.S. Department of Commerce.

1976



## CONTENTS

List of Figures. . . . .	iv
List of Tables . . . . .	v
Acknowledgments. . . . .	vi
Abstract . . . . .	vii
Part 1 . . . . .	1
Development of a Two-Dimensional Hydrodynamic Numerical Model for Use in a Shallow, Well-Mixed Estuary . . . . .	3
1 Equations . . . . .	4
2 Choice of a Finite Difference Scheme. . . . .	6
3 The Two-Dimensional Test Model. . . . .	20
4 Conservation of Mass. . . . .	31
5 Computation of the Moving Shoreline . . . . .	35
Appendix A . . . . .	43
Appendix B . . . . .	49
References . . . . .	52
Part 2 . . . . .	53
A Hydrodynamic Numerical Model of Tidal Flow through a Small Area of Brackish Marsh. . . . .	55
1 Equations and Solution Method . . . . .	61
2 The Moving Boundary Problem . . . . .	67
3 Results for the Implicit Method . . . . .	71
4 Results Using Leendertse's Implicit Scheme. . . . .	82
5 Effect of Increasing the Manning Coefficient. . . . .	91
6 Summary and Conclusions . . . . .	93
References . . . . .	167

FIGURES

Part 1

1	Grid scheme used by Leendertse 1970. . . . .	8
2	Grid scheme adopted in present modeling. . . . .	8
3	Stepped bottom topography showing flooding . . . . .	10
4	Unknown and boundary variables in one-dimensional model. . . .	14
5	Comparison of solutions in the two-dimensional model using the implicit/explicit and implicit methods . . . . .	26
6	Stepped bottom tank. . . . .	36
7	Topographical upstep and downstep. . . . .	36

Part 2

1	Computational grid . . . . .	56
2	Tide guage record near Airplane Lake for 15 October 1974 . . .	58
3	Grid scheme used to achieve solution of Equations 2. . . . .	66
4	Topographical upstep and downstep. . . . .	66
5	Current vector diagrams for the computation of Table 5 . . . .	76
6	Current vector diagrams for the computation of Table 4 . . . .	81
7	Schematic increase of the U-component of velocity after flooding of a dry square between time levels . . . . .	85
8	Comparison of U results ft/sec, at 2.5 hours for different computational schemes. . . . .	89
9	Comparison of U results ft/sec, at 2.5 hours for two different computational schemes. . . . .	90

TABLES

Part 1

1	Some computed values of water levels for the one-dimensional open-closed basin. . . . .	21
2	The square basin problems calculated with three solution methods at 21.0 hours tidal time parameters. . . . .	30

Part 2

1	Measured and interpolated elevations in feet relative to the base point . . . . .	97
2	Depth matrix . . . . .	98
3	Symbolic depth matrix. . . . .	99
4	Implicit computation . . . . .	100
5	Computation table. . . . .	139
6	U and V components of velocity for the Leendertse implicit computation. . . . .	147
7	U and V components of velocity for the implicit computation. .	149
8	U and V components for the implicit/explicit computation . . .	151
9	Computation table. . . . .	153
10	U and V components of velocity calculated implicitly . . . . .	163
11	U and V components of velocity calculated by the implicit/explicit scheme. . . . .	165

#### ACKNOWLEDGMENTS

This work is a result of research sponsored by the Louisiana Sea Grant Program, a part of the National Sea Grant Program maintained by the National Oceanic and Atmospheric Administration of the U.S. Department of Commerce. The U.S. Government is authorized to produce and distribute reprints for governmental purposes notwithstanding any copyright notation that may appear hereon. Citation of trade names does not constitute an official endorsement or approval of the use of such commercial products.

#### THE AUTHOR

Gerald F. McHugh is a research associate in the Office of Sea Grant Development, Louisiana State University Center for Wetland Resources, Baton Rouge, La. He is a native of Glenties, Donegal, Ireland. He holds the Ph.D. from the University of Manchester, England.

## ABSTRACT

Part 1 details the developmental steps that led to the creation of a two-dimensional hydrodynamic model capable of predicting water levels and current velocities within an area of arbitrary size, shape, and boundary nature (open or closed); and capable of predicting also the location of closed boundary segments as a function of time.

Restrictions on the applicability of the model are:

- 1) There must be negligible variation of horizontal velocity over most of the depth of the fluid layer
- 2) There must be negligible vertical velocity
- 3) There must be negligible vertical shear owing to horizontal velocity gradients
- 4) There must be negligible pressure and buoyancy forces arising from any small variations in salinity.

In Part 2, the feasibility of computing the tidal flow through a small area of marsh (roughly 1,000 x 600 sq.ft.) using equations and solution techniques described in Part 1, is demonstrated. The model allows for the inundation of and withdrawal of water from arbitrary areas of the marsh, and is quite general in regard to the size, shape, and open or closed nature of the boundaries.



Part 1  
Development of a Two-Dimensional Hydrodynamic Numerical Model  
for Use in a Shallow, Well-Mixed Estuary



The coast of Louisiana is characterized by several shallow estuarine systems, of which Barataria Bay is one of the largest. In the brackish regions of these systems, the parts not always under water consist of mud flats covered with marsh grass. Between the mud flats water depth will not usually exceed ten feet and is most often less than five feet. The elevation of a mud flat above mean tide level is about six inches. At low water at certain times of the year, mud flats may be exposed; at high water they are submerged. Offshore, in the Gulf of Mexico, the astronomical tide has a range of about one foot; and it is this small tidal range combined with the exceedingly flat nature of the terrain over many square miles that has made possible the vast extent of the brackish marsh.

Going inland from the Gulf, one finds water becoming less and less brackish, until finally it is fresh. The possibility exists, however, for the freshwater regions to be inundated with salt water as the result of storms blowing from the south. In this case, large areas of fresh marsh normally beyond the tidal reach and barely covered with water may suddenly be submerged to depths exceeding a foot.

Considerable interest exists in studying this transient storm-induced phenomenon from the point of view of its reaction upon the aquatic ecosystem. Hence a large-scale hydrodynamic model of an estuarine system such as Barataria Bay is indicated. Interest also exists in the ecology of the brackish mud flats that are intermittently covered with water; and here again a hydrodynamic model of the water exchange would be useful. For both of these models--the large and the small scale--a variable boundary feature is essential. The solid boundary must be allowed to

vary its position with time. In the following sections, the developmental steps leading to the creation of such a model or "solution strategy" are given.

Not included in this report is a description of the dispersive feature governing the concentration of suspended nutrients, which is important to biological studies. However, diffusive-dispersive effects may be combined with the basic hydrodynamical framework described here.

### 1. Equations

The two-dimensional vertically averaged equations governing a homogeneous hydrodynamic system in which Coriolis forces and wind stresses are present may be written (Hansen 1956, Leendertse 1967):

$$\frac{\partial \zeta}{\partial t} + \frac{\partial HU}{\partial x} + \frac{\partial HV}{\partial y} = 0$$

$$\frac{\partial U}{\partial t} + U \frac{\partial U}{\partial x} + V \frac{\partial U}{\partial y} - fV + g \frac{\partial \zeta}{\partial x} + \frac{1}{\rho} \frac{\partial P_0}{\partial x} + g \frac{U\sqrt{U^2+V^2}}{HC^2} - \frac{\tau_x^s}{\rho H} = 0 \quad (1.1)$$

$$\frac{\partial V}{\partial t} + U \frac{\partial V}{\partial x} + V \frac{\partial V}{\partial y} + fU + g \frac{\partial \zeta}{\partial y} + \frac{1}{\rho} \frac{\partial P_0}{\partial y} + g \frac{V\sqrt{U^2+V^2}}{HC^2} - \frac{\tau_y^s}{\rho H} = 0$$

where the symbols have the following meanings:

- $\zeta$  -- water level above a given horizontal reference plane
- $H$  -- depth of water above the bottom (=h +  $\zeta$ , where h is the depth of the bottom below the reference plane)
- $U, V$  -- vertically averaged x- and y- components respectively, of the horizontal velocity component
- $f$  -- Coriolis parameter (=2  $\Omega \sin \phi$ , where  $\Omega$  is the earth's angular velocity and  $\phi$  is the latitude)
- $g$  -- acceleration due to gravity (negative in the z-direction)
- $C$  -- Chezy function used to calculate the bottom stress. According to the Manning formula:

$$C = \frac{1.486H^{1/6}}{n}$$

where  $n$  is the Manning roughness coefficient

$\tau_x^s$ ,  
 $\tau_y^s$  -- x- and y- components respectively of the wind or surface stress  
 $P_0$  -- atmospheric pressure at the surface

Implicit in equations 1.1 are the approximations of constant horizontal velocity from top to bottom of the fluid layer, negligible vertical velocity, negligible vertical shear because of horizontal velocity gradients, and constant density. Indications of the accuracy with which these requirements are met can be obtained in either of two ways:

- i) Direct sampling of the currents and densities within the system
- ii) Computation of a model using equations 1.1 and comparison of results with observed data.

The second method is complicated by the fact that  $n$ , the Manning coefficient, is not known a priori; but a little experimentation with different values of  $n$  should indicate the appropriateness of the major assumptions.

In some cases there may be significant horizontal density gradients in the water owing to the presence of dissolved salts (salinity). These will create an additional forcing effect in the horizontal direction.

The terms to be added to the equations of motion are

$$\text{U-equation: } \left\langle \frac{g}{\rho} \int_z^{\zeta} \frac{\partial P}{\partial x} dz' \right\rangle, \quad \text{V-equation: } \left\langle \frac{g}{\rho} \int_z^{\zeta} \frac{\partial P}{\partial y} dz' \right\rangle$$

where the symbols  $\langle \rangle$  indicate vertical averaging from  $z = -h$  to  $z = \zeta$ .

A discussion of these additional force terms and of the simplifying assumptions described above, may be found in Pritchard (1971). In what follows, it will be assumed that the medium is sufficiently homogeneous that equations 1.1 are adequate to compute the motion.

## 2. Choice of a Finite Difference Scheme

Equations 1.1 must be expressed in finite difference form for the purpose of achieving a numerical solution.

The so-called "implicit" method of solution is used, since this has been shown, in the case of linear equations, to be unconditionally stable. A possible finite difference scheme for the implicit solution of the two-dimensional hydrodynamic equations was given by Leendertse (1970). The equation of continuity and the U-equation of motion in Leendertse's scheme can be written as follows:

$$\begin{aligned}
 & \frac{(\zeta_{i,j}^{n+1/2} - \zeta_{i,j}^n)}{\frac{\Delta t}{2}} + \frac{(\bar{H}\bar{U}_{i+1/2,j} U_{i+1/2,j}^{n+1/2} - \bar{H}\bar{U}_{i-1/2,j} U_{i-1/2,j}^{n+1/2})}{\Delta x} + \\
 & \frac{(\bar{H}\bar{V}_{i,j+1/2} V_{i,j+1/2}^n - \bar{H}\bar{V}_{i,j-1/2} V_{i,j-1/2}^n)}{\Delta y} = 0 \\
 & \frac{(U_{i+1/2,j}^{n+1/2} - U_{i+1/2,j}^{n-1/2})}{\Delta t} + \frac{U_{i+1/2,j}^{n+1/2} (U_{i+3/2,j}^{n-1/2} - U_{i-1/2,j}^{n-1/2})}{2\Delta x} + \\
 & V_{i+1/2,j}^* \frac{(U_{i+1/2,j+1}^{n-1/2} - U_{i+1/2,j-1}^{n-1/2})}{2\Delta y} - f V_{i+1/2,j}^* + \frac{g}{\Delta x} \left[ \frac{(\zeta_{i+1,j}^{n+1/2} + \zeta_{i+1,j}^{n-1/2})}{2} - \right. \\
 & \left. \frac{(\zeta_{i,j}^{n+1/2} - \zeta_{i,j}^{n-1/2})}{2} \right] + \frac{g (U_{i+1/2,j}^{n+1/2} + U_{i+1/2,j}^{n-1/2})}{2} \left[ (U_{i+1/2,j}^{n-1/2})^2 + (V_{i+1/2,j}^*)^2 \right]^{1/2} / \\
 & \bar{H}\bar{U}_{i+1/2,j} (\bar{C}\bar{U}_{i+1/2,j})^2 - \tau_x^s / \rho \bar{H}\bar{U}_{i+1/2,j} = 0
 \end{aligned} \tag{2.1}$$

In these equations a superscript ( $\bar{\quad}$ ) denotes 2-point averaging, and a superscript ( $\ast$ ) denotes 4-point averaging of a given variable.

The equation for  $\frac{\partial V}{\partial t}$  is analogous to the last above for  $\frac{\partial U}{\partial t}$  except that all times are increased by  $\Delta t/2$ . It need not be given here. The grid scheme utilized in writing Equations 2.1 is shown in Figure 1.

The separation of  $\zeta$  and  $h$  in space results in the following expressions for the averages  $\bar{H}^n_{i+1/2,j}$  and  $\bar{C}^n_{i+1/2,j}$  centered on  $U_{i+1/2,j}$ :

$$\bar{H}^n_{i+1/2,j} = \frac{h_{i+1/2,j+1/2} + h_{i+1/2,j-1/2}}{2} + \frac{\zeta^n_{i+1,j} + \zeta^n_{i,j}}{2}$$

$$\bar{C}^n_{i+1/2,j} = \frac{C^n_{i,j} + C^n_{i+1,j}}{2}$$

where

$$\bar{C}^n_{i,j} = \frac{1.486}{n} \left[ \frac{1}{4} (h_{i-1/2,j+1/2} + h_{i+1/2,j+1/2} + h_{i+1/2,j-1/2} + h_{i-1/2,j-1/2}) + \zeta^n_{i,j} \right]^{1/6}$$

Rather than separate the points of  $h$  and  $\zeta$  location it is more convenient mathematically to have both of these quantities refer to the same position in space. Then  $H_{i,j}$  is given by the simple addition:

$$H_{i,j} = h_{i,j} + \zeta_{i,j}$$

There are also two physical reasons for keeping  $h$  centralized with respect to the velocities, which will be described. Consequently, a grid scheme was adopted identical to one that has been used by several authors in the past for the explicit solution of the two-dimensional hydrodynamic equations. This is shown in Figure 2. According to the scheme of Figure 2,  $\bar{H}^n_{i+1,j}$  must be given by

$$\bar{H}^n_{i+1,j} = \frac{H_{i,j} + H_{i+1,j}}{2} = \frac{h_{i,j} + h_{i+1,j}}{2} + \frac{\zeta_{i,j} + \zeta_{i+1,j}}{2}$$

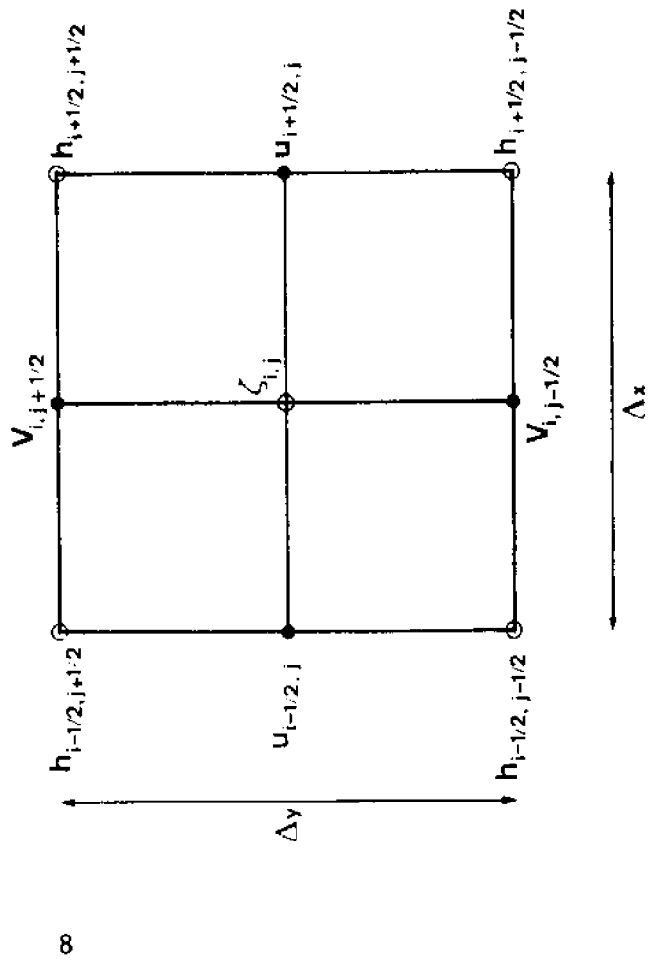


Fig. 1. Grid scheme used by Leendertse (1970).

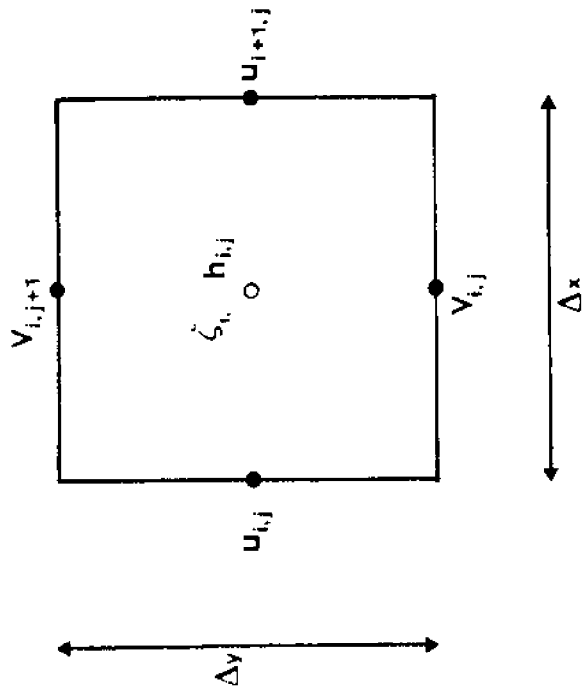


Fig. 2. Grid scheme adopted in present modeling.



Consequently, a pair of h's and a pair of  $\zeta$ 's are involved in the definition of  $\bar{H}_U^n$  as with Leendertse's scheme, the only difference being that the paired h's lie at right angles. However, the expression for  $\bar{C}_U^n$  is much simpler than Leendertse's above. We have for the point  $i+1, j$

$$\bar{C}_U^n_{i+1, j} = \frac{C_{i, j}^n + C_{i+1, j}^n}{2} = \frac{1.486}{n} \left[ \left( h_{i, j} + \zeta_{i, j} \right)^{1/6} + \left( h_{i+1, j} + \zeta_{i+1, j} \right)^{1/6} \right]$$

Only two h's are involved in defining  $\bar{C}_U^n$  instead of six in Leendertse's expression. The effect of the latter is to smooth out undulations in the bottom contour that have a width comparable to  $\Delta x$ . This might be considered advantageous in cases where the mean slope of the bottom (over many grid squares) determines the currents, and the small scale undulations are essentially accounted for in the Manning roughness coefficient  $n$ ; but in cases where undulations constitute important anomalies in the general contour, then clearly the weighting provided by remotely located h's is not conducive to accuracy. Consider a sinusoidal terrain running across the grid squares in the x- direction, of wavelength  $\lambda \approx \Delta x$ . Clearly, if  $h_{i-1/2, j+1/2}$  and  $h_{i-1/2, j-1/2}$  lie in the "next valley" they will have no relevance to the estimate of h at  $U_{i+1/2, j}$  which is what is required to evaluate C there. The scheme of Figure 2, which utilizes h's no further than  $\Delta x$  apart, must provide a better estimate of h at the locations between two adjacent h observations.

In the Louisiana estuarine systems there are many areas where the bottom is scoured by relatively deep channels on the order of tens of yards across. These are important conduits of the water flow. The width scale of such a submerged gully is much less than any practicable grid spacing. Consequently, it is not desirable to smooth out this type of irregularity in calculating C.

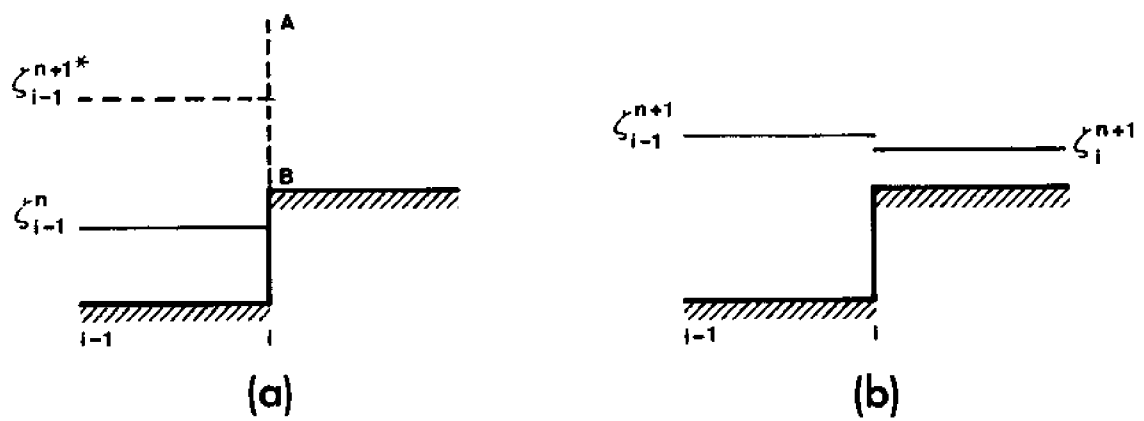


Fig. 3. Stepped bottom topography showing flooding.

But there is a second and more important reason for adopting a finite difference scheme where  $\zeta$  and  $h$  occur together in the center of a square. Whenever a canal or bayou occurs whose width is typically less than the grid interval, one must represent such a feature by a whole grid square, adjusting the constant depth  $h$  (across  $\Delta x$ , say) so that the flooded cross sectional area remains the same. Then all other factors being equal, the volume flux will be the same. Now, were the  $h$ 's to be given only at the corners of a grid square, then the bayou depth would be totally unrepresented. The model in fact would "see" no bayou! For this reason, a coincident  $h$  and  $\zeta$  are important. In the case of Barataria Bay, we have a main tidal pass whose width, about one mile, precludes any representation by multiple grid squares. And so here, a central depth  $h$  must be given.

A further simplification of Leendertse's finite difference scheme was adopted. Whereas Leendertse used a three-layer scheme in time-- $n-1/2$ ,  $n$ ,  $n+1/2$ --it seemed desirable to reduce the layers to two:  $n$ ,  $n+1$ .<sup>1</sup> A considerable saving in computer storage results therefrom;<sup>2</sup> and we obtain moreover, a simplification toward greater realism in the handling of a moving shoreline or boundary. To appreciate the latter point, consider Figure 3(a) and (b), which shows respectively, a grid "square" in vertical section just before flooding and just after flooding, from the adjacent square.

The calculation of the new level  $\zeta_{i-1}^{n+1*}$  after the time step  $\Delta t$  between the times  $n$  and  $n+1$ , proceeds as though there were a solid boundary extension AB at the edge  $i$ . In actual fact spill-over, or flooding, of square  $i$

---

<sup>1</sup>In his earlier models (1967) solved with an alternating Implicit-Explicit method, Leendertse used a two-layer scheme.

<sup>2</sup>See p. 28.

will have occurred during  $\Delta t$ , and so we must estimate a new level  $\zeta_i^{n+1}$  in square  $i$  based on some hydraulic formula. Next, we must deduct the volume of water transferred into  $i$  from the water initially calculated for square  $i-1$ , yielding a corrected level  $\zeta_{i-1}^{n+1}$  in square  $i-1$ . The boundary for further computations, i.e., for the next time step, has now been moved to the edge  $i+1$ .

The displacement of time levels requires that the new time  $n$  for the next step correspond to time level  $n+1$  for the old step. And the new  $n-1$  will correspond to the old level  $n$ . In square  $i-1$  we have  $\zeta_{i-1}^n$  defined, but what of  $\zeta_i^n$ ? It is undefined since no water existed in square  $i$  at the old time  $n$ . This is the difficulty created by a three-layer solution scheme in time. The two-layer scheme avoids this impasse since  $\zeta_i^{n-1}$  for the new time step is not required. The only levels needed to advance the computations are those shown in Figure 3(b). If by some expedient we avoid having to use  $\zeta_i^{n-1}$  in a square that became flooded at time level  $n$ , we must still incur the disadvantage of having to keep in memory the condition of every square, wet or dry, at time level  $n-1$ . This is so that the necessity of transfer to a modified equation of motion (one that does not use  $\zeta_i^{n-1}$ ) at time level  $n$  may be established. In a two-layer scheme, only the current condition of a square is recorded in memory, with consequent saving of computer storage.

At this stage of the analysis, the question remains whether the two-layer time scheme will be as numerically satisfactory as the three-layer scheme. To decide this question, one-dimensional models of estuarine-type geometry were computed using both schemes.

The one-dimensional three-layer system of equations utilizing the grid scheme of Figure 2 and corresponding in averaging symmetry to the system 2.1 is

$$\begin{aligned}
& \frac{(\zeta_i^{n+1} - \zeta_i^n)}{\Delta t} + \frac{(\bar{H}\bar{U}_{i+2} U_{i+1}^{n+1} - \bar{H}\bar{U}_i U_i^{n+1})}{\Delta x} = 0 \\
& \frac{(U_i^{n+1} - U_i^{n-1})}{2\Delta t} + U_i^{n+1} \frac{(U_{i+1}^{n-1} - U_{i-1}^{n-1})}{2\Delta x} + \frac{g}{\Delta x} \left[ \frac{(\zeta_i^{n+1} + \zeta_i^{n-1})}{2} - \frac{(\zeta_{i-1}^{n+1} + \zeta_{i-1}^{n-1})}{2} \right] + \\
& g \frac{(U_i^{n+1} + U_i^{n-1})}{2} |U_i^{n-1}| / \bar{H}\bar{U}_i (\bar{C}\bar{U}_i)^2 = 0
\end{aligned} \tag{2.2}$$

where the surface stress term has been dropped for convenience.

The one-dimensional two-layer system is

$$\begin{aligned}
& \frac{(\zeta_i^{n+1} - \zeta_i^n)}{\Delta t} + \frac{(\bar{H}\bar{U}_{i+1} U_{i+1}^{n+1} - \bar{H}\bar{U}_i U_i^{n+1})}{\Delta x} = 0 \\
& \frac{(U_i^{n+1} - U_i^n)}{\Delta t} + U_i^{n+1} \frac{(U_{i+1}^n - U_{i-1}^n)}{2\Delta x} + \frac{g}{\Delta x} \left[ \frac{(\zeta_i^{n+1} + \zeta_i^n)}{2} - \frac{(\zeta_{i-1}^{n+1} + \zeta_{i-1}^n)}{2} \right] + \\
& g \frac{(U_i^{n+1} + U_i^n)}{2} |U_i^n| / \bar{H}\bar{U}_i (\bar{C}\bar{U}_i)^2 = 0
\end{aligned} \tag{2.3}$$

Systems 2.2 and 2.3 were applied to a rectangular basin of constant bottom level, open at one end ( $i = 1$ ) and closed at the other ( $i = L$ ). A sinusoidal tide was applied at the open end. The disposition of variables to be computed is as shown in Figure 4.

$\zeta_1$  and  $U_L$  are the two known and necessary boundary variables, while  $U_2, \zeta_2, U_3, \zeta_3 \dots U_{L-1}, \zeta_{L-1}$  have to be determined as functions of time. A description of the implicit method is given in Appendix 1. Here it suffices to say that systems 2.2 and 2.3 lead to a system of  $2L-4$  algebraic equations for the  $2L-4$  unknowns. The quantity  $U_1$ , which occurs in the finite difference expression for the derivative  $\frac{\partial U}{\partial x}$  at  $i = 2$ , is outside the computation field, and this means that a modification must be made to either the equation of motion or the finite difference form of the

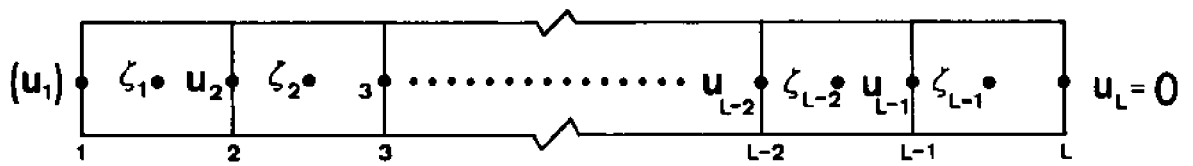


Fig. 4. Unknown and boundary variables in one-dimensional model.

derivative. Leendertse (1967) has reported that the replacement of a centrally symmetric spatial derivative at the boundary with a one-sided derivative that utilizes interior points may cause local numerical instability. He advises, consequently, that the derivative be dropped from the equation when one of its datum points is not available. The linearization should not introduce appreciable error in most physical cases. Hence, the equation of motion was partially linearized at the first computation point in the one-dimensional test models.

Length parameters were selected for comparability with the Barataria Bay estuarine system. They were:

$$\begin{aligned}L &= 21 \\ \Delta x &= 1 \text{ mile} \\ h &= 5 \text{ ft.}\end{aligned}$$

A Manning coefficient of 0.026 (following Hacker, Pike, and Wilkins 1973), tidal amplitude 0.4 ft., tidal period 12 hours, and time step 5 minutes were used. The tidal constants do not correspond to those of the Louisiana coast (where typically the amplitude is about 1 foot and the period 20 hours), but the shorter period reduces the computation time required for a given number of cycles.

It should be noted that the time step of 300 seconds closely approximates the Friedrich/Lewy/Courant limit  $\Delta t \leq \Delta s / \sqrt{2g\bar{h}_{\max}}^3$  for stability of an explicit scheme of solution. In the present model  $\Delta s / \sqrt{2g\bar{h}} \sim 295$  sec. It may also be noted that the choice  $L = 21$  for the number of grid lines insures that  $\lambda / \Delta x \sim 100$ , where  $\lambda$  is the wavelength of oscillation.<sup>4</sup> Sobey

---

<sup>3</sup>The symbol " $\Delta s$ " is used to represent a generalized grid interval: either  $\Delta x$ , for the one-dimensional model, or the lesser of  $\Delta x$  and  $\Delta y$  in a two-dimensional model.

<sup>4</sup>For a linear system of equations, solved in conjunction with a sinusoidal forcing function of period  $T$ , the wavelength of oscillation is given by  $\lambda = T\sqrt{g\bar{h}}$ . Hence, with  $T = 12$  hours and  $h = 5$  ft.,  $\lambda \sim 100$  miles.

(1970) has shown that Leendertse's Implicit-Explicit method of solving the two-dimensional linearized equations results in negligible phase distortion of the solution for  $\lambda/\Delta x \gtrsim 50$  when  $\Delta t = 1.25 \Delta s/\sqrt{gh}$ . Since the present one-dimensional model is wholly implicit, and  $\Delta t < \Delta s/\sqrt{gh}$ , one would expect the phase distortion to be even less. Amplitude distortion is zero for Leendertse's solution scheme.

With the above inputs both finite difference models behaved satisfactorily in computation, and negligible differences were observed in the results for  $\zeta(x,t)$  and  $U(x,t)$ . Table 1, p. 13, gives a few of these results, and also some results for another finite difference scheme to be discussed.

Although it was shown that schemes 2.2 and 2.3 yield virtually indistinguishable results, some doubt remains as to how closely these results approximate the true solution. In other words, are systems 2.2 and 2.3 the optimum schemes to use? To resolve this question empirically, it would be necessary to test a variety of numerical schemes and compare the results in each case with the analytical solution for the open-closed boundary initial value problem. But no such analytical solution is available, owing to the presence of the nonlinear terms

$$\frac{\partial HU}{\partial x} \quad \text{and} \quad \frac{gU|U|}{hC^2} \quad ,$$

not to mention the advective acceleration  $U \frac{\partial U}{\partial x}$ . If  $\frac{\partial HU}{\partial x}$  is linearized by replacing  $H$  with  $h$  (assuming  $\zeta \ll H$ ) and  $U \frac{\partial U}{\partial x}$  is dropped, we are still left with the nonlinear bottom friction term  $gU|U|/hC^2$ , which is an essential physical feature. It was therefore decided to investigate the numerical behavior of a rather different physical situation that does have a simple exact solution.



A level-bottomed frictionless rectangular basin, closed at both ends, was considered. Any disturbance in this basin at time  $t = 0$  will lead to a sustained oscillation with the natural or resonance period of the basin. The equations governing the phenomenon for small amplitude disturbances are:

$$\begin{aligned}\frac{\partial \zeta}{\partial t} + h \frac{\partial U}{\partial x} &= 0 \\ \frac{\partial U}{\partial t} + g \frac{\partial \zeta}{\partial x} &= 0\end{aligned}\tag{2.4}$$

Let  $l$  be the length and  $h$  the constant bottom-depth of the basin,  $A$  the oscillation amplitude and  $\omega$  the angular frequency. Then 2.4 with the boundary conditions  $U = 0$  at  $x = 0, l$  has the solution:

$$\begin{aligned}\zeta &= A \cos \left( \frac{\pi x}{l} \right) \cos (\omega t) \\ U &= A \sqrt{\frac{g}{h}} \sin \left( \frac{\pi x}{l} \right) \sin (\omega t)\end{aligned}$$

where

$$\omega = \frac{\pi}{l} \sqrt{gh}$$

The values  $l = 20$  miles,  $h = 5$  ft, and  $A = 0.4$  ft were chosen so as to render some comparison possible between the doubly closed and singly closed models. With these parameters, the natural period of oscillation turns out to be

$$T = \frac{2\pi}{\omega} = 4.64 \text{ hours}$$

At time zero, a constant slope of the water surface was assumed, equivalent to a straight line approximation of the function  $A \cos (\pi x/L)$ , with values  $\zeta = A$  and  $\zeta = -A$  at  $x = 0$  and  $x = L$  respectively, in order to simulate the artificial starting condition of a nonlinear model. With this initial situation, nine distinct finite difference schemes involving the implicit method were computed, and the corresponding numerical

solutions for the water height at a fixed point (near the end of the basin) were plotted at hourly intervals. Also plotted on the same diagram was the exact solution. This empirical approach was adopted as being more economical in time and effort than the analytical method pursued by Leendertse (1967) and Sobey (1970). Time and space steps were as for the open-closed model already described.

Only one of the numerical solutions became unstable, but six of the others showed marked damping. It was easy to rank these solutions in order of agreement with the exact sinusoidal function over the 9 hours plotted. The finite difference scheme yielding the best results (in which the fractional error deviation at times of maximum and minimum water level during the first cycle did not exceed 10 percent) was as follows:

$$\begin{aligned} \frac{(\zeta_i^{n+1} - \zeta_i^{n-1})}{2\Delta t} + \frac{h}{\Delta x} \left[ \frac{(U_{i+1}^{n+1} + U_{i+1}^{n-1})}{2} - \frac{(U_i^{n+1} + U_i^{n-1})}{2} \right] &= 0 \\ \frac{(U_i^{n+1} - U_i^{n-1})}{2\Delta t} + \frac{g}{\Delta x} \left[ \frac{(\zeta_i^{n+1} + \zeta_i^{n-1})}{2} - \frac{(\zeta_{i-1}^{n+1} + \zeta_{i-1}^{n-1})}{2} \right] &= 0 \end{aligned} \quad (2.5)$$

The second best solution corresponded to the two-layer scheme of equations 2.3, namely

$$\begin{aligned} \frac{(\zeta_i^{n+1} - \zeta_i^n)}{\Delta t} + h \frac{(U_{i+1}^{n+1} - U_i^{n+1})}{\Delta x} &= 0 \\ \frac{(U_i^{n+1} - U_i^n)}{\Delta t} + \frac{g}{\Delta x} \left[ \frac{(\zeta_i^{n+1} + \zeta_i^n)}{2} - \frac{(\zeta_{i-1}^{n+1} + \zeta_{i-1}^n)}{2} \right] &= 0 \end{aligned} \quad (2.6)$$

The linearized version of Leendertse's equations 2.2 ranked third, but was close in accuracy to 2.6.

It is noteworthy that the two-layer scheme corresponding to 2.5

$$\frac{(\zeta_i^{n+1} - \zeta_i^n)}{\Delta t} + \frac{h}{\Delta x} \left[ \frac{(U_{i+1}^{n+1} + U_{i+1}^n)}{2} - \frac{(U_i^{n+1} + U_i^n)}{2} \right] = 0$$

$$\frac{(U_i^{n+1} - U_i^n)}{\Delta t} + \frac{g}{\Delta x} \left[ \frac{(\zeta_i^{n+1} + \zeta_i^n)}{2} - \frac{(\zeta_{i-1}^{n+1} + \zeta_{i-1}^n)}{2} \right] = 0$$

gave the worst results, showing instability after 3 hours. Clearly, it is better to make use of the next-preceding solution point in time (n-1) as the known value with which to calculate the subsequent point (n+1), rather than to use the preceding point (n). This is in the context of the doubly closed frictionless basin. One would hope, however, that the introduction of friction and of a forcing function at an open boundary would render the distinction between the solutions obtained with the three-layer and two-layer schemes less marked; and indeed this has proven to be the case with schemes 2.2 and 2.3 applied to the one-dimensional open-closed basin discussed.

A third difference scheme was computed for the singly open basin with symmetrical terms corresponding to the linearized equations 2.5:

$$\frac{(\zeta_i^{n+1} - \zeta_i^{n-1})}{2\Delta t} + \frac{1}{\Delta x} \left[ \bar{H}\bar{U}_{i+1}^n \frac{(U_{i+1}^{n+1} + U_{i+1}^{n-1})}{2} - \bar{H}\bar{U}_i^n \frac{(U_i^{n+1} + U_i^{n-1})}{2} \right] = 0 \quad (2.7)$$

$$\frac{(U_i^{n+1} - U_i^{n-1})}{2\Delta t} + \frac{(U_{i+1}^{n+1} + U_{i+1}^{n-1})}{2} \frac{(U_{i+1}^n - U_{i-1}^n)}{2\Delta x} + \frac{g}{\Delta x} \left[ \frac{(\zeta_i^{n+1} + \zeta_i^{n-1})}{2} - \frac{(\zeta_{i-1}^{n+1} + \zeta_{i-1}^{n-1})}{2} \right] + g \frac{(U_i^{n+1} + U_i^{n-1}) |U_i^n|}{2 \bar{H}\bar{U}_i^n (\bar{C}\bar{U}_i^n)^2} = 0$$

The solution showed a smaller amplitude of oscillation at points within the basin than with scheme 2.3, and a phase lag of about 30 minutes relative to the solution for that scheme. Such phase lags had been predicted

by Leendertse (1967) in his comparative studies of wave deformation using various linear schemes. Some results for comparison with those of scheme 2.3 are given in Table 1.

We see, in conclusion, that the chosen scheme 2.3 for the open-closed basin, has a counterpart 2.6 for the doubly closed basin that ranks high among those schemes tested. Moreover, the introduction of bottom friction and a forcing function appears to render the numerical solutions less sensitive to the type of differencing used. Hence, even if there were no regular correspondence between the results obtained for two different physical situations using equivalent difference schemes, we may feel safe in selecting the two-layer scheme 2.3 as the basis for a real-world computational model.

### 3. The Two-Dimensional Test Model

Leendertse (1967), in his various hydrodynamic models, used an Alternating Directions Implicit-Explicit method to solve his equations. The solution strategy is as follows:

- i) The equation of continuity and the U-equation of motion are solved together implicitly at time level  $n$  to yield values of  $\zeta^{n+1/2}$  and  $U^{n+1/2}$  along each row.
- ii) The V-equation of motion is solved explicitly for  $V^{n+1/2}$  along each column. We now have  $\zeta^{n+1/2}$ ,  $U^{n+1/2}$ ,  $V^{n+1/2}$  everywhere in the field.
- iii) The equation of continuity and the V-equation of motion are solved together implicitly at time level  $n+1/2$  to yield values of  $\zeta^{n+1}$  and  $V^{n+1}$  along each column.
- iv) The U-equation of motion is solved explicitly for  $U^{n+1}$  along each row. We now have  $\zeta^{n+1}$ ,  $U^{n+1}$ ,  $V^{n+1}$  everywhere in the field.

TABLE 1. Some computed values of water level for the one-dimensional open-closed basin using finite difference schemes 2.2, 2.3, 2.7.

Hour	$\zeta(10, \text{Hour})$		
	Scheme (2.2)	Scheme (2.3)	Scheme (2.7)
35	-0.02	-0.03	-0.01
36	0.09	0.09	0.05
37	0.19	0.19	0.12
38	0.24	0.24	0.18
39	0.22	0.22	0.19
40	0.14	0.14	0.11
41	0.06	0.06	0.06
42	-0.05	-0.04	0.00
43	-0.14	-0.14	-0.07
44	-0.20	-0.20	-0.13
45	-0.20	-0.20	-0.16
46	-0.10	-0.10	-0.09
47	-0.02	-0.03	-0.01
48	0.09	0.09	0.05
49	0.19	0.19	0.12
50	0.24	0.24	0.18
51	0.22	0.22	0.19
52	0.14	0.14	0.11
53	0.06	0.06	0.05
54	-0.05	-0.05	0.00
55	-0.14	-0.14	-0.07
56	-0.20	-0.20	-0.13
57	-0.20	-0.20	-0.16
58	-0.10	-0.10	-0.09
59	-0.02	-0.03	-0.01
60	0.09	0.09	0.05

Note: The observation point is 9 miles from the open boundary.

The whole procedure is repeated for the next pair of half-time steps, and so on.

The two-dimensional equations adopted for the author's model, which follow in form those of Leendertse (1970), with the restriction to two time layers, are:

$$\frac{(\zeta_{i,j}^{n+1} - \zeta_{i,j}^n)}{\Delta t} + \frac{(\bar{H}\bar{U}_{i+1,j}^{n+1} U_{i+1,j}^{n+1} - \bar{H}\bar{U}_{i,j}^{n+1} U_{i,j}^{n+1})}{\Delta x} + \frac{(\bar{H}\bar{V}_{i,j+1}^n V_{i,j+1}^n - \bar{H}\bar{V}_{i,j}^n V_{i,j}^n)}{\Delta y} = 0$$

$$\frac{(U_{i,j}^{n+1} - U_{i,j}^n)}{\Delta t} + U_{i,j}^{n+1} \frac{(U_{i+1,j}^n - U_{i-1,j}^n)}{2\Delta x} + V_{i,j}^{*n} \frac{(U_{i,j+1}^n - U_{i,j-1}^n)}{2\Delta y} - f V_{i,j}^{*n} +$$

$$\frac{g}{\Delta x} \left[ \frac{(\zeta_{i,j}^{n+1} + \zeta_{i,j}^n)}{2} - \frac{(\zeta_{i-1,j}^{n+1} + \zeta_{i-1,j}^n)}{2} \right] + g \frac{(U_{i,j}^{n+1} + U_{i,j}^n)}{2} \left[ (U_{i,j}^n)^2 + (V_{i,j}^{*n})^2 \right]^{1/2} /$$

$$\bar{H}\bar{U}_{i,j}^n \left( \bar{C}\bar{U}_{i,j}^n \right)^2 + \frac{1}{\rho} \frac{\partial P_0}{\partial x} - \tau_x^s / \rho \bar{H}\bar{U}_{i,j}^n = 0$$

$$\frac{(\zeta_{i,j}^{n+2} - \zeta_{i,j}^{n+1})}{\Delta t} + \frac{(\bar{H}\bar{U}_{i+1,j}^{n+1} U_{i+1,j}^{n+1} - \bar{H}\bar{U}_{i,j}^{n+1} U_{i,j}^{n+1})}{\Delta x} + \frac{(\bar{H}\bar{V}_{i,j+1}^{n+1} V_{i,j+1}^{n+1} - \bar{H}\bar{V}_{i,j}^{n+1} V_{i,j}^{n+1})}{\Delta y} = 0$$

$$\frac{(V_{i,j}^{n+2} - V_{i,j}^{n+1})}{\Delta t} + U_{i,j}^{*n+1} \frac{(V_{i+1,j}^{n+1} - V_{i-1,j}^{n+1})}{2\Delta x} + V_{i,j}^{n+2} \frac{(V_{i,j+1}^{n+1} - V_{i,j-1}^{n+1})}{2\Delta y} + f U_{i,j}^{*n+1} +$$

$$\frac{g}{\Delta y} \left[ \frac{(\zeta_{i,j}^{n+2} + \zeta_{i,j}^{n+1})}{2} - \frac{(\zeta_{i,j-1}^{n+2} + \zeta_{i,j-1}^{n+1})}{2} \right] + g \frac{(V_{i,j}^{n+2} + V_{i,j}^{n+1})}{2} \left[ (U_{i,j}^{*n+1})^2 + (V_{i,j}^{n+1})^2 \right]^{1/2} /$$

$$\bar{H}\bar{V}_{i,j}^{n+1} \left( \bar{C}\bar{V}_{i,j}^{n+1} \right)^2 + \frac{1}{\rho} \frac{\partial P_0}{\partial y} - \tau_y^s / \rho \bar{H}\bar{V}_{i,j}^{n+1} = 0 \quad (3.1)$$

together with the explicit equations (Leendertse 1967):

$$\frac{(V_{i,j}^{n+1} - V_{i,j}^n)}{\Delta t} + U_{i,j}^{*n+1} \frac{(V_{i+1,j}^n - V_{i-1,j}^n)}{2\Delta x} + V_{i,j}^{n+1} \frac{(V_{i,j+1}^n + V_{i,j-1}^n)}{2\Delta y} + f U_{i,j}^{*n+1} +$$

$$\begin{aligned}
& \frac{g}{\Delta y} \left[ \frac{(\zeta_{i,j}^{n+1} + \zeta_{i,j}^n)}{2} - \frac{(\zeta_{i,j-1}^{n+1} + \zeta_{i,j-1}^n)}{2} \right] + g v_{i,j}^{n+1} \left[ (U_{i,j}^{*n+1})^2 + (v_{i,j}^n)^2 \right]^{1/2} / \bar{Hv}_{i,j}^{n+1} (\bar{Cv}_{i,j}^{n+1})^2 \\
& + \frac{1}{\rho} \frac{Po}{y} - \tau_y^s / \rho \bar{Hv}_{i,j}^{n+1} = 0 \\
& \frac{(U_{i,j}^{n+2} - U_{i,j}^{n+1})}{\Delta t} + U_{i,j}^{n+2} \frac{(U_{i+1,j}^{n+1} - U_{i-1,j}^{n+1})}{2\Delta x} + v_{i,j}^{*n+2} \frac{(U_{i,j+1}^{n+1} - U_{i,j-1}^{n+1})}{2\Delta y} - f v_{i,j}^{*n+2} + \\
& \frac{g}{\Delta x} \left[ \frac{(\zeta_{i,j}^{n+2} + \zeta_{i,j}^{n+1})}{2} - \frac{(\zeta_{i-1,j}^{n+2} + \zeta_{i-1,j}^{n+1})}{2} \right] + g U_{i,j}^{n+2} \left[ (U_{i,j}^{n+1})^2 + (v_{i,j}^{*n+2})^2 \right]^{1/2} / \bar{Hu}_{i,j}^{n+2} (\bar{Cu}_{i,j}^{n+2})^2 \\
& + \frac{1}{\rho} \frac{\partial Po}{\partial x} - \tau_x^s / \rho \bar{Hu}_{i,j}^{n+2} = 0 \tag{3.2}
\end{aligned}$$

The quantities with superscript  $(\bar{\quad})$  and  $(*\quad)$  are defined as follows:

$$\begin{aligned}
\bar{Hu}_{i,j} &= \frac{H_{i,j} + H_{i-1,j}}{2} & \bar{Cu}_{i,j} &= \frac{1.486}{n} \frac{(H_{i,j}^{1/6} + H_{i-1,j}^{1/6})}{2} \\
\bar{Hv}_{i,j} &= \frac{H_{i,j} + H_{i,j-1}}{2} & \bar{Cv}_{i,j} &= \frac{1.486}{n} \frac{(H_{i,j}^{1/6} + H_{i,j-1}^{1/6})}{2} \\
v_{i,j}^* &= \frac{1}{4} (v_{i-1,j+1} + v_{i,j+1} + v_{i,j} + v_{i-1,j}) \\
U_{i,j}^* &= \frac{1}{4} (U_{i,j} + U_{i+1,j} + U_{i+1,j-2} + U_{i,j-1})
\end{aligned}$$

The Alternating Directions Implicit-Explicit procedure was tested by applying a sinusoidal tidal function to a square basin of constant bottom depth, open at one side. Parameters of the model (calculated without atmospheric forcing) were:

Grid dimensions	21 X 21	Tidal amplitude	= 0.4 ft.
$\Delta x$	= 5280 ft.	Tidal period	= 12 h
$\Delta y$	= 5280 ft.	Coriolis parameter $f$	= $0.712 \times 10^{-4}$ rad sec <sup>-1</sup>
$h$	= 5 ft.	Manning coefficient	= 0.026

Initially, a 5-minute time step was used. It was then found that with both V-explicit and U-explicit intermediate steps, the model developed an increasingly strong oscillation of  $\zeta$ -values in the y-direction, of wavelength  $2\Delta y$ , after 5 hours of tidal time, leading to negative depths after 9 hours. With U-explicit only, the model showed an increasing oscillation in the x-direction of wavelength  $2\Delta x$  after 17 hours; but with no explicit steps at all, the computation proceeded satisfactorily for the full 24-hour test period.

The presence of numerical instability with either or both of the explicit intermediate steps is to be expected from the fact that  $\Delta t$  slightly exceeds the Friedrich/Lewy/Courant limit  $\Delta s/\sqrt{2gh_{\max}} \approx 295$  sec; and the reason that the V-explicit step introduces a much stronger instability than the U-explicit step is of course because the physical situation is essentially one-dimensional in the y-direction. Along this direction the principal driving force operates. The U-component of velocity is much weaker than the V-component and only exists in the present case as a consequence of the Coriolis terms. There is, therefore, almost no change of  $\zeta$  in the x-direction, at least under conditions such that the results do not contain spurious oscillations.

The experiment was made of calculating the model implicitly at three other time steps: 10 minutes, 2 minutes, and 1 minute. When the method is wholly implicit, one substitutes for the explicit steps by letting V at time level  $n+1$  equal V at the preceding time level  $n$ , and U at time level  $n+2$  equal U at time level  $n+1$ .<sup>5</sup>

---

<sup>5</sup>Although this procedure is also "explicit," the term "explicit step" will be understood to refer only to the case that the hydrodynamic equations are utilized, and without such step or steps, the method will be considered purely implicit.



The results for  $\Delta t = 10$  minutes showed a strong spurious oscillation of  $\zeta$  in the y-direction after 3 hours of tidal time. The results for  $\Delta t = 2$  minutes agreed very closely with those for  $\Delta t = 5$  minutes; and the results with  $\Delta t = 1$  minute were likewise almost identical to those for  $\Delta t = 2$  minutes. Clearly, solution convergence has been obtained at  $\Delta t = 2$  minutes.

The model was also calculated with both explicit steps included for the time steps 2 minutes and 1 minute. Results were virtually identical in both cases. It is therefore meaningful to compare the time histories of  $\zeta$  at a single point in the field as obtained with the implicit method on the one hand, and with the implicit-explicit method on the other, for the common time step of 2 minutes. Figure 5(a) shows the curves plotted for 40 hours of tidal time at the point (10,20). This is near the closed boundary, where the phase difference and amplitude difference between the curves for the two solution methods is greatest. It can be seen that the phase advance of the Implicit-Explicit method, relative to the other, is variable with time (probably owing to the distorting influence of the starting conditions  $\zeta = U = V = 0$  everywhere) and can be as much as one hour. At a point halfway between the open and closed boundaries, the phase differences are slightly reduced and the magnitudes of the maxima and minima of  $\zeta$  agree closely (see Figure 5[b]).

As a final experiment, the same two-dimensional problem was recalculated using Leendertse's 1970 approach (see also Leendertse and Gritton [1971]). The one-dimensional equations abstracted from the two-dimensional equations have already been given (2.1); it is therefore only necessary to say that in the second half-time step  $(n+1/2)\Delta t$  to  $(n+1)\Delta t$ , the variables  $\zeta^{n+1}$  and  $V^{n+1}$  are implicitly calculated. Translated to integer time levels, and using the grid scheme of Figure 2, the full equations are:

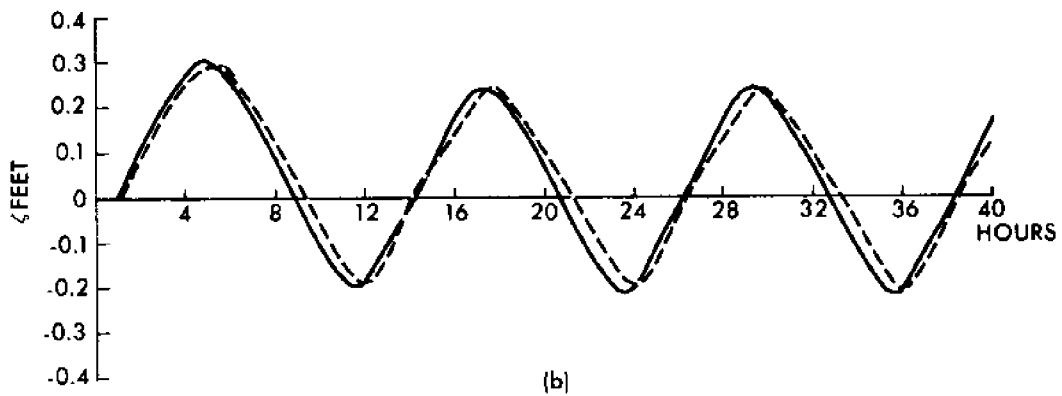
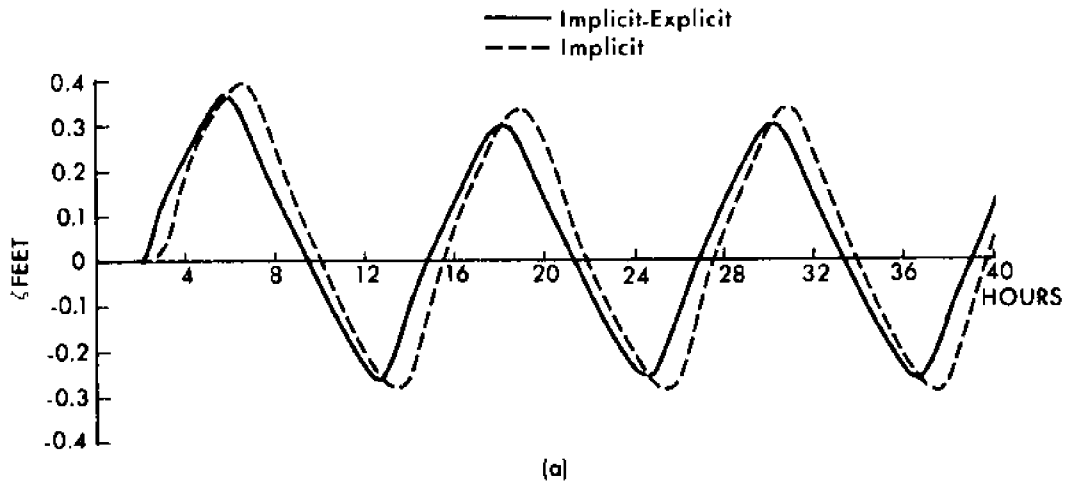


Fig. 5. Comparison of solutions in the two-dimensional model using the Implicit/Explicit and Implicit methods.

$$\begin{aligned}
& \frac{(\zeta_{i,j}^{n+1} - \zeta_{i,j}^n)}{\Delta t} + \frac{(\bar{H}\bar{U}_{i+1,j}^{n+1} U_{i+1,j}^{n+1} - \bar{H}\bar{U}_{i,j}^{n+1} U_{i,j}^{n+1})}{\Delta x} + \frac{(\bar{H}\bar{V}_{i,j+1}^n V_{i,j+1}^n - \bar{H}\bar{U}_{i,j}^n V_{i,j}^n)}{\Delta y} = 0 \\
& \frac{(U_{i,j}^{n+1} - U_{i,j}^{n-1})}{2\Delta t} + U_{i,j}^{n+1} \frac{(U_{i+1,j}^{n-1} - U_{i-1,j}^{n-1})}{2\Delta x} + V_{i,j}^{*n} \frac{(U_{i,j+1}^{n-1} - U_{i,j-1}^{n-1})}{2\Delta y} - f V_{i,j}^{*n} + \\
& \frac{g}{\Delta x} \left[ \frac{(\zeta_{i,j}^{n+1} + \zeta_{i,j}^{n-1})}{2} - \frac{(\zeta_{i-1,j}^{n+1} + \zeta_{i-1,j}^{n-1})}{2} \right] + g \frac{(U_{i,j}^{n+1} + U_{i,j}^{n-1})}{2} \left[ (U_{i,j}^{n-1})^2 + (V_{i,j}^{*n})^2 \right]^{1/2} / \\
& \bar{H}\bar{U}_{i,j}^n (\bar{C}\bar{U}_{i,j}^n)^2 = 0 \tag{3.3}
\end{aligned}$$

$$\begin{aligned}
& \frac{(\zeta_{i,j}^{n+2} - \zeta_{i,j}^{n+1})}{\Delta t} + \frac{(\bar{H}\bar{U}_{i+1,j}^{n+1} U_{i+1,j}^{n+1} - \bar{H}\bar{U}_{i,j}^{n+1} U_{i,j}^{n+1})}{\Delta x} + \frac{(\bar{H}\bar{V}_{i,j+1}^{n+2} V_{i,j+1}^{n+2} - \bar{H}\bar{V}_{i,j}^{n+1} V_{i,j}^{n+2})}{\Delta y} = 0 \\
& \frac{(V_{i,j}^{n+2} - V_{i,j}^n)}{2\Delta t} + U_{i,j}^{*n+1} \frac{(V_{i+1,j}^n - V_{i-1,j}^n)}{2\Delta x} + V_{i,j}^{n+2} \frac{(V_{i,j+1}^n - V_{i,j-1}^n)}{2\Delta y} + f U_{i,j}^{*n+1} + \\
& \frac{g}{\Delta y} \left[ \frac{(\zeta_{i,j}^{n+2} + \zeta_{i,j}^n)}{2} - \frac{(\zeta_{i,j-1}^{n+2} + \zeta_{i,j-1}^n)}{2} \right] + g \frac{(V_{i,j}^{n+2} + V_{i,j}^n)}{2} \left[ (U_{i,j}^{*n+1})^2 + (V_{i,j}^n)^2 \right]^{1/2} / \\
& \bar{H}\bar{V}_{i,j}^{n+1} (\bar{C}\bar{V}_{i,j}^{n+1})^2 = 0
\end{aligned}$$

The solution strategy is as follows:

- i) Solve the equation of continuity and the U-equation of motion together implicitly at time level n to yield values of  $\zeta^{n+1}$  and  $U^{n+1}$  along each row.  
Required in the calculation are  $\zeta^{n-1}$ ,  $U^{n-1}$ ,  $\zeta^n$ , and  $V^n$ .
- ii) Solve the equation of continuity and the V-equation of motion together implicitly at time level n+1 to yield values of  $\zeta^{n+2}$  and  $V^{n+2}$  along each column.  
Required in the calculation are  $\zeta^n$ ,  $V^n$ ,  $\zeta^{n+1}$ ,  $U^{n+1}$ .

Repeat this procedure for the next pair of time steps, and so on. Thus, while  $\zeta$  is found at every time level, the U and V components of velocity are only solved for at alternate time levels with respect to each other. In the above scheme,  $V^{n+1}$  is missing; likewise  $U^{n+2}$

If both components of velocity are required contemporaneously, then one component--say,  $U^n$ --must be found either by solving the appropriate equation of motion explicitly, or by interpolating between values at adjacent time levels.

Whether  $U^n$  is found from the formula

$$U_{i,j}^n = \frac{U_{i,j}^{n-1} + U_{i,j}^{n+1}}{2} ,$$

or derived by explicit solution of the U-equation of motion at time level  $n-1/2$ , storage must be reserved in the computer for the following velocity arrays:

$$U^{n-1}, U^n, V^n, U^{n+1}, V^{n+2}$$

since  $V^{n+2}$  cannot be stored in  $V^n$  (as would be desirable) on account of the cross-derivative  $\partial V/\partial x$  in the V-equation of motion, which requires  $V^n$  in the preceding column.

The velocity storage requirement for the Implicit-Explicit scheme represented by equations 3.1 and 3.2 is

$$U^n, V^n, U^{n+1}, V^{n+1}$$

since here,  $V^{n+2}$  can be stored in  $V^n$ .

Hence Leendertse's solution strategy requires one more velocity storage array. The same implicit equations, however, involve  $\zeta^{n-1}$ , and therefore require an additional  $\zeta$ -array also. This disadvantage of larger storage requirement has already been mentioned in Section 2.

The Leendertse Implicit model was computed at time steps equal to 10 minutes, 5 minutes, 2 minutes, and 1 minute. Almost identical results were obtained for all of these time steps. The  $\zeta$ -values also showed close agreement with those of the Implicit-Explicit Model.

Table 2 displays results from each of the three solution models at 21 hours tidal time, for each stable case computed. It can be seen that for any given model the effect of varying time step is manifest mostly in the part of the field furthest from the open boundary at  $j = 1$ . Furthermore, it would appear that for both the Implicit-Explicit model and the Leendertse Implicit model, solution convergence has been essentially obtained at  $\Delta t = 120$  sec.

For a computer run time of fifteen minutes and  $\Delta t = 60$  sec, the Implicit-Explicit model yielded hourly output up to 22 hours of tidal time. For the same computer run time and the same  $\Delta t$ , the Leendertse Implicit model (wherein  $U^n$  was calculated from the mean of  $U^{n+1}$  and  $U^{n-1}$ ) yielded hourly output up to 25 hours of tidal time. There is thus a slight time advantage, at a given  $\Delta t$ , in using the latter model, if one is content to interpolate for one velocity component. However, the time advantage becomes very great if the user is satisfied with less accuracy; for then a larger time step can be employed--and one larger, it would seem, than the maximum time step permissible to the Implicit model, equations 3.1.

Using Leendertse's implicit method, one retains, however, the disadvantages of larger computer storage requirements and unnatural treatment of the moving shoreline, as discussed in Section 2. A further point to be considered is that in cases of very small spatial interval  $\Delta s$  (<100 ft), where  $\Delta t$  must necessarily be of the order of a few seconds,



a tidal model could probably be computed with sufficient accuracy using the simple implicit scheme embodied in equations 3.1; for when  $\Delta t \ll$  tidal period, the phase and amplitude distortion introduced by equating  $V^{n+1}$  with  $V^n$ , and  $U^{n+2}$  with  $U^{n+1}$ , must be negligible.

#### 4. Conservation of Mass

The finite difference equations 3.1 adopted for the two-dimensional model must be shown to conserve mass in the sense that the only mass changes occurring within the boundaries are those arising from the flow of mass across the open boundaries.

Consider the equation of continuity in two dimensions:

$$\frac{\partial \zeta}{\partial t} + \frac{\partial HU}{\partial x} + \frac{\partial HV}{\partial y} = 0$$

If we perform a double integration on each term from  $x = 0$  to  $x = 1$ , and  $y = 0$  to  $y = k$ , we obtain

$$\begin{aligned} \frac{\partial}{\partial t} \int_0^1 \int_0^k \zeta \, dx dy &= - \int_0^k \int_0^1 \frac{\partial HU}{\partial x} \, dx dy - \int_0^1 \int_0^k \frac{\partial HV}{\partial y} \, dy dx = \\ & \int_0^k \left[ (HU)_0 - (HU)_1 \right] dy + \int_0^1 \left[ (HV)_0 - (HV)_k \right] dx \end{aligned}$$

The term on the left-hand side is the rate of increase of volume within the area  $lk$ . The first term on the right-hand side is the net flux of volume through sides  $k$  of the area  $lk$ , and the second term on the same side is the net flux of volume through sides  $l$  of the area  $lk$ . Hence the sum on the right-hand side is simply the rate of increase of volume within the area  $lk$  which is equal to the quantity on the left.

In the context of our finite difference form of the equation of continuity, we must replace the continuous integration with a discrete summation, taking the limits  $i = 1 \rightarrow L$  and  $j = 1 \rightarrow K$ .

It is therefore required to prove that

$$\sum_1^L \sum_1^K \left( \frac{\zeta_{i,j}^{n+1} - \zeta_{i,j}^n}{\Delta t} \right) \Delta x \Delta y + \sum_1^K \sum_1^L \left( \frac{\bar{H}\bar{U}_{i+1,j}^{n+1} U_{i+1,j}^{n+1} - \bar{H}\bar{U}_{i,j}^n U_{i,j}^{n+1}}{\Delta x} \right) \Delta x \Delta y +$$

$$\sum_1^L \sum_1^K \left( \frac{\bar{H}\bar{V}_{i,j+1}^n V_{i,j+1}^n - \bar{H}\bar{V}_{i,j}^n V_{i,j}^n}{\Delta y} \right) \Delta y \Delta x = 0$$

The first term above can be written

$$\sum_1^L \sum_1^K \left( \frac{\Delta \zeta}{\Delta t} \right)_{i,j}^{n,n+1} \Delta x \Delta y$$

and this is clearly the mean rate of increase of volume within the area defined by the limits (1,L) and (1,K) between time levels n and n+1.

Let the second term be expanded in the first subscript, keeping the second subscript (j) constant. We obtain

$$\sum_1^K \left[ \left( \bar{H}\bar{U}_{2,j}^{n+1} U_{2,j}^{n+1} - \bar{H}\bar{U}_{1,j}^n U_{1,j}^{n+1} \right) + \left( \bar{H}\bar{U}_{3,j}^{n+1} U_{3,j}^{n+1} - \bar{H}\bar{U}_{2,j}^n U_{2,j}^{n+1} \right) + \dots \right.$$

$$\left. \left( \bar{H}\bar{U}_{L,j}^{n+1} U_{L,j}^{n+1} - \bar{H}\bar{U}_{L-1,j}^n U_{L-1,j}^{n+1} \right) \right] \Delta y = \sum_1^K \left( -\bar{H}\bar{U}_{1,j}^n U_{1,j}^{n+1} + \bar{H}\bar{U}_{L,j}^n U_{L,j}^{n+1} \right) \Delta y$$

Similarly, the third term of the equation expanded in the second subscript keeping the first subscript (i) constant, yields

$$\sum_1^L \left( -\bar{H}\bar{V}_{i,1}^n V_{i,1}^n + \bar{H}\bar{V}_{i,K}^n V_{i,K}^n \right) \Delta x$$

The equation can now be written

$$\sum_1^L \sum_1^K \left( \frac{\Delta \zeta}{\Delta t} \right)_{i,j}^{n,n+1} \Delta x \Delta y = \left( \sum_1^K \bar{H}\bar{U}_{1,j}^n U_{1,j}^{n+1} - \sum_1^K \bar{H}\bar{U}_{L,j}^n U_{L,j}^{n+1} \right) \Delta y +$$

$$\left( \sum_1^L \bar{H}\bar{V}_{i,1}^n V_{i,1}^n - \sum_1^L \bar{H}\bar{V}_{i,K}^n V_{i,K}^n \right) \Delta x$$



The first expression in parentheses on the right-hand side is simply the mean net volume flux into the basin in the x-direction between time levels  $n$  and  $n+1$ . The second expression in parentheses on the right hand side is the net volume flux into the basin in the y-direction at time level  $n$ . If we discount the difference in time levels, then the sum of the two parenthesized terms is the total net volume flux into the basin at a given time instant, which equals the instantaneous rate of increase of volume within the basin. Since the left-hand term covers a time interval  $\Delta t$ , and the right-hand expression embraces the same time interval, we can say that on average the finite difference equations conserve mass. An increasing error will result as the time step is enlarged. But then, the equations generally become poor approximations of the true relationships when  $\Delta t$  is excessive.

There is a further consideration of mass conservation that arises on account of the possible variation of the boundary configuration. The effect to be described does not seem to have been noted in the literature.

It is evident that whenever a negative water depth is obtained after solving the equations implicitly along a row or column, then the square in which the negative depth occurs must drop out of the computation field, and a new boundary or set of boundaries is established. This is the reverse of the flooding of dry squares: one or more wet squares becomes dry. The question arises of what to do with the negative depth. It can be shown that conservation of mass requires that this negative depth be held in memory and added to the new positive depth temporarily established when the dry square is flooded again (or, alternatively, the negative depth may be added into the wet field depths in some distributive manner, but this is more difficult). It may happen that the sum so obtained is

still negative, in which case this sum must be added to the next temporary positive depth established when the square is flooded again, and so on until a total positive depth is obtained.

The necessity for keeping a running account of negative depths and adding them into the wet field may be shown in the following manner. Consider a rectangular tank (Figure 6) having a single-stepped bottom and a drain in the deepest corner. For convenience of calculation the tank has unit bottom area in each region, so that depths and volumes are numerically equal.

Figure 6(a) shows the initial state with depths of water  $H_1$  and  $H_2$  in the two depth regions of the tank. Figure 6(b) shows the final state after a volume of water  $\Delta V$  has been removed by opening the drain. The new depth established on the left is  $H_1'$ , and the right region is now dry. Clearly, the model simulates tidal ebbing from a flooded area of land.

The ebbing process can be broken down conceptually into an unstable intermediate state shown in Figure 6(c), and then into a redistribution of the water  $H_2$  such that the level in the higher bottom region is below the bottom surface, thus giving rise to a negative depth (Fig. 6[d]). Let the new theoretical depths established be  $H_1''$  and  $H_2''$  where  $H_2'' < 0$ . Clearly, conservation of volume gives

$$H_2 = [H_1'' - (H_1 - \Delta V)] + H_2'' \quad (1)$$

Physically, all the water  $H_2$  should have gone into the left region, so that the corrected level here is

$$H_1' = H_2 + H_1 - \Delta V \quad (11)$$

Eliminating  $H_2$  from (i) and (ii) we obtain

$$H_1' = H_1'' + H_2''$$

Thus, to conserve water, we must add the negative solution in the newly dry area to the solution in the adjacent wet area. Without the correction  $H_2''$  in the present example, the volume in the left-hand region will be too large.

For the tidal model it is more convenient to make the correction to the same square that developed the negative water depth, performing the addition when that square becomes flooded again. There is of course no rationale for choosing any particular wet square to be corrected; nor do we know how to distribute the correction among all the wet squares in a row or column.

A departure in the present work from Leendertse's published method (Leendertse and Gritton 1971) should be mentioned. Whenever there has been an adjustment of boundary in a row or column, the values of  $\zeta$  in that row or column are not recalculated at the same time level. Rather, a new time step is considered for every application of the implicit solution. In Leendertse's procedure, the adjusted row or column is re-solved at the same time step. It seems doubtful whether this doubling of computational effort is worth the possible increase of accuracy. Moreover, there is no reason why a row or column should be solved with the new boundary rather than the original boundary, at the time step in which the new boundary is established.

##### 5. Computation of the Moving Shoreline

The advance of the wet boundary by flooding over dry steps in the

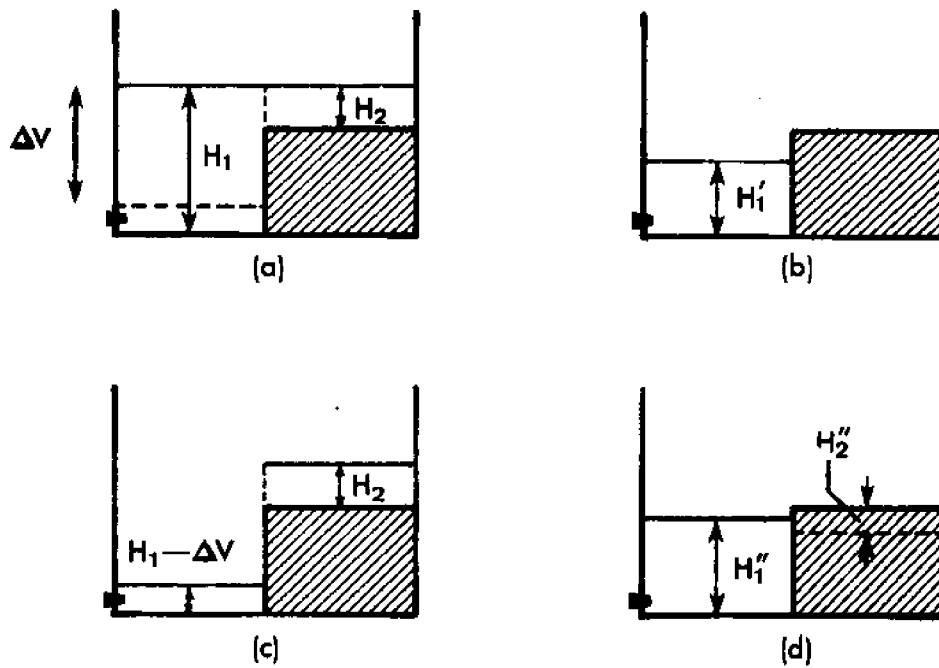


Fig. 6. Stepped Bottom Tank. (a) Full; (b) With Volume  $\Delta V$  Removed; (c) and (d) Conceptual Intermediate States.

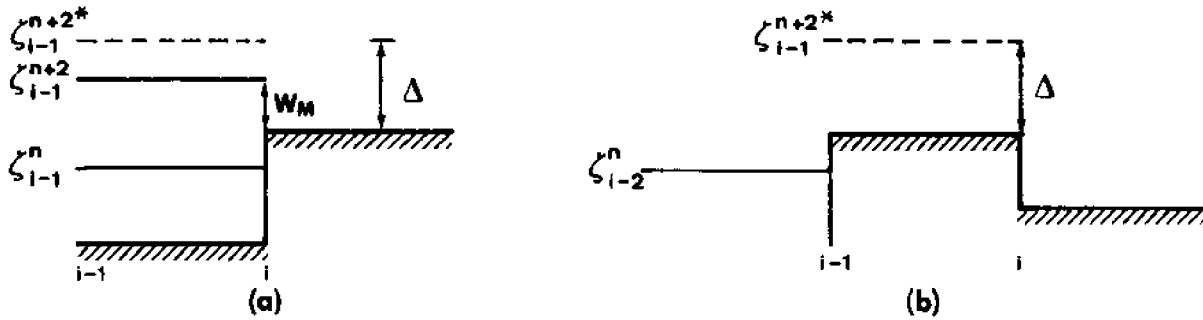


Fig. 7. (a) Topographical upstep; (b) topographical downstep.

topography is treated as a weir phenomenon,<sup>6</sup> for which a hydraulic formula exists. This is (cf. Giles [1962]):

$$Q = mW^{3/2} \quad (5.1)$$

where  $Q$  is the volume flow per second per unit width of the weir of height  $W$ . The empirical constant  $m$  depends on the actual weir. In the Francis formula, of which 5.1 is the limiting case when  $V^2/2g \ll W$ , where  $V$  is the velocity of approach to the weir,  $m$  has the value 3.33 ft<sup>1/2</sup>/sec.

Since it is proposed to determine the new shoreline, not after every time step, but after every pair of time steps, when the field equations have been applied along both rows and columns, the general problem may be stated thus: To determine the volume transferred in a time interval  $2\Delta t$  across one edge of a dry grid square. Two physical situations must be distinguished: the "upstep" and the "downstep." These are illustrated in Figures 7(a) and 7(b) respectively. The vertical section is arbitrarily taken perpendicular to the  $y$  direction, and the flooding is assumed to occur in the  $x$  direction.

Consider firstly the topographical upstep. At time  $n\Delta t$ , the level in square  $i-1$  is  $\zeta_{i-1}^n$ . If there were an infinite barrier at edge  $i$ , the final level in square  $i-1$  after time  $2\Delta t$  would be  $\zeta_{i-1}^{n+2*}$ . But owing to the spillover into dry square  $i$ , the final and maximum level reached in  $i-1$  will be  $\zeta_{i-1}^{n+2} < \zeta_{i-1}^{n+2*}$ . Corresponding to the level  $\zeta_{i-1}^{n+2}$ , there is a maximum weir height  $W_M$ . The minimum weir height is plainly zero. Suppose the weir height begins to increase from zero at time  $(n+2f)\Delta t$ , where  $0 < f < 1$ . At the time instant  $(n+2f)\Delta t$ , the water level in square  $i-1$  will equal the bottom level in square  $i$ . Making use of 5.1, the volume transferred across edge  $i$  in time  $2\Delta t$  must be given by

<sup>6</sup>See also Reid and Bodine (1968) for this assumption.

$$\text{Vol}_i = m\Delta y \int_{(n+2f)\Delta t}^{(n+2)\Delta t} W^{3/2} dt \quad (5.2)$$

Let us assume that  $W$  increases at a rate proportional to  $t' = t - (n+2f)\Delta t$ . Then we may write

$$W = \alpha t' \text{ and } W_M = \alpha(1-f)2\Delta t \quad (5.3)$$

Hence, from 5.2 and 5.3 and the definition of  $t'$

$$\begin{aligned} \text{Vol}_i &= m\Delta y \int_{(n+2f)\Delta t}^{(n+2)\Delta t} \alpha^{3/2} t'^{3/2} dt = m\Delta y \int_0^{(1-f)2\Delta t} \alpha^{3/2} t'^{3/2} dt' \\ &= \frac{2}{5} m\Delta y \alpha^{3/2} [(1-f)2\Delta t]^{5/2} \end{aligned}$$

or,

$$\text{Vol}_i = \frac{4}{5} m\Delta y (1-f) W_M^{3/2} \Delta t$$

The new depth in square  $i$  is given by

$$H_i^{n+2} = \text{Vol}_i / \Delta x \Delta y \quad (5.4)$$

Hence from 5.4 and the last equation,

$$H_i^{n+2} = \frac{4}{5} m \frac{(1-f) W_M^{3/2} \Delta t}{\Delta x}$$

Now the average value of the function  $1-f$ , assuming that all  $f$ 's are equally likely, is  $1/2$ . Thus on average we obtain

$$H_i^{n+2} = \frac{0.4 m W_M^{3/2} \Delta t}{\Delta x} \quad (5.5)$$

It is to be noted that formula 5.5 can only be successfully applied to an upstep when

$$H_i^{n+2} \ll W_M \quad (5.6)$$

If this condition is not met, then some interference of the weir flow will occur on account of the water built up in square  $i$ . In order to ensure condition 5.6, there will be an effective upper limit to the permissible magnitude of  $\Delta t$  for given  $\Delta x$ .

To conserve mass, the volume of water transferred to a dry square must be subtracted from the wet field. For convenience of computation, however, it was decided to deduct the flood volume  $H_i^{n+2} \Delta x \Delta y$  from the adjacent flooding square only. Hence we obtain

$$\zeta_{i-1}^{n+2} = \zeta_{i-1}^{n+2*} - H_i^{n+2},$$

and (referring to Figure 7[a])

$$W_M = \Delta - H_i^{n+2}.$$

The largest possible value of  $W_M$  is equal to  $\Delta$  when  $H_i^{n+2} = 0$ .

A special case arises if the corrected level  $\zeta_{i-1}^{n+2}$  in square  $i-1$  should be less than the new flood level  $\zeta_i^{n+2}$  in square  $i$ . Physically, this is an unrealizable situation. What must happen, according to the previous assumption of volume transfer from square  $i-1$  only, is that in the case of the upstep, a common level will be reached in both squares, and so

$$H_i^{n+2} = \frac{1}{2} \Delta \quad (5.7)$$

Thus a test should be made for the truth of the inequality  $\zeta_{i-1}^{n+2} < \zeta_i^{n+2}$ , and when this occurs, a revised depth is calculated by 5.7. However,  $\Delta t$  should be so chosen as to render this special case infrequent or absent altogether.

Where common levels are reached in both squares, it is clear that

$$W_M = \frac{1}{2} \Delta.$$

Hence the range of  $W_M$  is from  $\frac{1}{2}\Delta$  to  $\Delta$ . We assume on average that

$$W_M = \frac{3}{4} \Delta \quad (5.8)$$

Consider now the downstep situation. This will obtain when flooding occurs over a levee, as diagrammed in Figure 7(b). The process is more complicated than with the upstep, for here two flood stages occur almost simultaneously. During  $2\Delta t$  water will appear on top of the levee, and during the same time interval it will cascade down onto the next and lower step.

Assume that the weir height  $W$  above the levee (square  $i-1$  in Figure 7(b)) increases steadily from time  $(n+2f)\Delta t$  when  $W = 0$ , to time  $(n+2)\Delta t$  when  $W = W_M$ . Making the assumption as before that the water in square  $i$  comes only from  $i-1$ , we have

$$W_M = \Delta - H_i^{n+2}$$

and the largest possible value of  $W_M$  is equal to  $\Delta$  when  $H_i^{n+2} = 0$ .

The test  $\zeta_{i-1}^{n+2} < \zeta_i^{n+2}$  should be applied, and also a check to see if the corrected level  $\zeta_{i-1}^{n+2}$  is below the land surface in square  $i-1$ . If either of these tests prove positive, then formula 5.7 can be used; so that in this case  $W_M = \frac{1}{2} \Delta$ . It is assumed that on average for the downstep, equation 5.8 also holds.

Substituting  $W_M$  from 5.8 in equation 5.5, we obtain

$$H_i^{n+2} = \frac{0.26 m \Delta^{3/2} \Delta t}{\Delta x} \quad (5.9)$$

The use of equation 5.8 for  $W_M$  in the downstep situation is admittedly somewhat artificial. We justify it merely on the grounds that (1) the levee situation should be infrequent compared with the upstep situation and (2) an error in the volume transferred should be eventually removed by successive application of the equation of continuity to the new wet field. The last remark applies also, of course, to any error in the calculated volume for an upstep.



It is to be noted that 5.9 can only be successfully applied to a downstep when

$$\delta_{i-1}^{n+2} = \zeta_i^{n+2} + h_i \ll \Delta \quad (5.10)$$

To ensure condition 5.10, there will be an effective upper limit to the permissible magnitude of  $\Delta t$  for given  $\Delta x$ .

Since every grid square  $i$  not touching a boundary has four grid squares adjacent to it, flooding can conceivably occur from more than one of these squares at once. We handle this possibility by calculating the flooding from two or more perpendicular directions separately and then adding the separate contributions in square  $i$ . Thus a running total  $H_i^{n+2'}$  must be kept, composed of the sum of the individual  $H_i^{n+2}$ 's contributed by the adjacent flooding squares already considered.

Define a quantity  $\delta_i^{n+2'}$  as the amount by which the interim level in  $i$  exceeds the land surface in the next square whose flooding contribution is to be considered. Clearly, if for this square

$$\delta_i^{n+2'} \ll \Delta,$$

then we may safely apply formula 5.9. It was decided to adopt an arbitrary criterion

$$\delta_i^{n+2'} \leq F_c \Delta, \quad 0 < F_c < 1 \quad (5.11)$$

for calculating a successive flooding contribution. If condition 5.11 with some assigned value of  $F_c$  is not met, then the level in the flooded square currently reached by the addition of the previous flooding contributions is taken as the final level. Again, suitable choice of  $\Delta t$  for

given  $\Delta x$  and  $\Delta y$  should render this premature halt unlikely. But if it occurs, when we may expect the insufficiency in the new water level (in square  $i, j$ ) to be gradually eliminated over the next few time steps for the reason given earlier: namely, the successive application of the equation of continuity to the new wet field.

Plainly, the accuracy of the flooding procedure can be improved by reducing  $\Delta t$ , appropriately. There must be a trade-off between the desired accuracy in this area (within the limits of formula 5.9) and the computer running time of the model. The topographical sensitivity should enable the modeler to choose wisely here.

The flooding procedure is applied where necessary in a chain manner. It may happen that a newly flooded square is capable of flooding the next square, and so on. Since all these operations are carried out for one and the same time step, there will be an increasing error in the estimated magnitude of the flooding as one moves down the chain. Only experience with a given model and time step can tell if this cumulative error is important. If it should seem that the chain is too long and that it occurs in a crucial area, then one may have to restrict the flooding to one or two squares at a time before applying the field equations again, or alternatively, reduce  $\Delta t$ .

APPENDIX A

Principles of the Implicit Method

Referring to equations 3.1, we write the first pair in the form

$$\begin{aligned} \zeta_{i,j}^{n+1} + \left( \bar{H}_{i+1,j}^u \frac{\Delta t}{\Delta x} \right) U_{i+1,j}^{n+1} + \left( -\bar{H}_{i,j}^u \frac{\Delta t}{\Delta x} \right) U_{i,j}^{n+1} &= \zeta_{i,j}^n - \left( \bar{H}_{i,j+1}^v V_{i,j+1}^n - \right. \\ &\left. \bar{H}_{i,j}^v V_{i,j}^n \right) \frac{\Delta t}{\Delta y} \\ U_{i,j}^{n+1} \left\{ 1 + \left( U_{i+1,j}^n - U_{i-1,j}^n \right) \frac{\Delta t}{\Delta x} + g \frac{\Delta t}{2} \left[ \left( U_{i,j}^n \right)^2 + \right. \right. \\ &\left. \left. \left( v_{i,j}^{*n} \right)^2 \right]^{1/2} / \bar{H}_{i,j}^u \left( \bar{C}_{i,j}^u \right)^2 \right\} + \left( \frac{g\Delta t}{2\Delta x} \right) \zeta_{i,j}^{n+1} + \left( \frac{-g\Delta t}{2\Delta x} \right) \zeta_{i-1,j}^{n+1} \\ &= U_{i,j}^n - v_{i,j}^{*n} \left( U_{i,j+1}^n - U_{i,j-1}^n \right) \frac{\Delta t}{2\Delta y} + f\Delta t v_{i,j}^{*n} - \frac{g\Delta t}{2\Delta x} \left( \zeta_{i,j}^n - \zeta_{i-1,j}^n \right) - \\ &\frac{g\Delta t}{2} U_{i,j}^n \left[ \left( U_{i,j}^n \right)^2 + \left( v_{i,j}^{*n} \right)^2 \right]^{1/2} / \bar{H}_{i,j}^u \left( \bar{C}_{i,j}^u \right)^2 - \frac{1}{\rho} \frac{\partial P_0}{\partial x} + \tau_x^s / \rho \bar{H}_{i,j}^u \end{aligned}$$

Let

$$a_{i+1,j} = \bar{H}_{i+1,j}^u \frac{\Delta t}{\Delta x}$$

$$a'_{i,j} = -\bar{H}_{i,j}^u \frac{\Delta t}{\Delta x}$$

$$A_{i,j} = \zeta_{i,j}^n - \left( \bar{H}_{i,j+1}^v V_{i,j+1}^n - \bar{H}_{i,j}^v V_{i,j}^n \right) \frac{\Delta t}{\Delta y}$$

$$b_{i,j} = \frac{g\Delta t}{2\Delta x}$$

$$b'_{i-1,j} = \frac{-g\Delta t}{2\Delta x}$$

$$b''_{i,j} = 1 + \left( U_{i+1,j}^n - U_{i-1,j}^n \right) \frac{\Delta t}{2\Delta x} + \frac{g\Delta t}{2} \left[ \left( U_{i,j}^n \right)^2 + \left( v_{i,j}^{*n} \right)^2 \right]^{1/2} / \bar{H}_{i,j}^u \left( \bar{C}_{i,j}^u \right)^2$$

$$B_{i,j} = U_{i,j}^n - v_{i,j}^{*n} \left( U_{i,j+1}^n - U_{i,j-1}^n \right) \frac{\Delta t}{2\Delta y} F_1 + f\Delta t v_{i,j}^{*n} - \frac{g\Delta t}{2\Delta x} \left( \zeta_{i,j}^n - \zeta_{i-1,j}^n \right) - \frac{g\Delta t}{2} U_{i,j}^n \left[ \left( U_{i,j}^n \right)^2 + \left( v_{i,j}^{*n} \right)^2 \right]^{1/2} / \bar{H}_{i,j}^n \left( \bar{C}_{i,j}^n \right)^2 - \frac{1}{\rho} \frac{\partial P_0}{\partial x} + \tau_x^s / \rho \bar{H}_{i,j}^n$$

The multiplier  $F_1$  (=0 or 1) is introduced into the expression for  $B_{i,j}$  in order to take cognizance of the fact that the derivative  $(U_{i,j+1}^n - U_{i,j-1}^n) / 2\Delta y$  may be unavailable for computation. In this case we set  $F_1 = 0$ . Otherwise  $F_1 = 1$ . In the case that  $j = 1$ , we omit the derivative altogether, as the U-array must properly begin with subscripts 1, 1 in FORTRAN language. The conditions requiring  $F_1$  to be zero are:

- a) Proximity of dry land or an open boundary, rendering either  $U_{i,j+1}$  or  $U_{i,j-1}$  undefined
- b) The case  $j = K-1$  in which  $U_{i,K}$  lies outside the computation field. (Here K is the maximum value of j.)

Thus the equations to be solved for  $\zeta_{i,j}^{n+1}$  and  $U_{i,j}^{n+1}$  are

$$\zeta_{i,j}^{n+1} + a_{i+1,j} U_{i+1,j}^{n+1} + a'_{i,j} U_{i,j}^{n+1} = A_{i,j} \tag{A.1}$$

$$b'' U_{i,j}^{n+1} + b_{i,j} \zeta_{i,j}^{n+1} + b'_{i-1,j} \zeta_{i-1,j}^{n+1} = B_{i,j}$$

Suppose that the boundaries in the jth row occur at  $i=I$  and  $i=L$ .

The boundary situations to be considered are:

$i = I$	$i = L$	Reference
Open	Closed	UOPEN1
Closed	Open	UOPEN2
Open	Open	UOPEN3
Closed	Closed	UCLOSE

The system of equations A.1 may be written in expanded form, dropping the subscript j for convenience:

$$a'_I U_I^{n+1} + \zeta_I^{n+1} + a_{I+1} U_{I+1}^{n+1} = A_I \quad (i)$$

$$b'_I \zeta_I^{n+1} + b''_{I+1} U_{I+1}^{n+1} + b_{I+1} \zeta_{I+1}^{n+1} = B_{I+1} \quad (ii)$$

$$a'_{I+1} U_{I+1}^{n+1} + \zeta_{I+1}^{n+1} + a_{I+2} U_{I+2}^{n+1} = A_{I+1} \quad (iii)$$

$$b'_{I+1} \zeta_{I+1}^{n+1} + b''_{I+2} U_{I+2}^{n+1} + b_{I+2} \zeta_{I+2}^{n+1} = B_{I+2} \quad (iv) \quad (A.2)$$

$$a'_{I+2} U_{I+2}^{n+1} + \zeta_{I+2}^{n+1} + a_{I+3} U_{I+3}^{n+1} = A_{I+2} \quad (v)$$

.....

$$b'_{L-2} \zeta_{L-2}^{n+1} + b''_{L-1} U_{L-1}^{n+1} + b_{L-1} \zeta_{L-1}^{n+1} = B_{L-1} \quad (N-1)$$

$$a'_{L-1} U_{L-1}^{n+1} + \zeta_{L-1}^{n+1} + a_L U_L^{n+1} = A_{L-1} \quad (N)$$

where

$$N = 2(L-I)-1$$

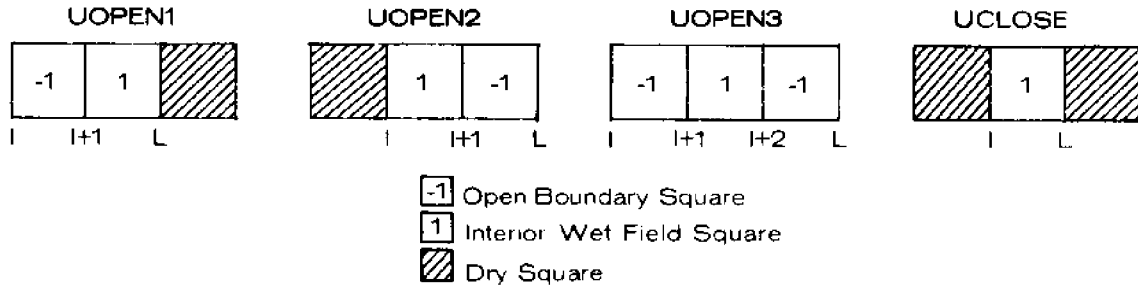
For each of the cases in Table 3, we must select a subset of equations from system A.2 as detailed in Table 4.

It is to be noted that  $U_I^{n+1} = U_L^{n+1}$  are usually zero when they are given quantities.

Reference	Given Quantities	Equations Used	No. of Equations (M)
UOPEN1	$\zeta_I^{n+1}, U_L^{n+1}$	(ii) - (N)	$2(L-I)-2$
UOPEN2	$U_I^{n+1}, \zeta_{L-1}^{n+1}$	(i) - (N-1)	$2(L-I)-2$
UOPEN3	$\zeta_I^{n+1}, \zeta_{L-1}^{n+1}$	(ii) - (N-1)	$2(L-I)-3$
UCLOSE	$U_I^{n+1}, U_L^{n+1}$	(i) - (N-1)	$2(L-I)-2$



Certain special cases must now be considered where the general solution algorithm is inapplicable. These are illustrated below with the reference names over each.



### UOPEN1

The equations for this case are

$$b'_{I+1} U_{I+1}^{n+1} + b_{I+1} \zeta_{I+1}^{n+1} = B_{I+1} - b'_I \zeta_I^{n+1}$$

$$a'_{I+1} U_{I+1}^{n+1} + \zeta_{I+1}^{n+1} = A_{I+1}$$

These have the solution:

$$\zeta_{I+1}^{n+1} = \frac{a'_{I+1} (B_{I+1} - b'_I \zeta_I^{n+1}) - b'_{I+1} A_{I+1}}{b_{I+1} a'_{I+1} - b'_{I+1}}$$

$$U_{I+1}^{n+1} = \frac{A_{I+1} b_{I+1} - (B_{I+1} - b'_I \zeta_I^{n+1})}{b_{I+1} a'_{I+1} - b'_{I+1}}$$

### UOPEN2

The equations for this case are

$$\zeta_I^{n+1} + a_{I+1} U_{I+1}^{n+1} = A_I$$

$$b'_I \zeta_I^{n+1} + b'_{I+1} U_{I+1}^{n+1} = B_{I+1} - b_{I+1} \zeta_{I+1}^{n+1}$$

These have the solution:

$$\zeta_I^{n+1} = \frac{a_{I+1} (B_{I+1} - b_{I+1} \zeta_{I+1}^{n+1}) - b'_{I+1} A_I}{b'_I a_{I+1} - b'_{I+1}}$$

### UOPEN3

The equations for this case are

$$U_{I+1}^{n+1} = \frac{b'_{I+1} A_I - (B_{I+1} - b'_{I+1} \zeta_{I+1}^{n+1})}{b'_{I+1} a_{I+1} - b'_{I+1}}$$

$$b'_{I+1} U_{I+1}^{n+1} + b'_{I+1} \zeta_{I+1}^{n+1} = B_{I+1} - b'_{I+1} \zeta_I^{n+1}$$

$$a'_{I+1} U_{I+1}^{n+1} + \zeta_{I+1}^{n+1} + a_{I+2} U_{I+2}^{n+1} = A_{I+1}$$

$$b'_{I+1} \zeta_{I+1}^{n+1} + b'_{I+2} U_{I+2}^{n+1} = B_{I+2} - b'_{I+2} \zeta_{I+2}^{n+1}$$

These have the solution:

$$\zeta_{I+1}^{n+1} = \frac{b'_{I+2} a'_{I+1} (B_{I+1} - b'_{I+1} \zeta_I^{n+1}) - b'_{I+2} b'_{I+1} A_{I+1} + b'_{I+1} a_{I+2} (B_{I+2} - b'_{I+2} \zeta_{I+2}^{n+1})}{b'_{I+2} (a'_{I+1} b_{I+1} - b'_{I+1}) + a_{I+2} b'_{I+1} b'_{I+1}}$$

$$U_{I+1}^{n+1} = \frac{(a_{I+2} b'_{I+1} - b'_{I+2}) (B_{I+1} - b'_{I+1} \zeta_I^{n+1}) + b_{I+1} b'_{I+2} A_{I+1} - a_{I+2} b_{I+1} (B_{I+2} - b'_{I+2} \zeta_{I+2}^{n+1})}{b'_{I+2} (a'_{I+1} b_{I+1} - b'_{I+1}) + a_{I+2} b'_{I+1} b'_{I+1}}$$

$$U_{I+2}^{n+1} = \frac{b'_{I+1} b'_{I+1} A_{I+1} + (a'_{I+1} b_{I+1} - b'_{I+1}) (B_{I+2} - b'_{I+2} \zeta_{I+2}^{n+1}) - a'_{I+1} b'_{I+1} (B_{I+1} - b'_{I+1} \zeta_I^{n+1})}{b'_{I+2} (a'_{I+1} b_{I+1} - b'_{I+1}) + a_{I+2} b'_{I+1} b'_{I+1}}$$

### UCLOSE

Here, a single equation determines the unknown  $\zeta_I^{n+1}$ :

$$\zeta_I^{n+1} = A_I$$

Similar cases to the four above may, of course, occur along columns.



APPENDIX B

Use of a Stretched Coordinate System

Suppose that for reasons of field resolution the coordinate lines  $i = 1, 2, 3 \dots$  are not equispaced but observe a functional relationship with the distance  $x$  from the origin. That is

$$i = I(x)$$

Similarly, if the  $j$  coordinate lines are also stretched by a functional relationship with the distance  $y$  from the origin, we have

$$j = J(y)$$

The chain rule of differentiation requires that

$$\frac{\partial}{\partial x} = \frac{\partial}{\partial I} \frac{\partial I}{\partial x}, \quad \frac{\partial}{\partial y} = \frac{\partial}{\partial J} \frac{\partial J}{\partial y},$$

For the finite difference representation of the derivatives, these operator relationships translate to

$$\frac{\partial}{\partial x} = \frac{\Delta}{\Delta I} \frac{\partial I}{\partial x}, \quad \frac{\partial}{\partial y} = \frac{\Delta}{\Delta J} \frac{\partial J}{\partial y},$$

where  $\Delta$  is the difference operator.

Since  $\Delta I = \Delta J = 1$ , it will be convenient to replace  $\Delta I$  and  $\Delta J$  by  $\Delta s (=1)$ . Then equations 3.1 with stretched coordinates can be written in an obvious shorthand:

$$\frac{(\zeta_{i,j}^{n+1} - \zeta_{i,j}^n)}{\Delta t} + \left( \frac{\quad}{\Delta s} \right) \bar{I}'_{i+1/2,j} + \left( \frac{\quad}{\Delta s} \right) \bar{J}'_{i,j+1/2} = 0$$

$$\frac{(U_{i,j}^{n+1} - U_{i,j}^n)}{\Delta t} + U_{i,j}^{n+1} \left( \frac{\quad}{2\Delta s} \right) I'_{i,j} + V_{i,j}^{*n} \left( \frac{\quad}{2\Delta s} \right) J'_{i,j} - f V_{i,j}^{*n} +$$

$$\frac{g}{\Delta s} \left[ \left( \quad \right)_{i,j} - \left( \quad \right)_{i-1,j} \right] \bar{I}'_{i-1/2,j} + g \frac{(U_{i,j}^{n+1} + U_{i,j}^n)}{2} \left[ \quad \right]^{1/2} /$$

$$\bar{H}\bar{u}_{i,j}^n (\bar{C}\bar{u}_{i,j}^n)^2 + \frac{1}{\rho} \frac{\partial P_0}{\partial x} - \tau_x^s / \rho \bar{H}\bar{u}_{i,j}^n = 0$$

$$\frac{(z_{i,j}^{n+2} - z_{i,j}^{n+1})}{\Delta t} + \left( \quad \right)_{\Delta s} \bar{I}'_{i+1/2,j} + \left( \quad \right)_{\Delta s} \bar{J}'_{i,j+1/2} = 0$$

$$\frac{(v_{i,j}^{n+2} - v_{i,j}^{n+1})}{\Delta t} + U_{i,j}^{*n+1} \left( \quad \right)_{2\Delta s} I'_{i,j} + V_{i,j}^{n+2} \left( \quad \right)_{2\Delta s} J'_{i,j} + U_{i,j}^{*n+1} +$$

$$\frac{g}{\Delta s} \left[ \left( \quad \right)_{i,j} - \left( \quad \right)_{i,j-1} \right] \bar{J}'_{i,j-1/2} + g \frac{(V_{i,j}^{n+2} + V_{i,j}^{n+1})}{2} \left[ \quad \right]^{1/2} /$$

$$\bar{H}\bar{v}_{i,j}^{n+1} (\bar{C}\bar{v}_{i,j}^n)^2 + \frac{1}{\rho} \frac{\partial P_0}{\partial y} - \tau_y^s / \rho \bar{H}\bar{v}_{i,j}^{n+1} = 0$$

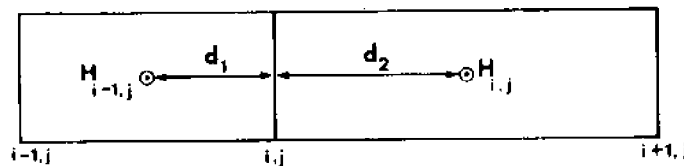
The contents of the parentheses where blank are the same as the contents of the corresponding parentheses in equations 3.1. The symbol  $\bar{I}'_{i+1/2,j}$  means the average value of  $\frac{\partial I}{\partial x}$  between the points (i,j) and (i+1,j).

Thus

$$\bar{I}'_{i+1/2,j} = \frac{I'_{i,j} + I'_{i+1,j}}{2}$$

Similarly with the other averaged derivatives.

The averaging involved in calculating  $\bar{H}\bar{u}$ ,  $\bar{H}\bar{v}$ ,  $\bar{C}\bar{u}$ ,  $\bar{C}\bar{v}$ ,  $V^*$ , and  $U^*$  is now a little more complicated. Let X(i) and Y(j) be the distances from the origin to the ith and jth coordinate lines respectively.



It is evident that

$$\bar{H}u_{i,j} = H_{i,j} \left( \frac{d_1}{d_1+d_2} \right) + H_{i-1,j} \left( 1 - \frac{d_1}{d_1+d_2} \right)$$

Let

$$P_x(i) = \frac{d_1}{d_1+d_2}$$

Then

$$P_x(i) = \frac{x_1 - x_{i-1}}{x_{i+1} - x_{i-1}}$$

and

$$\bar{H}u_{i,j} = H_{i,j} P_x(i) + H_{i-1,j} (1 - P_x(i)) \quad i = 2 \dots L - 1$$

If we define

$$P_y(j) = \frac{y_j - y_{j-1}}{y_{j+1} - y_{j-1}}$$

we obtain similarly

$$\bar{H}v_{i,j} = H_{i,j} P_y(j) + H_{i,j-1} (1 - P_y(j)) \quad j = 2 \dots K - 1$$

The averages  $\bar{C}u$  and  $\bar{C}v$  are defined as follows

$$\bar{C}u_{i,j} = \frac{1.486}{n} \left[ H_{i,j}^{1/6} P_x(i) + H_{i-1,j}^{1/6} (1 - P_x(i)) \right]$$

$$\bar{C}v_{i,j} = \frac{1.486}{n} \left[ H_{i,j}^{1/6} P_y(j) + H_{i,j-1}^{1/6} (1 - P_y(j)) \right]$$

The above four averages are subject of course to the proviso that all quantities H are defined where necessary.

It may be easily shown that with the above definitions of  $P_x(i)$  and  $P_y(j)$

$$V_{i,j}^* = \frac{1}{2} \left[ (v_{i,j} + v_{i,j+1}) P_x(i) + (v_{i-1,j} + v_{i-1,j+1}) (1 - P_x(i)) \right]$$

$$U_{i,j}^* = \frac{1}{2} \left[ (u_{i,j} + u_{i+1,j}) P_y(j) + (u_{i,j-1} + u_{i+1,j-1}) (1 - P_y(j)) \right]$$

subject again to the proviso that all quantities V or U required on the right hand sides are defined.

## REFERENCES

- Giles, R. V. 1962. Fluid Mechanics and Hydraulics, McGraw Hill, New York. pp. 135-136.
- Hacker, S. 1973. Transport phenomena in estuaries. Ph.D. diss., Louisiana State University, Baton Rouge.
- Hansen, W. 1956. Theorie zur errechnung des wasserstandes und der stromungen in randmeeren nebst anwedungen, Tellus 8,3:287-300.
- Leendertse, J. J. 1967. Aspects of a computational model for long-period water-wave propagation. Rand Corp. Memorandum RM-5294-PR.
- \_\_\_\_\_. 1970. A water-quality simulation model for well-mixed estuaries and coastal seas: Vol. I, Principles of Computation. Rand Corp. Memorandum RM-6230-RC.
- \_\_\_\_\_ and E. C. Gritton. 1971. A water-quality simulation model for well-mixed estuaries and coastal seas: Vol. II, Computation Procedures. Rand Corp. Memorandum R-708-NYC.
- Pritchard, D. W. 1971. Estuarine modelling: an assessment. Tracor, Inc., pp. 11-12.
- Reid, R. O. and B. R. Bodine. 1968. Numerical model for storm surges in Galveston Bay, Proc. ASCE Waterways and Harbors Div. 94, no. WWI:37-57.
- Sobey, R. J. 1970. Finite-difference schemes compared for wave-deformation characteristics in mathematical modelling of two-dimensional long-wave propagation, U.S. Army Corps of Engineers, Coastal Engineering Research Center, Tech. Memorandum no. 32.

Part 2

A Hydrodynamic Numerical Model of Tidal Flow Through A  
Small Area of Brackish Marsh

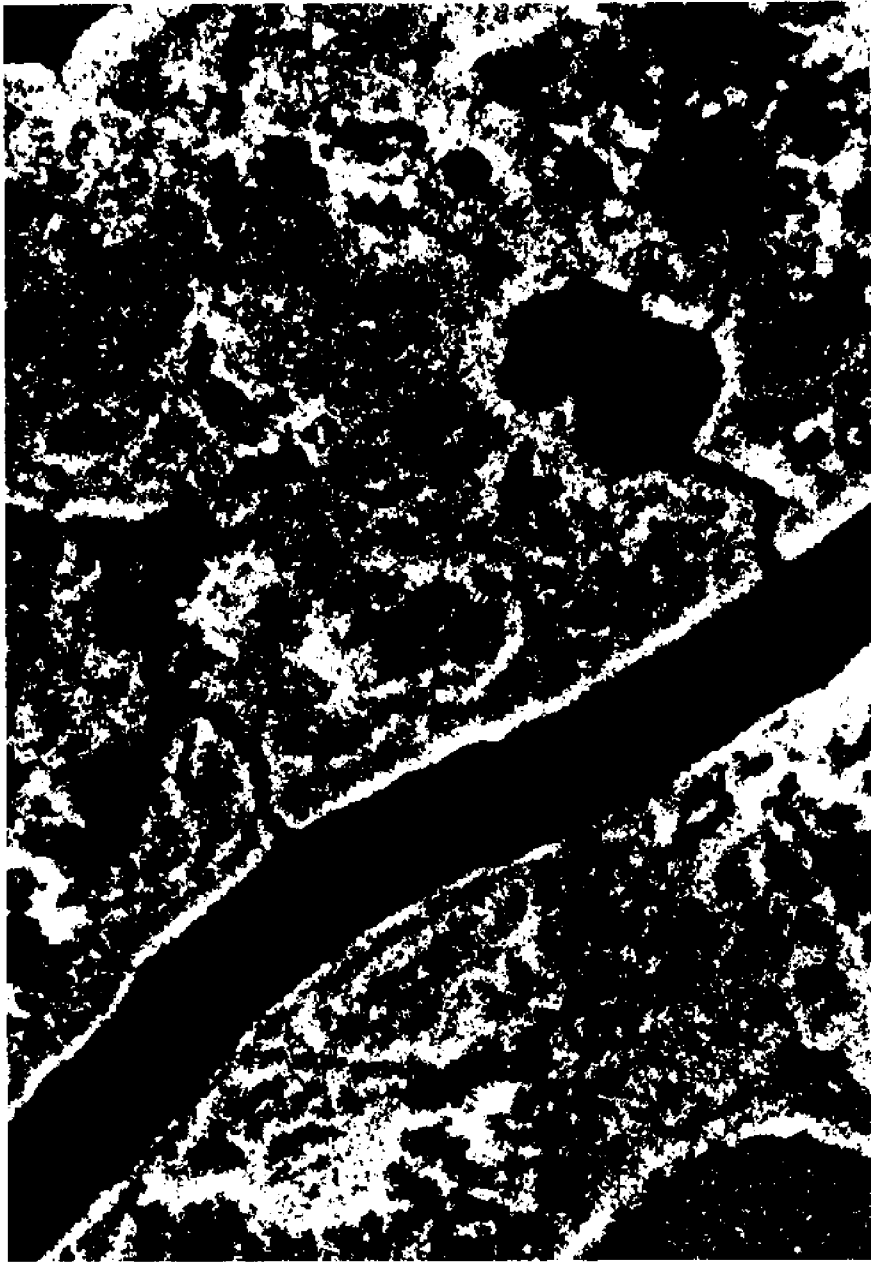


Plate 1. Aerial view of marsh study area.

A segment of Louisiana brackish marsh in the neighborhood of Airplane Lake was selected in October 1974 as a test case for demonstrating the feasibility of modeling the movement of water over such a terrain.

An aerial view of the marsh is shown as Plate 1. The salient features are a broad channel in the south<sup>1</sup> of the picture and two tributary channels running northward that form three open boundaries of the area to be modeled. The northern boundary of this area (henceforward to be known as the Model Area) is mixed in nature, being open for part of the way from west to east and temporarily closed and open for the rest of its length, depending on the state of the tide.

Such a piece of marsh was selected because it has the advantages of being nearly enclosed by open boundaries, and it is a size convenient for surveying in a matter of hours. A mixed boundary is far more difficult to handle computationally than one that is always open. The mixed boundary is also complicated to handle from the observational viewpoint, for an installed tide gauge will only function intermittently.

The channels shown in Plate 1 lie essentially on the margin of Barataria Bay and about 7 km from the Gulf of Mexico.

In character the marsh consists of soft mud covered with Spartina grass about 2-3 ft in height. It may or may not be left "dry" at low water; but it is certainly flooded at high water. Thus at high water the Model Area becomes a shallow lake with open boundaries all around. Only the grass projecting above the water surface still delineates the shape and extent of the land underneath.

For computational purposes it is necessary to superimpose a grid on

---

<sup>1</sup>Compass directions are relative to the orientation of the paper only.

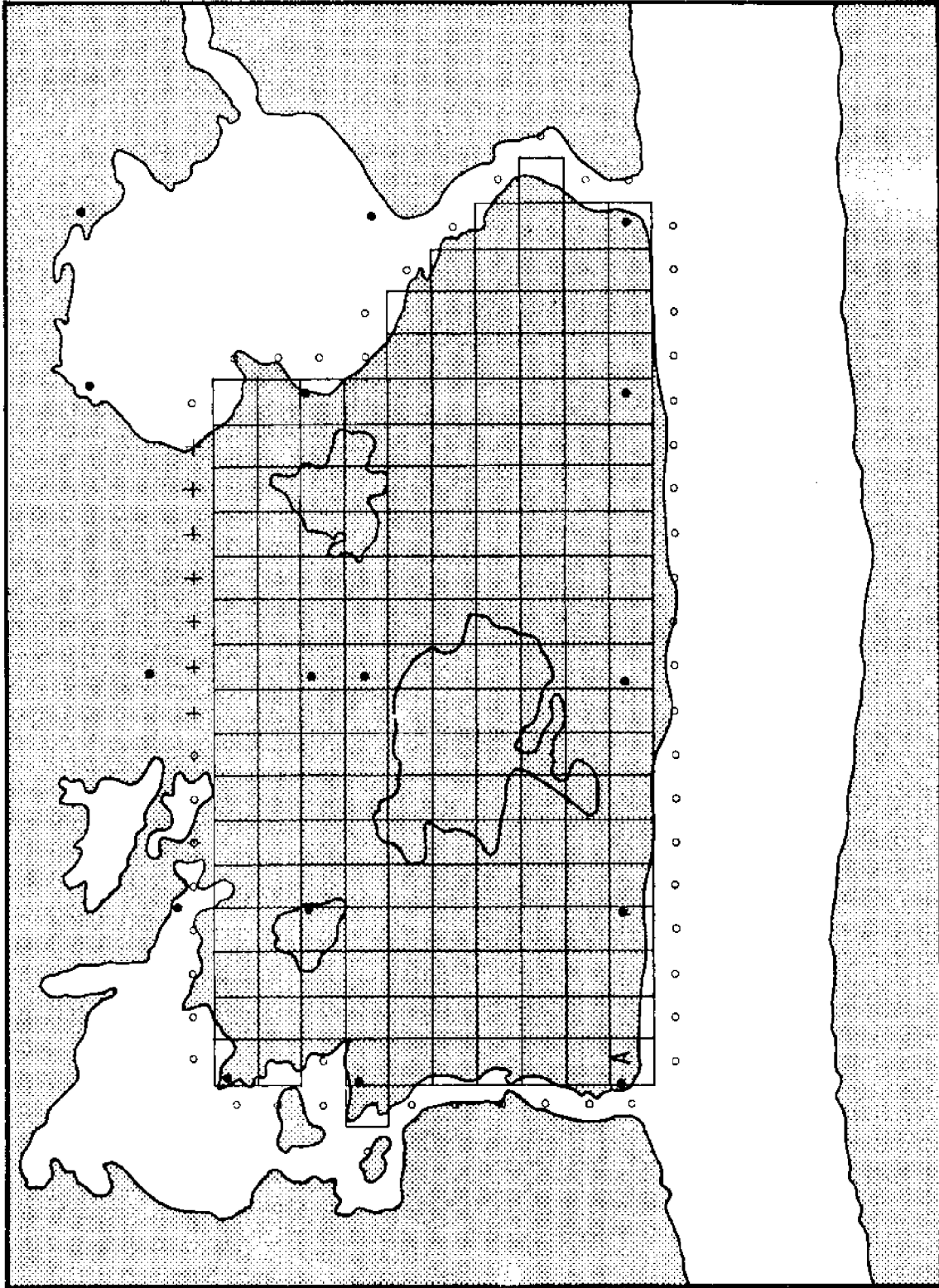


Fig. 1. Computational grid. o = open boundary points; + = intermittently open boundary points.



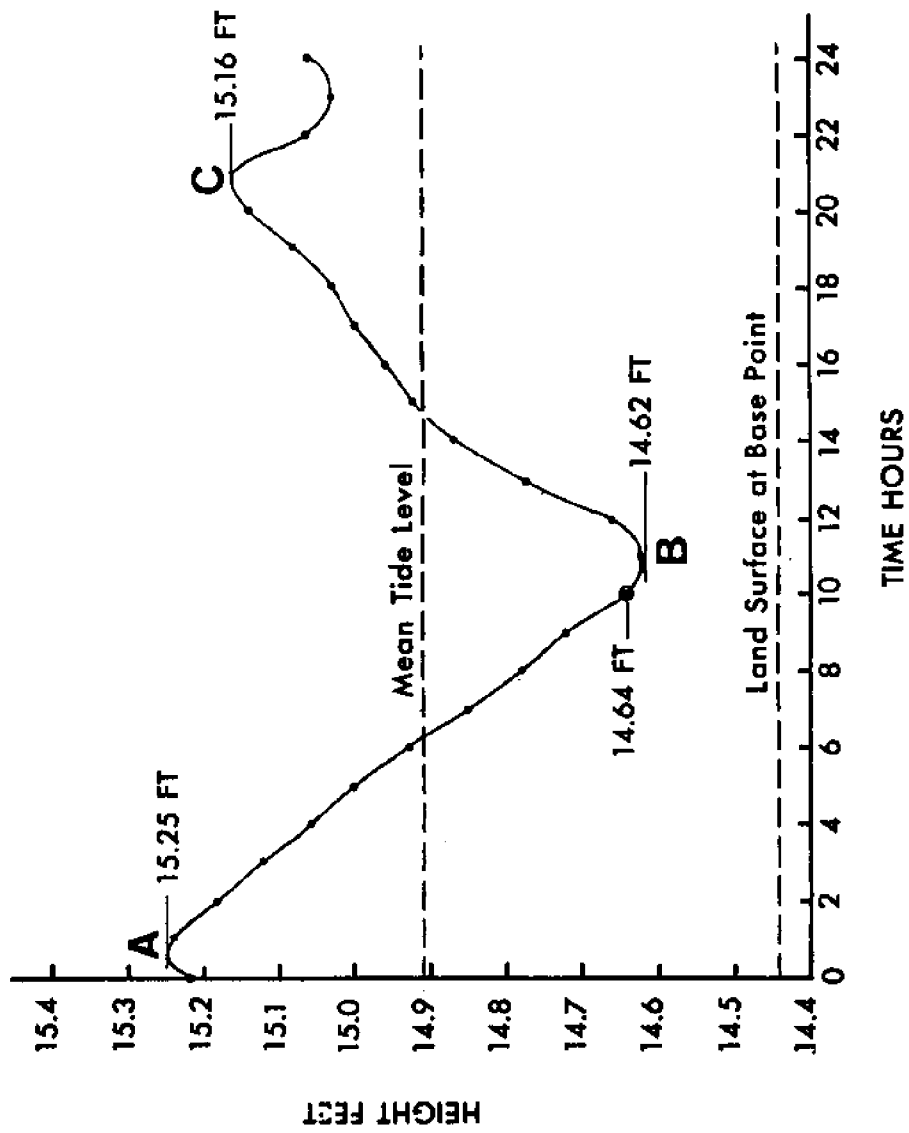
the Model Area, whose rectangular border substitutes for the real configuration of the land. Figure 1 shows the grid selected, the interval being 51.28 ft. Grid lines number from 1 to 25 in the west-east direction, and from 1 to 13 in the south-north direction. A greater density of grid lines than this is of course possible, but high resolution of the Model Area was not justified in the present case, owing to the sparsity of the topographical data.

The solid circles in Figure 1 indicate points whose elevation was measured by theodolite relative to the Base Point A situated in the lower left-hand corner of the Model Area. It can be appreciated from the scarcity of measured points that there are large areas of intervening land whose elevation is a matter of guesswork. Although one can safely predict that any inferred elevation between two widely separated datum points will not be in error by more than 0.5 feet, owing to the near-flat nature of the Louisiana salt marshes, yet small differences in elevation of the order of an inch or two may be important in determining the distribution of waters over the Model Area during the period between low and mean tide levels. However, the present study is less concerned with predictive accuracy than with demonstrating the feasibility of a mathematical technique. Consequently, the half-measured/half-guessed character of the topographical input is not considered damaging for the present purpose.

Elevations were obtained for the centers of all the grid squares in the Model Area by linear interpolation between the measured points. These are given in Table 1.<sup>2</sup> For the open boundary squares (indicated by

---

<sup>2</sup>Tables begin on p. 97.



Range AB= 0.63FEET  
 Range BC= 0.54FEET  
 Half-Period AB= 10.5 HOURS  
 Half-Period BC= 10.0 HOURS

Fig. 2. Tide gauge record near Airplane Lake for 15 October 1974.

open circles in Fig. 1) it was necessary to estimate a typical depth of the bottom of the channels below the mean water level during the period of measurement. Here again, observational thoroughness was neglected in the interest of convenience. A constant channel depth of 1.5 ft. was assumed. It is now necessary to relate the measured elevations (or essentially the Base Point) to the mean tide level on the day for which computations are to be carried out.

Figure 2 shows the tide gauge record for 15 October 1974, obtained at a station some hundreds of yards from the Model Area. This station is a permanent installation; and whereas in a predictive study an in situ tide gauge would be desirable (if possible several), in the present case the remote reading was judged sufficient.

The curve shows two maxima and one minimum yielding two values for the tidal range on 15 October, namely 0.63 and 0.54 feet. Likewise two "half-period" magnitudes are obtained, which are 10.5 and 10.0 hours. The following tidal constants were selected for the model

$$\begin{aligned} \text{Amplitude} &= 0.3 \text{ ft.} \\ \text{Period} &= 20.0 \text{ hrs.} \end{aligned}$$

Thus the tide was idealized to a pure sinusoid with the above parameters.

Now, at 1000 hours on 15 October it was estimated that the land surface at the Base Point lay approximately 0.2 ft. below the water surface at the Base Point. Consequently, the land surface at the Base Point should be drawn at  $Y_{BP} = 14.44$  ft. in Figure 2. The mean tide level ( $Y_{MT}$ ) was estimated from the formula

$$Y_{MT} = \left[ \frac{(Y_A + Y_B)}{2} + \frac{(Y_B + Y_C)}{2} \right] / 2$$

where  $Y_A$ ,  $Y_B$ ,  $Y_C$  are the ordinates of points A, B, and C in Figure 2. One could of course have used some other formula, such as finding the

first moment of the figure, considered as an area, about the time axis. But such elaboration is not necessary here.

With the above formula for  $Y_{MT}$  we find that  $Y_{MT} = 14.91$  ft. Hence, the correction to be made to the measured elevations to relate them to mean tide level is

$$C = Y_{MT} - Y_{BP} = 0.47 \text{ ft.}$$

Let us adopt the convention that depths below the mean tide level are positive, and "depths" above it are negative. The symbol  $h$  is used to represent the topographical depth relative to mean tide level. Let  $E$  stand for the topographical elevation relative to the Base Point. Then clearly,

$$h = -(E-C) \tag{1}$$

Equation 1 shows the manner in which the corrections are to be made.

A glance at Figure 2 reveals that the Base Point will always be covered by water since the tidal minimum occurs 0.18 ft. above it. Inspection of Table 1 shows, moreover, that the whole Model Area will always be under water since the maximum elevation relative to the Base Point is only 0.04 ft. It appears then that a day of exceptionally high mean tide level had been chosen to make the measurements. From the point of view of modeling, such a high mean tide level is not advantageous. The decision was made therefore to reposition the mean tide level relative to the marsh. It was desired that at mean tide at least some of the marsh should be above water. The new correction increment chosen was

$$C = -0.2 \text{ ft.}$$

Applying this correction to the elevations in Table 1 in the manner of equation 1, and correcting also the open boundary depths, we derive an

h-table (Table 2); and from this table it is possible to derive what is here called a "symbolic depth matrix." The latter matrix contains as elements the numbers -1, 1, 0, and 2, each element corresponding to a grid square. The assignment of element values proceeds on the following basis:

- 1 -- open boundary square
- 1 -- square under water, not open boundary
- 0 -- dry square
- 2 -- square outside computation field

Thus if, at the start of the model we assume that the water level is constant everywhere that water exists and equal to the mean tide level, and that all topographical depressions below the mean tide level contain water, then we obtain the symbolic depth matrix shown in Table 2.

Clearly, there is a wet zone in the northeast of the Model Area and another smaller one in the midsouth. These starting conditions will provide a more interesting and technically significant model history as the tide goes through its cycles than will a direct application of the curve in Figure 1.

#### 1. Equations and Solution Method

The two-dimensional, vertically averaged equations governing a homogeneous hydrodynamic system in which Coriolis forces and wind stresses are present may be written (Hansen 1956; Leendertse 1967):

$$\begin{aligned}
 \frac{\partial \zeta}{\partial t} + \frac{\partial HU}{\partial x} + \frac{\partial HV}{\partial y} &= 0 \\
 \frac{\partial U}{\partial t} + U \frac{\partial U}{\partial x} + V \frac{\partial U}{\partial y} - fV + g \frac{\partial \zeta}{\partial x} + g \frac{U \sqrt{U^2+V^2}}{HC^2} - \frac{\tau_x^s}{\rho H} &= 0 \\
 \frac{\partial V}{\partial t} + U \frac{\partial V}{\partial x} + V \frac{\partial V}{\partial y} + fU + g \frac{\partial \zeta}{\partial y} + g \frac{V \sqrt{U^2+V^2}}{HC^2} - \frac{\tau_y^s}{\rho H} &= 0
 \end{aligned}
 \tag{2}$$

where the symbols have the following meanings:

- $\zeta$  -- water level above a given horizontal reference plane (in this case mean tide level)  
H -- depth of water above the bottom (=  $h + \zeta$ , where  $h$  is as defined earlier)  
U,V -- vertically averaged x- and y- components respectively, on the horizontal velocity component  
f -- Coriolis parameter (=  $2 \Omega \sin\phi$ , where  $\Omega$  is the earth's angular velocity, and  $\phi$  is the latitude. For  $29^{\circ}18' N$ , the mean latitude of Barataria Bay,  $f = 0.712 \times 10^{-4}$  rad/sec)  
g -- acceleration due to gravity  
C -- function used to compute the bottom stress. According to the Chezy-Manning formula:

$$C = \frac{1.486H^{1/6}}{n}$$

where  $n$  is a constant that has the approximate value 0.026 for estuarine bottoms (Hacker, Pike, and Wilkins 1973)

- $\tau_x^s, \tau_y^s$  -- x and y components respectively of the wind or surface stress.

Implicit in the derivation of equations 2 are the following assumptions:

- 1) There is negligible variation of the horizontal velocity component from top to bottom of the fluid layer.
- 2) The vertical velocity component is negligible.
- 3) There is negligible vertical shear due to horizontal velocity gradients.
- 4) There are negligible pressure and buoyancy effects due to small variations in the density.

Assumptions 1 and 3 remain to be validated by computational experience with the model, backed by observations of water level in different places as a function of time.

Assumptions 2 and 4 are expected to be valid for well mixed estuarine waters flowing over mud flats.

Equations 2 must be expressed in finite difference form for the purpose of achieving a numerical solution. In Part 1 some numerical experiments together with other considerations led to the choice of the

following finite difference equations as appropriate "implicit" approximations to 2:

$$\begin{aligned}
& \frac{(\zeta_{i,j}^{n+1} - \zeta_{i,j}^n)}{\Delta t} + \frac{(\bar{H}_{u_{i+1,j}}^n U_{i+1,j}^{n+1} - \bar{H}_{u_{i,j}}^n U_{i,j}^{n+1})}{\Delta x} + \frac{(\bar{H}_{v_{i,j+1}}^n V_{i,j+1}^n - \bar{H}_{v_{i,j}}^n V_{i,j}^n)}{\Delta y} = 0 \\
& \frac{(U_{i,j}^{n+1} - U_{i,j}^n)}{\Delta t} + U_{i,j}^{n+1} \frac{(U_{i+1,j}^n - U_{i-1,j}^n)}{2\Delta x} + V_{i,j}^{*n} \frac{(U_{i,j+1}^n - U_{i,j-1}^n)}{2\Delta y} - fV_{i,j}^{*n} + \\
& \frac{g}{\Delta x} \left[ \frac{(\zeta_{i,j}^{n+1} + \zeta_{i,j}^n)}{2} - \frac{(\zeta_{i-1,j}^{n+1} + \zeta_{i-1,j}^n)}{2} \right] + g \frac{(U_{i,j}^{n+1} + U_{i,j}^n)}{2} \left[ (U_{i,j}^n)^2 + \right. \\
& \left. (V_{i,j}^{*n})^2 \right]^{1/2} / \bar{H}_{u_{i,j}}^n (\bar{C}_{u_{i,j}}^n)^2 - \tau_x^s / \rho \bar{H}_{u_{i,j}}^n = 0 \\
& \frac{(V_{i,j}^{n+2} - V_{i,j}^{n+1})}{\Delta t} + U_{i,j}^{*n+1} \frac{(V_{i+1,j}^{n+1} - V_{i-1,j}^{n+1})}{2\Delta x} + V_{i,j}^{n+2} \frac{(V_{i,j+1}^{n+1} - V_{i,j-1}^{n+1})}{2\Delta y} + fU_{i,j}^{*n+1} + \\
& \frac{g}{\Delta y} \left[ \frac{(\zeta_{i,j}^{n+2} + \zeta_{i,j}^{n+1})}{2} - \frac{(\zeta_{i,j-1}^{n+2} + \zeta_{i,j-1}^{n+1})}{2} \right] + g \frac{(V_{i,j}^{n+2} + V_{i,j}^{n+1})}{2} \left[ (U_{i,j}^{*n+1})^2 + \right. \\
& \left. (V_{i,j}^{n+1})^2 \right]^{1/2} / \bar{H}_{v_{i,j}}^{n+1} (\bar{C}_{v_{i,j}}^{n+1})^2 - \tau_y^s / \rho \bar{H}_{v_{i,j}}^{n+1} = 0
\end{aligned} \tag{3a}$$

The superscript n denotes time level t. Thus  $t = n\Delta t$ .

Equations 3a are similar in form to the implicit equations of Leendertse (Leendertse and Gritton 1971), with the exception that only two layers in time are considered (n, n+1) instead of three (n-1, n, n+1). The restriction of two layers did not, in the case of a two-dimensional test model with bottom friction and forcing function, lead to results that were significantly different from those obtained with a three-layer scheme. Consequently, the two-layer scheme seemed to show a better relationship of computer storage requirement to solution accuracy than the other. But more important, the elimination of the lower time level allows a more natural treatment of the moving boundary problem. A

grid square that was dry at time level  $n-1$  (but is now wet at time level  $n$ ) poses a difficulty in that  $\zeta^{n-1}$  for that square is not defined. The grid scheme corresponding to equations 3a is shown in Figure 3.

In Leendertse's initial work (1967) an Alternating Directions Implicit-Explicit method of solution was employed. It would be advantages however, in terms of computational effort, if the two explicit steps could be avoided.

Part 1 showed that the phase and amplitude distortion introduced into a tidal solution of period 12 hours by omission of the two explicit steps, can be expected to be small if  $\Delta t$  is less than 2 minutes and also less than the Friedrich/Lewy/Courant limit  $\Delta s / \sqrt{2gh_{\max}}$ , for stability of an explicit technique.

In the present model  $\Delta s$  ( $= \Delta x = \Delta y$ ) = 51.28 ft.,  $h_{\max} = 1.3$  ft., and so

$$\sqrt{2gh_{\max}} = 5.6 \text{ secs.}$$

With a time step of order 5 seconds and a tidal period equal to 20 hours, it is highly likely that the difference between the solutions obtained with a pure implicit method and a mixed implicit-explicit method, will be negligible. Accordingly, it was decided to begin the computations using the following strategy:

- 1) Solve the equation of continuity and the U-equation of motion together implicitly along rows at time level  $n$  to yield  $\zeta^{n-1}$  and  $U^{n+1}$  all over the wet computation field.
- 2) Equate  $V^{n+1}$  with  $V^n$  for all wet squares.
- 3) Solve the equation of continuity and the V-equation of motion together implicitly along columns at time level  $n+1$  to yield  $\zeta^{n+2}$  and  $V^{n+2}$  all over the wet computation field.



4) Equate  $U^{n+2}$  with  $U^{n+1}$  for all wet squares.

This procedure is repeated for each succeeding pair of time steps.

Steps 2 and 4 replace the explicit steps of Leendertse's method.

In terms of the present grid scheme, the relevant "explicit" equations are:

$$\begin{aligned}
 & \frac{(v_{i,j}^{n+1} - v_{i,j}^n)}{\Delta t} + U_{i,j}^{*n+1} \frac{(v_{i+1,j}^n - v_{i-1,j}^n)}{2\Delta x} + v_{i,j}^{n+1} \frac{(v_{i,j+1}^n - v_{i,j-1}^n)}{2\Delta y} + \\
 & fU_{i,j}^{*n+1} + \frac{g}{\Delta y} \left[ \frac{(\zeta_{i,j}^{n+1} + \zeta_{i,j}^n)}{2} - \frac{(\zeta_{i,j-1}^{n+1} + \zeta_{i,j-1}^n)}{2} \right] + g v_{i,j}^{n+1} \left[ (U_{i,j}^{*n+1})^2 + \right. \\
 & \left. (v_{i,j}^n)^2 \right]^{1/2} / \bar{H}_{v_{i,j}}^{n+1} (\bar{C}_{v_{i,j}}^{n+1})^2 - \tau_y^s / \rho \bar{H}_{i,j}^{n+1} = 0 \\
 & \frac{(U_{i,j}^{n+2} - U_{i,j}^{n+1})}{\Delta t} + U_{i,j}^{n+2} \frac{(U_{i+1,j}^{n+1} - U_{i-1,j}^{n+1})}{2\Delta x} + v_{i,j}^{*n+2} \frac{(U_{i,j+1}^{n+1} - U_{i,j-1}^{n+1})}{2\Delta y} - \\
 & f v_{i,j}^{*n+2} + \frac{g}{\Delta x} \left[ \frac{(\zeta_{i,j}^{n+2} + \zeta_{i,j}^{n+1})}{2} - \frac{(\zeta_{i-1,j}^{n+2} + \zeta_{i-1,j}^{n+1})}{2} \right] + g U_{i,j}^{n+2} \left[ (U_{i,j}^{n+1})^2 + \right. \\
 & \left. (v_{i,j}^{*n+2})^2 \right]^{1/2} / \bar{H}_{u_{i,j}}^{n+2} (\bar{C}_{u_{i,j}}^{n+2})^2 - \tau_x^s / \rho \bar{H}_{i,j}^{n+2} = 0
 \end{aligned} \tag{3b}$$

Although 2 and 4 above are still explicit in form, no use is made of the hydrodynamic equations to calculate  $v^{n+1}$  and  $U^{n+2}$ ; consequently, the method will be regarded as purely implicit, and the term "explicit step" reserved for the case that the hydrodynamic equations are utilized.

For details of the implicit method itself, reference can be made to Part 1. Here it suffices to say that two boundary conditions are required, one at each end of a row or column of the grid. The four possible combinations are:

- i) Open-Closed
- ii) Closed-Open
- iii) Open-Open
- iv) Closed-Closed

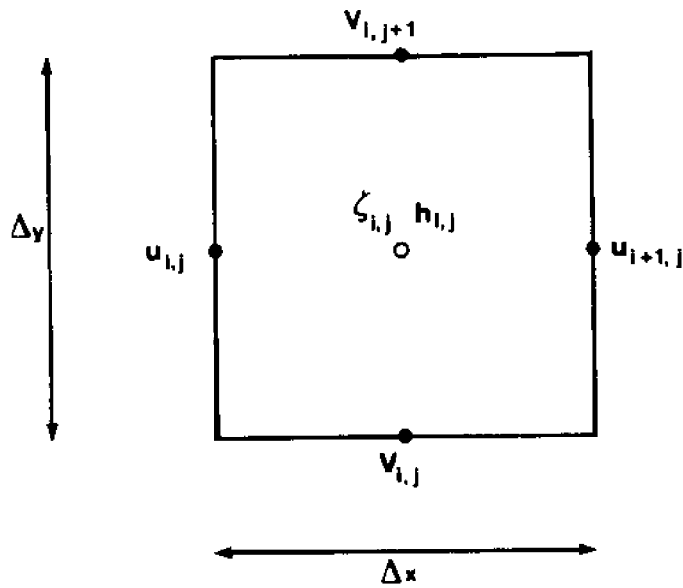


Fig. 3. Grid scheme used to achieve a solution of Equations 2.

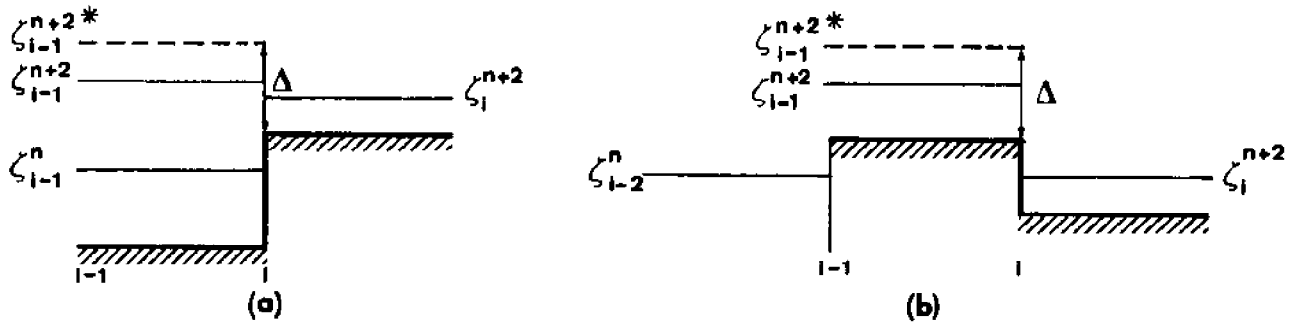


Fig. 4. (a) Topographical upstep and (b) topographical downstep.

In the case of an open boundary,  $\zeta$  is given; in the case of a closed boundary U or V is given depending on whether the vector of unknowns lies along a row or column respectively. When U or V is given they have the value zero.

## 2. The Moving Boundary Problem

Here we come to a part of the solution technique that assumes a special importance for the class of problem dealt with in this study, that is, flow over small scale, highly irregular topographical fields whose features may become alternately wet and dry. A full discussion of the method by which the extension of the boundary closed by the rising water level was calculated is given in Part 1. A summary of the salient features is presented here.

The new wet boundary is determined after every successive pair of time steps. Figure 4(a) and (b) show the two topographical situations that can arise, referred to as the "upstep" and "downstep" situations. Vertical grid sections in the x-z plane are shown by way of example.

In the upstep situation, water from "square"  $i-1$  floods onto the higher square  $i$ . In the downstep situation, the water from square  $i-2$  first floods over an upstep  $i-1$  and then onto a lower square  $i$ . Hence, Figure 4(b) corresponds to a levee situation. The condition for flooding in both cases is that  $\zeta_{i-1}^{n+2*}$ , which is the computed level in square  $i-1$  prior to allowing any movement of the closed boundary from  $i$  to  $i+1$ , exceeds the level of the dry land surface in square  $i$ .

The volume of water transferred in both cases is estimated from a hydraulic formula developed by engineers to calculate weir flows (cf. Giles 1962). It states that

$$Q = mW^{3/2} \tag{4}$$

where  $Q$  is the volume flow per second per unit width of weir,  $W$  is the weir height, and  $m$  is an empirical constant. In the Francis formula, of which 4 is the limiting case when  $V^2/2g \ll W$ , where  $V$  is the velocity of approach to the weir,  $m$  has the value  $3.33 \text{ ft}^{1/2}/\text{sec}$ ; and this is the value adopted for the present study.

From averaging considerations, the volume transferred in time  $2\Delta t$  from square  $i-1$  to square  $i$  was estimated in Part 1 to be

$$\text{Vol}_i = 0.26 m \Delta^{3/2} \Delta t \Delta y$$

where  $\Delta$  is the excess of  $\zeta_{i-1}^{n+2*}$  over the land surface in square  $i$  for the upstep, or the excess of  $\zeta_{i-1}^{n+2*}$  over the land surface in square  $i-1$  for the downstep, and  $\Delta y$  is the dimension of a grid "square" in the  $y$ -direction. Since the "squares" have area  $\Delta x \Delta y$ , the depth of water established in square  $i$  must be

$$H_i^{n+2} = \frac{0.26 m \Delta^{3/2} \Delta t}{\Delta x} \quad (5)$$

To conserve mass, the volume of water transferred to a dry square must be subtracted from the wet field. It is convenient to make this correction to the adjacent, transferring, wet square. Let  $\zeta_{i-1}^{n+2}$  be the new depth after correction, in square  $i-1$ . Then it follows that

$$\zeta_{i-1}^{n+2} = \zeta_{i-1}^{n+2*} - H_i^{n+2}$$

Now it may happen that the following condition is fulfilled:

$$\zeta_{i-1}^{n+2} < \zeta_i^{n+2} \quad (6)$$

Clearly, this is not physically realizable. As an alternative to this condition holding, we distribute the water between  $i$  and  $i-1$  so that

$$H_i^{n+2} = \frac{1}{2} \Delta \quad (7)$$

In the case of the upstep, equation 7 means that

$$\zeta_{i-1}^{n+2} = \zeta_i^{n+2} ,$$

i.e., equal levels are established. In the case of the downstep, equation 7 is somewhat artificial. But choice of a suitably small value of  $\Delta t$  should make occurrence of the physically imaginary condition discussed here sufficiently rare as to maintain good solution accuracy.

Very often flooding can occur from more than one direction at once. In the context of the finite difference grid we have to consider the possibility of flooding of dry square  $i$  from each of the squares  $(i-1,j)$ ,  $(i+1,j)$ ,  $(i,j-1)$  and  $(i,j+1)$ . Thus at the same time step  $\Delta t$  we must test for flooding of square  $i$  from each of the four directions and apply formula 5 in cumulative fashion if necessary. By this is meant that a running total  $H_i^{n+2'}$  must be kept, composed of the sum of the individual  $H_i^{n+2'}$ 's contributed by the adjacent flooding squares already considered.

Before each addition to  $H_i^{n+2'}$  a test must be made, however. This test has to do with the fact that additional flooding cannot occur by formula 5 if the depth of water already established is such as to impede the weir flow. Define a quantity  $\delta_i^{n+2'}$  as the amount by which the interim level in  $i$  exceeds the land surface in the next square whose flooding contribution is to be considered. Clearly, if for this square

$$\delta_i^{n+2'} \ll \Delta$$

then we may safely apply formula 5. It was decided to adopt a criterion

$$\delta_i^{n+2'} \leq F_c \Delta, \quad 0 < F_c < 1 \quad (8)$$

for calculating a successive flooding contribution. If condition 8 isn't met, with some choice of  $F_c$ , then the level in the flooded square currently reached by the addition of the previous flooding contributions

is taken as the final level. Again, suitable choice of  $\Delta t$  for given  $\Delta x$  or  $\Delta y$  should render this premature halt unlikely. But if it occurs, then we may expect the insufficiency in the new water level (in square  $i$ ) to be gradually eliminated over the next few time steps as a result of the successive application of the equation of continuity to the new wet field. The same remark applies to single-square flooding where equation 7 has to be used.

The flooding procedure is applied, where necessary, in a chain manner. It may happen that a newly flooded square is capable of flooding the next square, and so on. There will be a cumulative error in this chain procedure, which can only be kept small in the case of a potentially long chain, by reducing the number of links. This reduction may be affected by reducing  $\Delta t$ , so that the volume transferred in the first step is small.

It should be noted that when flooding of dry squares occurs from the open boundary, it is not necessary to make any correction of volume to the open boundary squares, for the latter represent in effect an infinite source. Consequently, the open boundary squares in the printed tables of  $\zeta$  always show  $\zeta$ - values equal to those of the imposed tide.

In the present implementation of the flooding calculations, the new wet boundary was sought for after every successive pair of time steps. That is, the field equations were solved for two time steps as outlined in Section 2; then every dry square was examined for potential flooding, and adjustments of the wet field boundary were carried out where appropriate; next, the field equations were solved again for the next two time steps, and so on.

Word must be said finally about the way in which the temporarily

closed and open segment of the model boundary was handled. Inspection of Table 2 will show that grid squares (11,12), (12,12)...(17,12) must become alternately wet and dry as the tide evolves. When these squares are dry they constitute a closed boundary, and when they are wet, the boundary is of course open. It is necessary then to take cognizance of the moment when such a boundary square as those enumerated becomes flooded from the interior of the model, after having been dry. At that moment it is assumed that the proper water level in the square concerned is equal to the open boundary tidal level at the same instant. The  $\zeta$ -value is therefore adjusted accordingly. When, however, the neighboring tide drops so far that a boundary square becomes dry, then that square simply vanishes from the computation field.

A dilemma arises if a boundary square becomes dry at the time level for which its  $\zeta$ -value is required as part of the solution along a column. Letting  $n+2$  be that time level, then the problem referred to arises when at time level  $n+1$  the boundary is open, and at time level  $n+2$  it is closed. Which boundary condition do we use? It is likely that for small enough  $\Delta t$ , either condition will yield similar results in the interior of the wet field. However, it was decided to make sure of this by computing the model in both ways, i.e., with the boundary square still considered as open at the final time level--albeit with a negative depth--and with the boundary square considered to be dry during the whole of the time step, and therefore removed from the computation field.

### 3. Results for the Implicit Method

Before referring to the tables of results (p. 97 ff) it is necessary to mention an important modification of the computational theory that was made because of the presence of round-off error.

After the computation of a new depth  $H_{i,j}$  in the subroutine that computes the movement of the wet boundary due to flooding of dry squares, the following criteria were applied:

$$\begin{aligned} H_{i,j} \leq H_c = .001 \text{ ft} & \quad \text{No flooding; square remains} \\ & \quad \text{dry} \\ H_{i,j} > H_c & \quad \text{Flooding occurs} \end{aligned} \tag{9}$$

Hence, minuscule depths were ignored for the purposes of computing the new wet boundary. The logical criteria

$$\begin{aligned} H_{i,j} \leq 0 & \quad \text{No flooding} \\ H_{i,j} > 0 & \quad \text{Flooding} \end{aligned}$$

were found to be computationally unworkable. The reason for this is that the water level  $\zeta_{ij}$  must be computed immediately afterwards from the formula

$$\zeta_{ij} = H_{i,j} - h_{i,j} \quad , \tag{10}$$

and if  $H_{i,j}$  is so small as to be essentially unrepresentable in the fixed-point format X.XXX... where the X's are decimal digits, then the results of the subtraction in equation 10 will be

$$\zeta_{i,j} = -h_{i,j}$$

and consequently when  $H_{i,j}$  is reconstituted in the main program from the equation

$$H_{i,j} = \zeta_{i,j} + h_{i,j}$$

we will obtain

$$H_{i,j} = 0 \quad ,$$

an exact zero. This exact zero must certainly lead to trouble when



the logarithm of  $H_{i,j}$  is required, as in the calculation of the Chezy-Manning friction function  $C$ .

For consistency, a similar artificial criterion was applied to the test for dry squares after solving along a row or column using the field equations. Logically, a square  $i,j$  will become dry when

$$\zeta_{i,j} \leq -h_{i,j}$$

However, this condition was changed to

$$\zeta_{i,j} \leq -h_{i,j} + H_c \quad (11)$$

with  $H_c$  defined as in criteria 9. The use of condition 11 will certainly improve the readability or interpretation of the output, when, instead of the printed result,

$$\zeta_{i,j} = -h_{i,j}$$

which is the consequence in a case where  $\zeta_{i,j}$  actually exceeds  $-h_{i,j}$  by a negligibly small amount but suffers round-off of the rightmost digits in output, we have instead a blank or coded location, meaning that the square is dry. In most cases computed, the selected value of  $H_c$  was 0.001 ft. The difference between a truly dry area and one covered by less than 0.001 ft. of water is academic. The small depth of water that may be present when a square is removed from the computation field is of course retained in memory so as to be added back into the field when flooding occurs.

In section 2, it was stated that the Manning coefficient  $n$  has the approximate value 0.026 for estuarine bottoms. Since no value has been determined for marsh grass in flat tidal regions, it was decided to

begin with this same value of 0.026 in the present model. A working assumption like this should suffice to demonstrate the feasibility of the mathematical technique, which is all that is aimed at here.

With these preliminary remarks, we may now turn to an examination of the computations.

A number of trials of the model were made, using the solution procedure outlined on page 64, and covering a range of time steps from in excess of 1 minute to as small as 5 seconds. It soon became apparent that in order to avoid spurious oscillations along rows and columns,  $\Delta t$  had to be less than 20 seconds. In fact, solution convergence for the implicit method was obtained at  $\Delta t = 10$  secs; for with  $\Delta t = 5$  sec, the few differences in  $\zeta$  were negligible. Comparing the printed values of U and V for the 10 and 5 second cases (which were output every 2.5 hours of tidal time) there were but rare occurrences of any differences, and these were unimportant.

The spurious east-west oscillations of  $\zeta$  obtained with  $\Delta t = 20$  secs, could be clearly recognized as such, for their wavelength was twice the grid interval. Moreover, minima were so pronounced in some locations at times between mean and high water as to be negative. Oscillations in the north-south direction seemed generally to be of longer wavelength.

Table 4 shows selected output (the print-out was half-hourly) obtained with  $\Delta t = 10$  secs. There is no trace of an oscillation of  $\zeta$  across the wet area; for the water surface moves, when the entire Model Area is flooded, almost as a uniformly elevated sheet. That this behavior should be expected can be seen from consideration of the minimum shallow water wave velocity,  $\sqrt{gH}_{\min} = 2.2$  ft/sec, at high water over the most elevated marsh point, where  $H = 0.15$  ft. Clearly, with this minimum

velocity a disturbance of elevation will have propagated from one open boundary to the center of the Model Area in the north-south direction in about 2.3 minutes; and since (a) the difference in  $\zeta$ -elevation for a phase difference corresponding to 2.3 minutes is only 0.01 ft approximately, and (b) the wave velocity will be considerably higher over the depressed areas of the marsh where  $H > H_{\min}$ , we may expect the elevation differences involved to be less than 0.01 ft at any given time during the flood stage and therefore unnoticeable with two decimal place accuracy.

Returning to consideration of the effect of differing length of time step in the pure implicit solution technique, it is evident that  $\Delta t$  is quite critical in the region 10-20 seconds for the given grid spacing of approximately 51 ft. In order to test the idea that  $\Delta t/\Delta s$  is the controlling ratio in determining the presence of spurious oscillations for the implicit as well as the explicit method of solution, the case  $\Delta t = 20$  secs was recomputed, but with the grid interval doubled. Thus for this test case

$$\Delta x = \Delta y = 102.56 \text{ ft.}$$

Representative results for the first 5 hours of tidal time are shown in Table 5. Clearly, spurious oscillations are no longer present, and the  $\zeta$ - values are in fact closely similar to those of Table 4. However, the velocities in the double grid-size model are generally larger (see Figs. 5 and 6).

For the present model, the F-L-C limit on  $\Delta t/\Delta s$  is given by

$$\frac{\Delta t}{\Delta s} \leq \frac{1}{\sqrt{2 gh_{\max}}} = 0.11 \text{ sec/ft.}$$

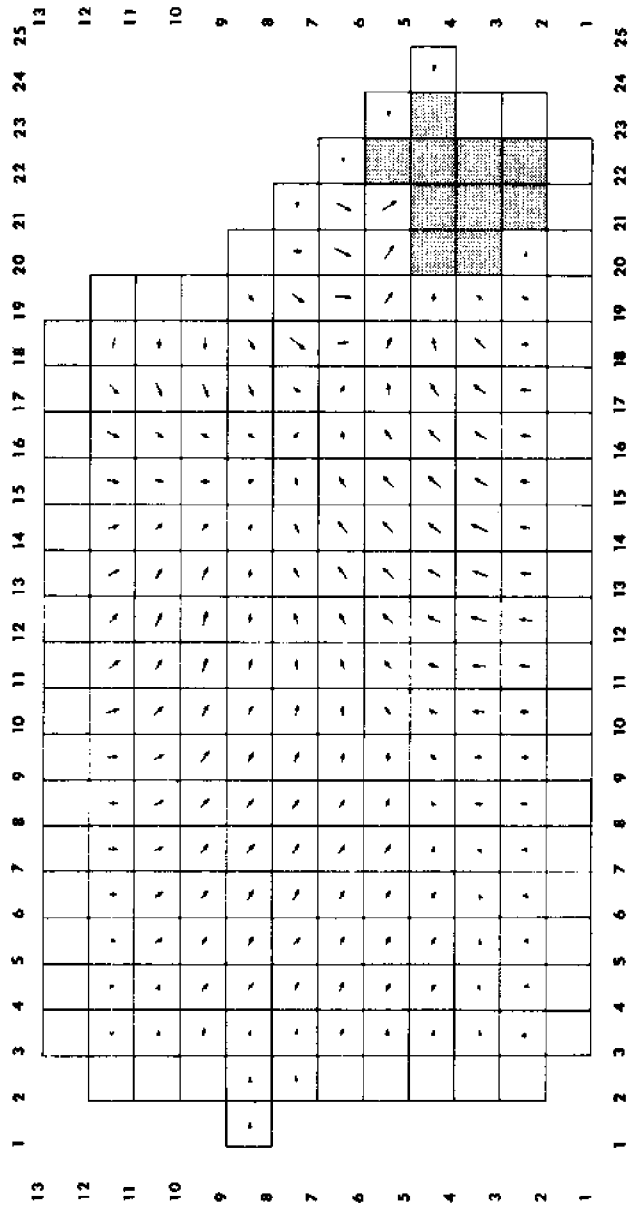


Fig. 5. Current vector diagrams for the computation of Table 4.

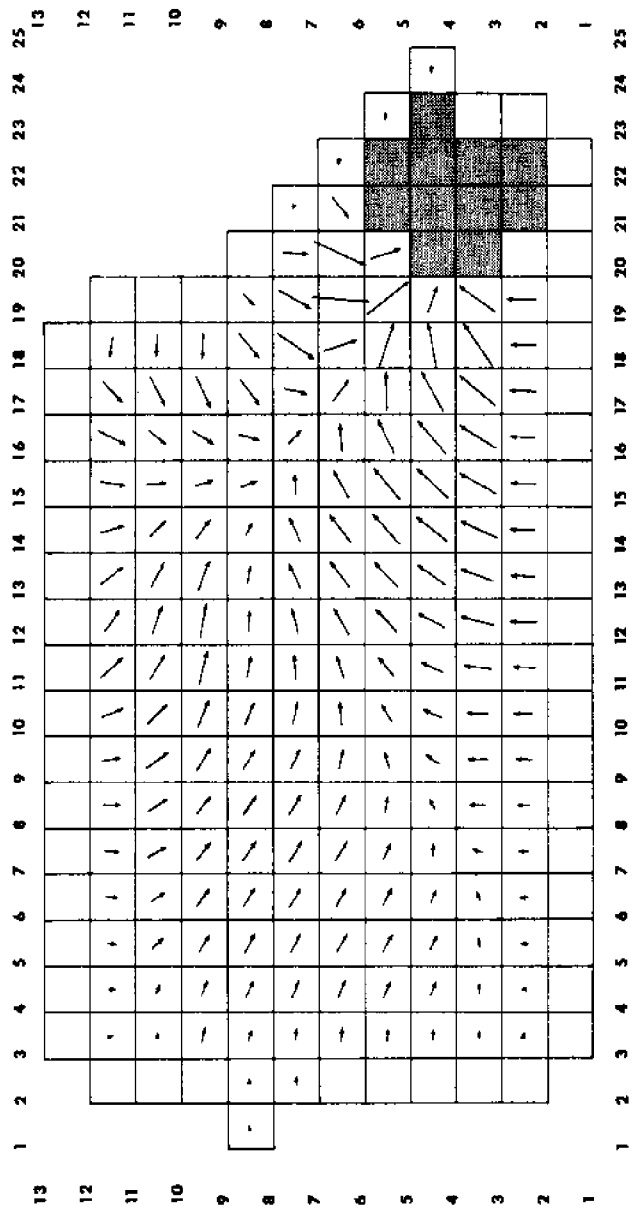


Fig. 6. Current vector diagrams for the computation of Table 5.

Hence it appears that for accurate results with the Alternating Directions Implicit method of page 64,

$$\frac{\Delta t}{\Delta s} < \frac{3.6}{\sqrt{2gh_{\max}}} = \frac{2.5}{\sqrt{gh_{\max}}}$$

One can compare this result with the finding of Sobey (1970), who showed analytically that Leendertse's Implicit-Explicit method will yield accurate results for the linear equations when  $\lambda/\Delta s$  (where  $\lambda$  is the wavelength of fluid motion) is as small as 50, provided  $\Delta t/\Delta s < 1.25/\sqrt{gh}$ . Hence the present criterion, relating to the pure implicit method, appears to be more restrictive, since  $\lambda/\Delta s \gg 50$ .<sup>3</sup>

Having obtained what appears to be a satisfactory solution using the pure implicit technique, it was decided to test the accuracy of this solution by including the explicit steps represented by equations (3b).

With  $\Delta t = 10$  secs, and other parameters as in Table 4, the Implicit-Explicit method proved unstable, with spurious oscillations manifested after 1.0 hours of tidal time.

With  $\Delta t = 5$  secs, the Implicit-Explicit method gave results virtually identical to those of Table 4 over the 10.0 hours of tidal time computed, there being six differences in  $\zeta$ , each of one unit in the second place of decimals, in the first 4.0 hours. The  $\zeta$  results with  $\Delta t = 2$  secs, computed for 4.0 hours, differed in only five values (again by one unit in the second place of decimals) from those in Table 4. Hence, the original surmise that there would be no advantage in calculating  $v^{n+1}$  and  $U^{n+2}$  with explicit steps appears to have been proven.

---

<sup>3</sup>For a linear system of equations solved in conjunction with a sinusoidal forcing function of period T, the wavelength is  $T\sqrt{gh}$ . Hence, with T = 20 hrs, h = 1.3 ft,  $\lambda \sim 467 \times 10^3$  ft.

Examination must now be made of the success of the moving boundary procedure. In the following description, all computations will refer to solutions obtained with the pure implicit technique.

We note first that the instability in the results computed with  $\Delta t \geq 20$  secs renders it impossible to detect any effect, if present, of diminishing time step upon the new boundary depths established in the dry areas. However, we can note that there is a diminishing occurrence of conditions of type 6, Section 3, as the time step is reduced. Thus, in the computation with  $\Delta t = 20$  secs,  $F_c = 0.5$ ,  $H_c = 0.001$  ft, there were 265 flood error messages of type 6 in the first 10 hours, yielding an average of approximately 1 message per 7 time steps. With  $\Delta t = 10$  secs, however (and other parameters the same) there were only 7 flood error messages in 10 hours, yielding an average of 1 message per 514 time steps. With  $\Delta t = 5$  secs, the message rate was 13 in 10 hours, or an average of approximately 1 per 554 time steps. Clearly then, even with large time steps, the flooding computation as regards the nonoccurrence of conditions of type 6 is physically meaningful.

One also wishes to know the frequency with which a multidirectional flooding procedure is aborted because of the achievement of an excessive flood depth in any initially dry square. The relevant error condition is given by the violation of condition 8 in Section 3. Messages indicating violation of condition 8 were printed out during one run of the standard case corresponding to Table 4. It was noticed that they became more frequent as tidal time increased. Between 9.0 and 9.5 hours there were 314 messages, yielding an average of approximately 2 messages per time step. It appears then that with  $\Delta t = 10$  secs, multidirectional flooding is not significantly cut off.

A word must now be said on the subject of the question raised at

end of Section 3. Two numerical cases were computed to decide whether there was a significant difference between the results obtained with a negative depth allowed in the open northern boundary at time level  $n+2$  (see p. 71) and the results obtained with no negative depth allowed. The first case (with  $(\zeta_{1,12}^{n+2} \geq -h_{1,12})$ ) has already been considered, it being the standard model of Table 4. The second case ( $\zeta_{1,12}^{n+2} \leq -h_{1,12}$ ) was computed with the same parameters as for Table 4. No difference in  $\zeta$  for the two cases over the 23 hours computed was observed. It appears then that the type of boundary condition used in row 12 is immaterial. The decision was made to compute the remaining cases studied with no restriction placed upon  $\zeta_{1,12}^{n+2}$ .

A further question remains concerning the best value of the parameter  $F_c$ , which determines the degree of multidirectional flooding that may occur in a given square. To test the sensitivity of the model to varying  $F_c$ , solutions were obtained with  $F_c = 0.2$  and  $F_c = 1.0$ , other parameters being as in Table 4. The results for the 8.5 hours and 12.0 hours computed respectively in the two cases were virtually identical to those of Table 4 in which  $F_c = 0.5$ . The few differences in  $\zeta$  observed were mostly of the type that either a zero was printed indicating a dry square in the one case, where in the other a two-decimal place number equal to  $-h$  was printed, or vice-versa. Thus condition 11 had been satisfied in the instance of a zero being printed, but not when the  $\zeta$ -value printed was equal to  $-h$  for the square concerned. Consequently, the indicated difference of  $\zeta$  must be less than 0.005 ft. From these results it may be assumed that the choice of  $F_c$  is not critical.

Returning to a discussion of the results in Table 4 obtained with  $\Delta t = 10$  secs, it will be seen that  $\zeta$ -values are only given for a little over one tidal cycle of 20.0 hours. The second tidal cycle yielded



results similar to the first, with but minor differences in a few locations during the flood stage. There is thus a rapid achievement of cyclic equilibrium using such a short time step. Shaded areas in Table 4 indicate dry parts of the grid, or at least parts that are "dry" within the limit of  $H_c = 0.001$  ft. But where a water level has been printed within a shaded square, this indicates that the level, to two-place precision, equals  $-h$ . Consequently, in these locations the local water depth exceeds  $H_c$ , but by such a small amount as to be insignificant.

With every computation of the model, there were also output at 2.5 hour intervals, the U and V components of velocity. Inspection of U and V at 2.5 hours and 22.5 hours showed that the start-up error consequent on setting  $U=V=0$  everywhere in the wet field at time zero (when  $\zeta = 0$ ), had become essentially eliminated at 2.5 hours, since there was good agreement between the velocity fields at both times, one tidal cycle apart.

Current vector diagrams were plotted by the computer for the cases of Tables 4 and 5. These are shown in Figures 5 and 6 respectively. In both figures, velocity vectors were eliminated from squares in which a thin film of water remained after the square had become hydrodynamically isolated from the source. By the expression "hydrodynamically isolated" is meant that the water surface in a square is discontinuous with the water surface in adjacent squares (if such surface is defined), owing to the land surface in the square concerned being above the water surface in one or more adjacent squares. In this case, spurious values of the velocity components may be generated by applying the field equations.

Velocity components were less than 0.1 ft/sec.

Comparing the vector diagram for the double size grid at 2.5 hours (Fig. 6) with that for the same time in Figure 5, shows at once that the current magnitudes are greater for the former model.

#### 4. Results Using Leendertse's Implicit Scheme

In Section 2 allusion was made to the implicit equations of Leendertse (Leendertse and Gritton 1971), which used three layers in time:  $n-1$ ,  $n$ , and  $n+1$  for the solution at time level  $n+1$ . Part 1 has shown that in a simple two-dimensional model with rectangular boundaries, open at one side, the use of Leendertse's three-layer scheme affords a much larger time step than is possible using the implicit-explicit two-layer scheme already described. If the time step of a given model is small enough compared to the tidal period so that the implicit two-layer scheme can give accurate results, the question then exists as to whether an implicit three-layer scheme will prove to be temporally more advantageous. To answer this question in the present instance, it was decided to recompute the results using the following finite-difference equations:

$$\begin{aligned}
 & \frac{(\zeta_{i,j}^{n+1} - \zeta_{i,j}^n)}{\Delta t} + \frac{(\bar{H}_{u_{i+1,j}}^n U_{i+1,j}^{n+1} - \bar{H}_{u_{i,j}}^n U_{i,j}^{n+1})}{\Delta x} \\
 & \frac{(\bar{H}_{v_{i,j+1}}^n V_{i,j+1}^n - \bar{H}_{u_{i,j}}^n V_{i,j}^n)}{\Delta y} = 0 \\
 & \frac{(U_{i,j}^{n+1} - U_{i,j}^{n-1})}{2\Delta t} + U_{i,j}^{n+1} \frac{(U_{i+1,j}^{n-1} - U_{i-1,j}^{n-1})}{2\Delta x} + V_{i,j}^{*n} \frac{(U_{i,j+1}^{n-1} - U_{i,j-1}^{n-1})}{2\Delta y} - \\
 & fV_{i,j}^{*n} + \frac{g}{\Delta x} \left[ \frac{(\zeta_{i,j}^{n+1} + \zeta_{i,j}^{n-1})}{2} - \frac{(\zeta_{i-1,j}^{n+1} + \zeta_{i-1,j}^{n-1})}{2} \right] + g \frac{(U_{i,j}^{n+1} + U_{i,j}^{n-1})}{2} \\
 & \left[ (U_{i,j}^{n-1})^2 + (V_{i,j}^{*n})^2 \right]^{1/2} / \bar{H}_{u_{i,j}}^n (\bar{C}_{u_{i,j}}^n)^2 = 0
 \end{aligned} \tag{12}$$

$$\begin{aligned}
& \frac{(\zeta_{i,j}^{n+2} - \zeta_{i,j}^{n+1})}{\Delta t} + \frac{(\bar{H}_{u_{i+1,j}}^{n+1} U_{i+1,j}^{n+1} - \bar{H}_{u_{i,j}}^{n+1} U_{i,j}^{n+1})}{\Delta x} + \\
& \frac{(\bar{H}_{v_{i,j+1}}^{n+1} v_{i,j+1}^{n+2} - \bar{H}_{v_{i,j}}^{n+1} v_{i,j}^{n+2})}{\Delta y} = 0 \\
& \frac{(v_{i,j}^{n+2} - v_{i,j}^n)}{2\Delta t} + U_{i,j}^{n+1} \frac{(v_{i+1,j}^n - v_{i-1,j}^n)}{2\Delta x} + v_{i,j}^{n+2} \frac{(v_{i,j+1}^n - v_{i,j-1}^n)}{2\Delta y} + \\
& fU_{i,j}^{n+1} + \frac{g}{\Delta y} \left[ \frac{(\zeta_{i,j}^{n+2} + \zeta_{i,j}^n)}{2} - \frac{(\zeta_{i,j-1}^{n+2} + \zeta_{i,j-1}^n)}{2} \right] + g \frac{(v_{i,j}^{n+2} + v_{i,j}^n)}{2} \\
& \left[ (U_{i,j}^{n+1})^2 + (v_{i,j}^n)^2 \right]^{1/2} / \bar{H}_{v_{i,j}}^{n+1} (\bar{C}_{v_{i,j}}^{n+1})^2 = 0
\end{aligned}$$

It will be observed that in the above solution scheme neither  $U^n$  nor  $v^{n+1}$  is determined. In order to obtain contemporaneous components  $U^n$  and  $v^n$  of the velocity field, the following strategy was adopted: Write

$$U_{i,j}^n = \frac{U_{i,j}^{n-1} + U_{i,j}^{n+1}}{2} \quad (13)$$

For a small enough time step, equation 13 should obviate the necessity of determining  $U^n$  explicitly from the U-equation of motion.

The use of equations 12 implies some error when a square which is now wet at time level  $n$  was dry at time level  $n-1$ . For then  $\zeta^{n-1}$  for that square is not defined. This problem was mentioned in the discussion of Section 2, and was one of the factors leading to the initial choice of a two-layer solution scheme in time. Moreover, the time derivative of  $U$  centered at time level  $n$ , which involves the difference  $(U^{n+1} - U^{n-1})$  is likely to be in error if for part of the interval  $(n-1, n+1)$  the square concerned was dry.

The definition of  $U_{i,j}^{n-1}$  for a square  $i,j$  dry at time level  $n-1$ , which has a wet square  $i-1,j$  adjacent to it, poses no problem; we have simply

$U_{i,j}^{n-1} = 0$ . If however, both squares  $i,j$  and  $i-1, j$  are dry at time level  $n-1$ , the  $U_{i,j}^{n-1}$  is not defined, for no water exists at the position of  $U_{i,j}^{n-1}$ . The simplest recourse is to assume again that  $U_{i,j}^{n-1} = 0$ .

In the case of deciding what to use for  $\zeta_{i,j}^{n-1}$ , when it is undefined, the simplest strategy is to write

$$\zeta_{i,j}^{n-1} = -h_{i,j} ;$$

then the depth of water in the dry square at time level  $n-1$  will be appropriately defined as zero.

The effect of assuming  $U^{n-1} = 0$  as regards the calculation of  $\partial U / \partial t$  at time level  $n$ , can be appreciated from the schematic diagram Figure 7(a); and the effect of assuming  $\zeta^{n-1} = -h$  in the calculation of  $\partial \zeta / \partial x$  at time level  $n$  can be appreciated from the schematic diagram Figure 7(b). (Note that the error that would be introduced into the calculation of  $\partial \zeta / \partial t$  at time level  $n$  if  $\zeta^{n-1}$  were to be used in the derivative, is avoided in the first of equations 12 by using  $\zeta^n$ .)

In both diagrams of Figure 7 the point F on the time axis denotes the instance at which a dry square  $i,j$  begins to be flooded. The velocity  $U_{i,j}$  will rise from zero at F and reach some value  $U_{i,j}^{n+1}$  at time level  $n+1$ . Similarly, the water level  $\zeta_{i,j}$  will start at the bottom surface at time point F and rise to some value  $\zeta_{i,j}^{n+1}$  at time level  $n+1$ . For convenience, linear increases have been assumed in both cases.

When  $U_{i,j}^{n-1}$  is set equal to zero in the expression  $\frac{(U_{i,j}^{n+1} - U_{i,j}^{n-1})}{2\Delta t}$  for  $(\partial U / \partial t)_{i,j}$  at time level  $n$ , we will have

$$\left(\frac{\partial U}{\partial t}\right)_{i,j}^n \equiv \frac{U_{i,j}^{n+1}}{2\Delta t} \quad (14)$$

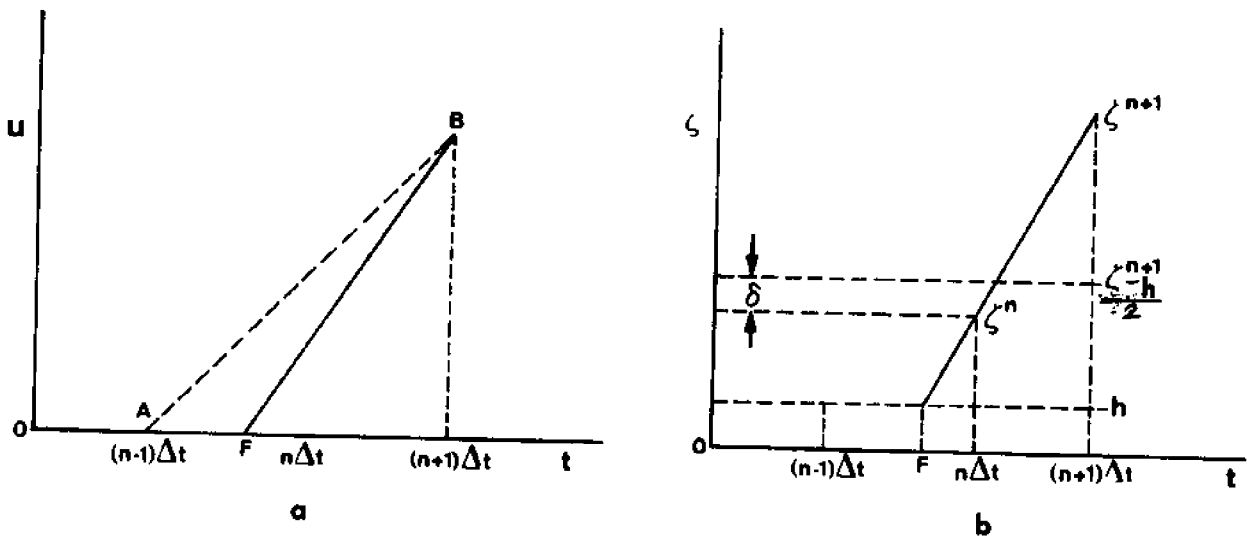


Fig. 7. (a) Schematic increase of the  $U$ -component of velocity after flooding of a dry square between time levels  $n-1$  and  $n+1$ . (b) Schematic increase of  $\zeta$  in the same square between time levels  $n-1$  and  $n+1$ .

In effect then, the ideal gradient of line FB (Fig. 7[a]) will have been replaced by the artificial gradient of line AB.

When  $\zeta_{i,j}^{n-1}$  is set equal to  $-h_{i,j}$  in the expression  $\frac{(\zeta_{i,j}^{n+1} + \zeta_{i,j}^{n-1})}{2}$  as the estimate of  $(\zeta_{i,j})^n$  for use in calculating  $(\partial \zeta / \partial x)^n$  at the position of  $U_{i,j}$ , we will have

$$(\zeta_{i,j})^n \equiv \frac{\zeta_{i,j}^{n+1} - h_{i,j}}{2} \quad (15)$$

The error is indicated as the interval  $\delta$  in Figure 7(b).

Hopefully, the use of equations 14 and 15 in solving the first two equations of 12 will not significantly affect the accuracy of the results. We do not expect errors in the convective acceleration terms consequent on setting one or more of their velocity components at time level  $n-1$  equal to zero, to have serious effect, since these terms are expected to be of second order.

Results were computed, using the above strategies, for time steps  $\Delta t = 60, 30, 20, 10,$  and  $2$  seconds, with other parameters as in Table 4. Comparing the  $\zeta$ -values obtained respectively with the first three time steps over the 23 hours of tidal time computed to those of Table 4, there were observed to be scattered differences between the former and the latter at corresponding times. These discrepancies never exceeded one unit in the second place of decimals. At  $\Delta t = 10$  seconds, many of the differences in  $\zeta$  were of the type discussed in connection with the tests of varying  $F_c$ ; i.e., the differing value printed is either a zero (indicating negligible water) or  $-h$ ; hence these differences were trivial. In the first 4.0 hours there were only nine differing values of  $\zeta$ , the discrepancy being one unit in the second place of decimals. At  $\Delta t = 2$  seconds, five differences from Table 4 were observed over the 4.5 hours

computed, all of one unit in the second place of decimals. Two differences in the first 4.0 hours were observed at the same time step on comparing  $\zeta$  with the results obtained using the Implicit-Explicit method and  $\Delta t = 2$  seconds. One may surmise from these considerations that in regard to the water levels the solution is convergent for Leendertse's Implicit scheme at  $\Delta t = 2$  seconds, and approximately so at  $\Delta t = 10$  seconds. Thus, in spite of the greater stability of the Leendertse scheme, one must still descend to approximately the same step of 10 seconds as was found to be adequate for the earlier implicit scheme studied, in order to obtain comparable accuracy of  $\zeta$ .

The situation with regard to the velocity solution is not so favorable. The velocities obtained with the Leendertse Implicit scheme would appear to require an even smaller step for comparable accuracy with those obtained by the earlier implicit scheme (to be referred to hereafter as the "Implicit scheme" without qualifier). This fact is revealed by an inspection of Tables 6, 7, and 8. In these tables the U and V components of velocity calculated using the Leendertse Implicit scheme, the Implicit scheme, and the Implicit-Explicit scheme, are given for the same time level of 2.5 hours.

One easily notices in Table 6 that certain velocity components in the upper left corner of the Model Area are large compared with those for the same locations in Tables 7 and 8. Moreover, the values in the latter two tables agree well, a fact inspiring confidence in their general validity. While a convergent solution for  $\zeta$  appears to have been approximately obtained for the Leendertse Implicit scheme at  $\Delta t = 10$  seconds, it would appear likely that local sensitivity in the velocity determination to the ratio  $\Delta s/\Delta t$ , renders this magnitude of  $\Delta t$  still too large for convergence

of the velocity solution. Looking at the form of the finite difference expressions for the time derivatives of U and V (equations 12) shows that the relevant time step here is not  $\Delta t$  but  $2\Delta t$ . Hence, as far as the velocity determination is concerned, we are dealing with a time step of 20 seconds when  $\Delta t = 10$  seconds. This is well above the Friedrich/Lewy/Courant limit of 5.6 seconds for the model (see Sec. 2).

In Figure 8 selected values of the U component are shown as found by three methods, and for various time steps. Since the Implicit and the Implicit-Explicit schemes yield identical values, to two place accuracy, at widely differing time steps (10 seconds and 2 seconds respectively), these values of U will be taken as convergent. It can then be seen that even with  $\Delta t = 2$  seconds, the Leendertse Implicit scheme has not yielded a convergent solution for U in the locations indicated. This is surprising, in that the relevant time step for the acceleration terms is a mere 4 seconds, less than the F-L-C limit.

In order to demonstrate further the likelihood of the assumption that the effect limiting the accuracy of the velocity determination is the relative magnitude of  $\Delta s/\Delta t$  as compared with the local value of  $\sqrt{gh}$ , it was decided to recompute the double-sized grid model using the Leendertse Implicit scheme. With  $\Delta t = 10$  seconds, the latter scheme showed seven differences of  $\zeta$  (not exceeding one unit in the second place of decimals) from those of the Implicit scheme ( $\Delta t = 20$  seconds) in the 5 hours computed. With  $\Delta t = 2$  seconds, the differences (again not exceeding one unit in the second place of decimals) were reduced to five in the 5 hours computed. Hence the  $\zeta$ -solution can be regarded as approximately convergent. Figure 9, similar to Figure 8, shows that U, when  $\Delta t = 2$  seconds, while not convergent in the locations indicated, does agree



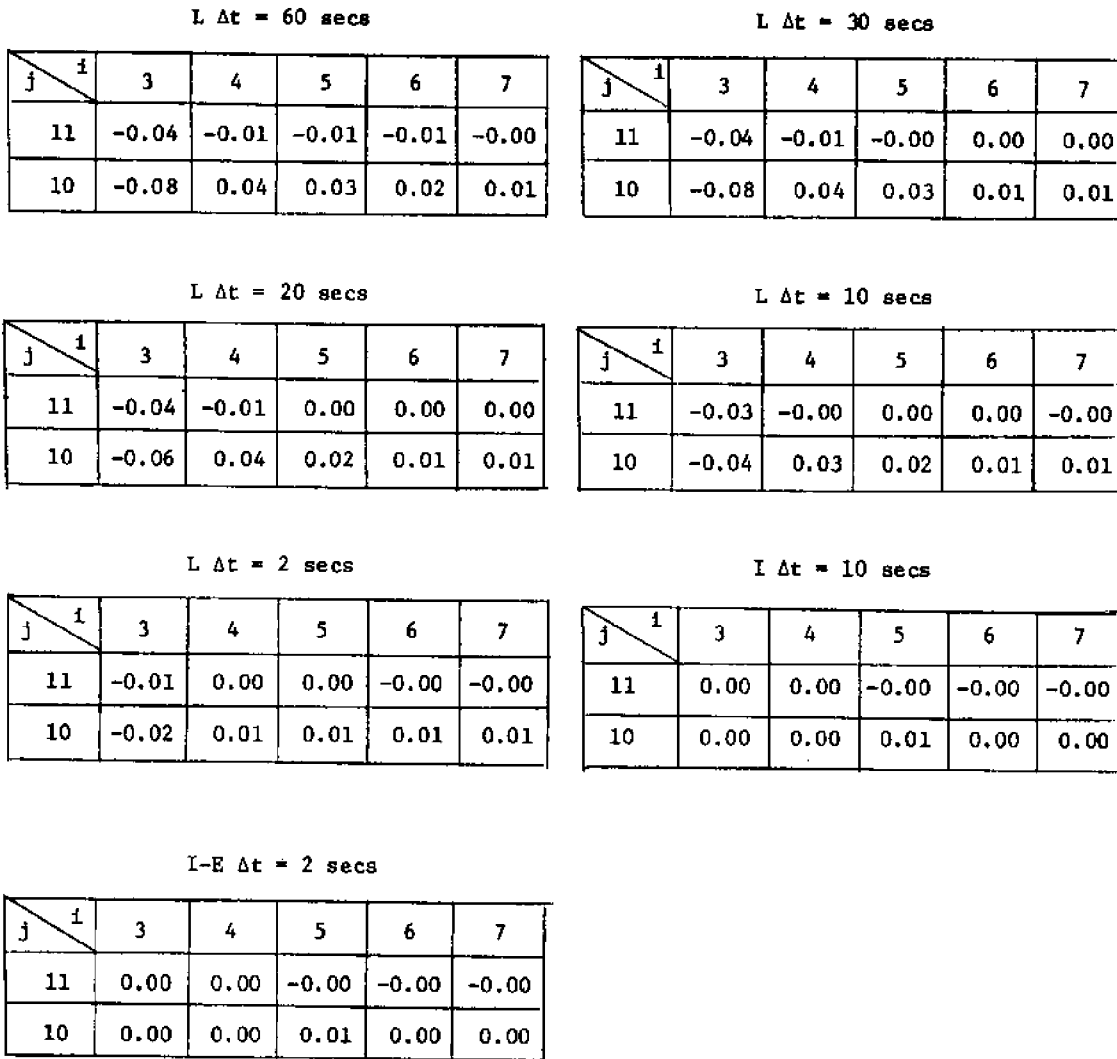


Fig. 8. Comparison of U Results Ft/Sec, at 2.5 Hours for Different Computational Schemes and Time Steps

- L - Leendertse Implicit Scheme
- I - Implicit Scheme Table 4.
- I-E - Implicit-Explicit Scheme

All Parameters Except  $\Delta t$  the Same as in Table 4.

L  $\Delta t = 10$  secs

j \ i	1	3	4	5	6	7
11		-0.01	0.00	0.00	-0.00	-0.00
10		-0.03	0.02	0.02	0.01	0.01

L  $\Delta t = 2$  secs

j \ i	1	3	4	5	6	7
11		-0.00	0.00	0.00	-0.00	-0.00
10		-0.01	0.01	0.01	0.01	0.01

I  $\Delta t = 20$  secs

j \ i	1	3	4	5	6	7
11		0.00	0.00	-0.00	-0.00	-0.00
10		0.00	0.01	0.01	0.01	0.01

Fig. 9. Comparison of U Results Ft/Sec, at 2.5 Hours for Two Different Computational Schemes

L - Leendertse Implicit Scheme

I - Implicit Scheme Table 5

All Parameters Except  $\Delta t$  the Same as in Table 5.

better with the Implicit solution than does U in Figure 8 (determined by Leendertse's Implicit scheme at the same time step) agree with its accurate solution. The same consideration holds when we compare the Leendertse Implicit solutions for the two grids at  $\Delta t = 10$  seconds, with their respective Implicit solutions. Hence, lengthening the spatial step for a given time step has improved the convergence of the velocity determination using Leendertse's Implicit scheme. The conviction must be however, that in the case of the present model, we are safer relying on the Implicit scheme of solution described by equations (3a).

#### 5. Effect of Increasing the Manning Coefficient

A final test of the model was made with a considerably larger value of the Manning roughness coefficient  $n$ . Subsequent to beginning the work described in this report, some values of  $n$  published by R. E. Horton (Engineering News, 24 February and 4 May 1916), were brought to the author's attention (J. D. O'Connor, pers. comm.). One of these values 0.070 was recommended for "sluggish river reaches, weedy." Accordingly, the Implicit model with parameters as in Table 4, was re-run, except that  $n$  was changed to 0.07.

Selected results for  $\zeta$  are shown in Table 9. A general similarity with the corresponding results in Table 4 is immediately obvious. Over the deeper areas,  $\zeta$  is the same; and in these squares the water level continues to rise and fall uniformly. Some differences from Table 4 occur in the shallower squares close to the wet/dry boundary. It can be observed that depths in the latter squares are generally shallower than in Table 4 on the flood tide and deeper during ebb. The reason must be, of course, that the greater bottom friction resulting from larger  $n$  retards the incoming flow in the first case and the outgoing flow in the

second. Qualitatively then, it can be seen that the model behaves as it should.

Regarding the velocities obtained with the larger value of  $n$ , these show a close similarity to those obtained using the smaller coefficient, but there are some noticeable differences. In Table 10 the  $U$  and  $V$  components of velocity computed for  $n = 0.07$  and  $\Delta t = 10$  seconds at 2.5 hours are given. They may be compared with the corresponding components in Table 7 for  $n = 0.026$  and  $\Delta t = 10$  seconds. Where identical values occur, to two-place accuracy, it is evident that the possible differences between  $U$  or  $V$  in the two tables respectively must be less than 0.005 ft/sec. The larger values of  $U$  and  $V$  that occur over the shallower or right-hand half of the field in Table 10 do not have a ready explanation. To help render them accountable, the computation with  $n = 0.07$  was repeated for a time step of 2 seconds and using the Implicit-Explicit scheme of solution.

Table 11 shows the results for  $U$  and  $V$  at 2.5 hours computed with  $\Delta t = 2$  seconds and using the Implicit-Explicit scheme. It can be seen by comparing Tables 10 and 11 that significant changes have occurred to certain of the velocity components in the extreme right-hand field. These changes are such as to bring either  $U$  or  $V$  in a few locations closer to the values obtained with  $n = 0.026$  and  $\Delta t = 10$  seconds (Table 7), or to those obtained with  $n = 0.026$  and  $\Delta t = 2$  seconds, and the Implicit-Explicit scheme (Table 8). Since Tables 8 and 7 show good agreement, either may be used for comparison with Table 11.

Clearly then, it would appear that using a larger Manning coefficient decreases the accuracy of the velocity solution somewhat for a given  $\Delta t$ . In particular, with  $n = 0.07$  and  $\Delta t = 10$  seconds, the implicitly

computed velocity components have not yet converged to the correct solution in certain shallow parts of the field.

For water levels, one may regard the Implicit solution for  $\zeta$  when  $n = 0.07$  as convergent at  $\Delta t = 10$  seconds. Over the 4 hours computed with  $\Delta t = 2$  seconds, and using the Implicit-Explicit scheme, there were only 17 differences in  $\zeta$  from the corresponding results in Table 9, none of these exceeding one unit in the second place of decimals.

## 6. Summary and Conclusions

The feasibility, from the mathematical standpoint, of computing the tidal flow through a small area of marshland using the Alternating Directions Implicit technique of numerical solution combined with a special flooding procedure based upon a hydraulic formula has been demonstrated. The most reliable finite difference scheme, for the minimum of computational effort, appears to be that given by equations 3a. This is a two-layer scheme in time; and in its implementation one avoids the necessity of determining explicitly the velocity components at every alternate time level, by equating the unknowns  $U$  and  $V$ , to the previously determined values one time step in the past. With a time step of 10 seconds, in conjunction with a spatial step of not less than 50 feet, this procedure appears to be adequate.

While the present model, using the above method of solution, requires some 46 minutes of running time on the IBM System 360/Model 65 to compute one 20-hour tidal cycle, the running time would be quite reasonable on one of the newer, large machines.

In the calculations, two Manning roughness coefficients were used:  $n = 0.026$  and  $0.07$ . The value was found to be not critical, since similar results were obtained with both coefficients, especially in the deeper areas where exact similarity of  $\zeta$  obtained. The smaller value had an

advantage from the point of view of computational testing: it reduces the bottom friction and so allows a greater current velocity over the marsh. This in turn allows the water surface to rise uniformly everywhere not close to the dry boundary. One thus has a quick means of estimating the accuracy of the water level solution obtained with a given time step; for, then, deviations from uniformity introduced by computational error are easily noticed. A more real study of course, must attempt to establish close limits on the value of  $n$  appropriate to mud flats covered in Spartina grass. This can only be done rigorously by comparing the predictions of the model with observation.

Of necessity, the temporarily open and closed boundary in the model was treated in isolation from the field outside the Model Area. Thus it could only be flooded (when "dry") from within that area. In a real-data study, a temporarily open and closed boundary would have to be observationally monitored by one or more tide gauges.

Provided that the hydrodynamic model can be successfully tuned in regard to the Manning roughness coefficient, it should provide a useful tool for the study of marsh circulation, water exchange rates, wind effects, and even dissolved or suspended organic components--if it be suspected that the latter may vary in horizontal space over small areas. For a study of water composition, there would of course be necessary an additional equation: the diffusion-dispersion equation.

However, even without proper tuning of the Manning coefficient, one should be able to use the present model for relative studies, an example being to ascertain the relational effects of different boundary configurations on the net volume flow over a given area per second. It is easy to introduce theoretical obstructions into the Model Area--such as canal

banks--and recompute the current field. The modified field may then be compared with the unobstructed field, and the result of comparison used as a basis for decision-making in the placement of linear obstructions across the marsh. From the biological viewpoint one would wish to maintain the circulation as vigorous as possible, over as much marsh area as possible, in order to ensure a high exchange of dissolved and suspended nutrients.









TABLE 3.  
SYMBOLIC DEPTH MATRIX

13	1	2	3	4	5	6	7	8	9	10	11	12	13	14	15	16	17	18	19	20	21	22	23	24	25
12	2	-1	1	1	1	1	1	-1	-1	-1	0	0	0	0	0	0	0	0	-1	2	2	2	2	2	2
11	2	-1	1	1	1	1	1	1	1	0	0	0	0	0	0	0	0	0	-1	2	2	2	2	2	2
10	2	-1	1	1	1	1	1	1	1	1	0	0	0	0	0	0	0	0	-1	2	2	2	2	2	2
9	2	-1	1	1	1	1	1	1	1	1	0	0	0	0	0	0	0	0	-1	2	2	2	2	2	2
8	-1	1	1	1	1	1	1	1	1	1	0	0	0	0	0	0	0	0	-1	-1	2	2	2	2	2
7	2	-1	1	1	1	1	1	1	1	1	0	0	0	0	0	0	0	0	0	0	0	-1	2	2	2
6	2	-1	1	1	1	1	1	1	1	0	0	0	0	0	0	0	0	0	0	0	0	0	-1	2	2
5	2	-1	1	1	1	1	0	0	0	0	0	0	0	1	0	0	0	0	0	0	0	0	-1	2	2
4	2	-1	1	0	0	0	0	0	0	0	1	1	0	0	0	0	0	0	0	0	0	0	0	-1	2
3	2	-1	0	0	0	0	0	0	0	1	1	1	1	1	0	0	0	0	0	0	0	0	-1	2	2
2	2	-1	0	0	0	0	0	0	0	1	1	1	1	1	0	0	0	0	0	0	0	0	-1	2	2
1	2	2	-1	-1	-1	-1	-1	-1	-1	-1	-1	-1	-1	-1	-1	-1	-1	-1	-1	-1	-1	-1	-1	2	2





TABLE 4. Continued

TIME = 1.0 HOURS

13	1	2	3	4	5	6	7	8	9	10	11	12	13	14	15	16	17	18	19	20	21	22	23	24	25
12		0.09	0.09	0.09	0.09	0.09	0.09	0.09	0.09	0.09	0.09	0.09	0.09	0.09	0.09	0.09	0.09	0.09	0.09	0.09	0.09	0.09	0.09	0.09	0.09
11		0.09	0.09	0.09	0.09	0.09	0.09	0.09	0.09	0.09	0.09	0.09	0.09	0.09	0.09	0.09	0.09	0.09	0.09	0.09	0.09	0.09	0.09	0.09	0.09
10		0.09	0.09	0.09	0.09	0.09	0.09	0.09	0.09	0.09	0.09	0.09	0.09	0.09	0.09	0.09	0.09	0.09	0.09	0.09	0.09	0.09	0.09	0.09	0.09
9		0.09	0.09	0.09	0.09	0.09	0.09	0.09	0.09	0.09	0.09	0.09	0.09	0.09	0.09	0.09	0.09	0.09	0.09	0.09	0.09	0.09	0.09	0.09	0.09
8		0.09	0.09	0.09	0.09	0.09	0.09	0.09	0.09	0.09	0.09	0.09	0.09	0.09	0.09	0.09	0.09	0.09	0.09	0.09	0.09	0.09	0.09	0.09	0.09
7		0.09	0.09	0.09	0.09	0.09	0.09	0.09	0.09	0.09	0.09	0.09	0.09	0.09	0.09	0.09	0.09	0.09	0.09	0.09	0.09	0.09	0.09	0.09	0.09
6		0.09	0.09	0.09	0.09	0.09	0.09	0.09	0.09	0.09	0.09	0.09	0.09	0.09	0.09	0.09	0.09	0.09	0.09	0.09	0.09	0.09	0.09	0.09	0.09
5		0.09	0.09	0.09	0.09	0.09	0.09	0.09	0.09	0.09	0.09	0.09	0.09	0.09	0.09	0.09	0.09	0.09	0.09	0.09	0.09	0.09	0.09	0.09	0.09
4		0.09	0.09	0.09	0.09	0.09	0.09	0.09	0.09	0.09	0.09	0.09	0.09	0.09	0.09	0.09	0.09	0.09	0.09	0.09	0.09	0.09	0.09	0.09	0.09
3		0.09	0.09	0.09	0.09	0.09	0.09	0.09	0.09	0.09	0.09	0.09	0.09	0.09	0.09	0.09	0.09	0.09	0.09	0.09	0.09	0.09	0.09	0.09	0.09
2		0.09	0.09	0.09	0.09	0.09	0.09	0.09	0.09	0.09	0.09	0.09	0.09	0.09	0.09	0.09	0.09	0.09	0.09	0.09	0.09	0.09	0.09	0.09	0.09
1		0.09	0.09	0.09	0.09	0.09	0.09	0.09	0.09	0.09	0.09	0.09	0.09	0.09	0.09	0.09	0.09	0.09	0.09	0.09	0.09	0.09	0.09	0.09	0.09

























TABLE 4. Continued

TIME = 8.5 HOURS

13	1	2	3	4	5	6	7	8	9	10	11	12	13	14	15	16	17	18	19	20	21	22	23	24	25
12			0.14	0.14	0.14	0.14	0.14	0.14	0.14	0.14	0.14	0.14	0.14	0.14	0.14	0.14	0.14	0.14	0.14	0.14	0.14	0.14	0.14	0.14	0.14
11		0.14	0.14	0.14	0.14	0.14	0.14	0.14	0.14	0.14	0.14	0.14	0.14	0.14	0.14	0.14	0.14	0.14	0.14	0.14	0.14	0.14	0.14	0.14	0.14
10		0.14	0.14	0.14	0.14	0.14	0.14	0.14	0.14	0.14	0.14	0.14	0.14	0.14	0.14	0.14	0.14	0.14	0.14	0.14	0.14	0.14	0.14	0.14	0.14
9		0.14	0.14	0.14	0.14	0.14	0.14	0.14	0.14	0.14	0.14	0.14	0.14	0.14	0.14	0.14	0.14	0.14	0.14	0.14	0.14	0.14	0.14	0.14	0.14
8	0.14	0.14	0.14	0.14	0.14	0.14	0.14	0.14	0.14	0.14	0.14	0.14	0.14	0.14	0.14	0.14	0.14	0.14	0.14	0.14	0.14	0.14	0.14	0.14	0.14
7		0.14	0.14	0.14	0.14	0.14	0.14	0.14	0.14	0.14	0.14	0.14	0.14	0.14	0.14	0.14	0.14	0.14	0.14	0.14	0.14	0.14	0.14	0.14	0.14
6		0.14	0.14	0.14	0.14	0.14	0.14	0.14	0.14	0.14	0.14	0.14	0.14	0.14	0.14	0.14	0.14	0.14	0.14	0.14	0.14	0.14	0.14	0.14	0.14
5		0.14	0.14	0.14	0.14	0.14	0.14	0.14	0.14	0.14	0.14	0.14	0.14	0.14	0.14	0.14	0.14	0.14	0.14	0.14	0.14	0.14	0.14	0.14	0.14
4		0.14	0.14	0.14	0.14	0.14	0.14	0.14	0.14	0.14	0.14	0.14	0.14	0.14	0.14	0.14	0.14	0.14	0.14	0.14	0.14	0.14	0.14	0.14	0.14
3		0.14	0.14	0.14	0.14	0.14	0.14	0.14	0.14	0.14	0.14	0.14	0.14	0.14	0.14	0.14	0.14	0.14	0.14	0.14	0.14	0.14	0.14	0.14	0.14
2		0.14	0.14	0.14	0.14	0.14	0.14	0.14	0.14	0.14	0.14	0.14	0.14	0.14	0.14	0.14	0.14	0.14	0.14	0.14	0.14	0.14	0.14	0.14	0.14
1		0.14	0.14	0.14	0.14	0.14	0.14	0.14	0.14	0.14	0.14	0.14	0.14	0.14	0.14	0.14	0.14	0.14	0.14	0.14	0.14	0.14	0.14	0.14	0.14





TABLE 4. Continued

TIME = 10.0 HOURS

13	1	2	3	4	5	6	7	8	9	10	11	12	13	14	15	16	17	18	19	20	21	22	23	24	25	
12	0.00	0.00	0.00	0.00	0.00	0.00	0.00	0.00	0.00	0.00	0.00	0.00	0.00	0.00	0.00	0.00	0.00	0.00	0.00	0.00	0.00	0.00	0.00	0.00	0.00	
11	0.00	0.00	0.00	0.00	0.00	0.00	0.00	0.00	0.00	0.00	0.00	0.00	0.00	0.00	0.00	0.11	0.11	0.11	0.00	0.00	0.00	0.00	0.00	0.00	0.00	0.00
10	0.00	0.00	0.00	0.00	0.00	0.00	0.00	0.00	0.00	0.00	0.00	0.00	0.00	0.00	0.00	0.00	0.00	0.00	0.00	0.00	0.00	0.00	0.00	0.00	0.00	0.00
9	0.00	0.00	0.00	0.00	0.00	0.00	0.00	0.00	0.00	0.00	0.02	0.07	0.10	0.10	0.10	0.10	0.10	0.00	0.00	0.00	0.00	0.00	0.00	0.00	0.00	0.00
8	0.00	0.00	0.00	0.00	0.00	0.00	0.00	0.00	0.00	0.00	0.00	0.00	0.00	0.00	0.00	0.00	0.00	0.00	0.00	0.00	0.00	0.00	0.00	0.00	0.00	0.00
7	0.00	0.00	0.00	0.00	0.00	0.00	0.00	0.00	0.00	0.01	0.00	0.00	0.00	0.00	0.00	0.12	0.12	0.12	0.12	0.00	0.00	0.00	0.00	0.00	0.00	0.00
6	0.00	0.00	0.00	0.00	0.00	0.00	0.00	0.00	0.00	0.01	0.00	0.00	0.00	0.00	0.00	0.10	0.11	0.12	0.00	0.00	0.00	0.00	0.00	0.00	0.00	0.00
5	0.00	0.00	0.00	0.00	0.00	0.00	0.00	0.00	0.00	0.02	0.00	0.00	0.00	0.00	0.06	0.09	0.10	0.00	0.00	0.00	0.00	0.00	0.00	0.00	0.00	0.00
4	0.00	0.00	0.00	0.00	0.00	0.00	0.00	0.00	0.00	0.02	0.01	0.00	0.00	0.00	0.00	0.00	0.00	0.00	0.00	0.00	0.00	0.00	0.00	0.00	0.00	0.00
3	0.00	0.00	0.00	0.00	0.00	0.00	0.00	0.00	0.00	0.00	0.00	0.00	0.00	0.00	0.01	0.00	0.00	0.00	0.00	0.00	0.00	0.00	0.00	0.00	0.00	0.00
2	0.00	0.00	0.00	0.00	0.00	0.00	0.00	0.00	0.00	0.00	0.00	0.00	0.00	0.00	0.00	0.00	0.00	0.00	0.00	0.00	0.00	0.00	0.00	0.00	0.00	0.00
1	0.00	0.00	0.00	0.00	0.00	0.00	0.00	0.00	0.00	0.00	0.00	0.00	0.00	0.00	0.00	0.00	0.00	0.00	0.00	0.00	0.00	0.00	0.00	0.00	0.00	0.00



TABLE 4. Continued

TIME = 11.0 HOURS

13	1	2	3	4	5	6	7	8	9	10	11	12	13	14	15	16	17	18	19	20	21	22	23	24	25
12		-0.09	-0.09	-0.09	-0.09	-0.09	-0.09	-0.09	-0.09	-0.09	-0.09	-0.09	-0.09	-0.09	-0.09	-0.09	-0.09	-0.09	-0.09	-0.09	-0.09	-0.09	-0.09	-0.09	-0.09
11		-0.09	-0.09	-0.09	-0.09	-0.09	-0.09	-0.09	-0.09	-0.09	-0.09	-0.09	-0.09	-0.09	-0.09	-0.09	-0.09	-0.09	-0.09	-0.09	-0.09	-0.09	-0.09	-0.09	-0.09
10		-0.09	-0.09	-0.09	-0.09	-0.09	-0.09	-0.09	-0.09	-0.09	-0.09	-0.09	-0.09	-0.09	-0.09	-0.09	-0.09	-0.09	-0.09	-0.09	-0.09	-0.09	-0.09	-0.09	-0.09
9		-0.09	-0.09	-0.09	-0.09	-0.09	-0.09	-0.09	-0.09	-0.09	0.02	0.07	0.08	0.09	0.09	0.10	-0.09	-0.09	-0.09	-0.09	-0.09	-0.09	-0.09	-0.09	-0.09
8		-0.09	-0.09	-0.09	-0.09	-0.09	-0.09	-0.09	-0.09	-0.09	-0.09	-0.09	-0.09	-0.09	-0.09	-0.09	-0.09	-0.09	-0.09	-0.09	-0.09	-0.09	-0.09	-0.09	-0.09
7		-0.09	-0.09	-0.09	-0.09	-0.09	-0.09	-0.09	-0.09	-0.09	-0.09	-0.09	-0.09	-0.09	-0.09	-0.09	-0.09	-0.09	-0.09	-0.09	-0.09	-0.09	-0.09	-0.09	-0.09
6		-0.09	-0.09	-0.09	-0.09	-0.09	-0.09	-0.09	-0.09	-0.09	-0.09	-0.09	-0.09	-0.09	-0.09	-0.09	-0.09	-0.09	-0.09	-0.09	-0.09	-0.09	-0.09	-0.09	-0.09
5		-0.09	-0.09	-0.09	-0.09	-0.09	-0.09	-0.09	-0.09	-0.09	-0.09	-0.09	-0.09	-0.09	-0.09	-0.09	-0.09	-0.09	-0.09	-0.09	-0.09	-0.09	-0.09	-0.09	-0.09
4		-0.09	-0.09	-0.09	-0.09	-0.09	-0.09	-0.09	-0.09	-0.09	-0.09	-0.09	-0.09	-0.09	-0.09	-0.09	-0.09	-0.09	-0.09	-0.09	-0.09	-0.09	-0.09	-0.09	-0.09
3		-0.09	-0.09	-0.09	-0.09	-0.09	-0.09	-0.09	-0.09	-0.09	-0.09	-0.09	-0.09	-0.09	-0.09	-0.09	-0.09	-0.09	-0.09	-0.09	-0.09	-0.09	-0.09	-0.09	-0.09
2		-0.09	-0.09	-0.09	-0.09	-0.09	-0.09	-0.09	-0.09	-0.09	-0.09	-0.09	-0.09	-0.09	-0.09	-0.09	-0.09	-0.09	-0.09	-0.09	-0.09	-0.09	-0.09	-0.09	-0.09
1		-0.09	-0.09	-0.09	-0.09	-0.09	-0.09	-0.09	-0.09	-0.09	-0.09	-0.09	-0.09	-0.09	-0.09	-0.09	-0.09	-0.09	-0.09	-0.09	-0.09	-0.09	-0.09	-0.09	-0.09



TABLE 4. Continued

TIME = 12.0 HOURS

13	1	2	3	4	5	6	7	8	9	10	11	12	13	14	15	16	17	18	19	20	21	22	23	24	25
12			-0.18	-0.18	-0.18	-0.18	-0.18	-0.18	-0.18	-0.18	-0.18	-0.18	-0.18	-0.18	-0.18	-0.18	-0.18	-0.18	-0.18	-0.18	-0.18	-0.18	-0.18	-0.18	-0.18
11			-0.18	-0.18	-0.18	-0.18	-0.18	-0.18	-0.18	-0.18	-0.18	-0.18	-0.18	-0.18	-0.18	-0.18	-0.18	-0.18	-0.18	-0.18	-0.18	-0.18	-0.18	-0.18	-0.18
10			-0.18	-0.18	-0.18	-0.18	-0.18	-0.18	-0.18	-0.18	-0.18	-0.18	-0.18	-0.18	-0.18	-0.18	-0.18	-0.18	-0.18	-0.18	-0.18	-0.18	-0.18	-0.18	-0.18
9			-0.18	-0.18	-0.18	-0.18	-0.18	-0.18	-0.18	-0.18	-0.18	-0.18	-0.18	-0.18	-0.18	-0.18	-0.18	-0.18	-0.18	-0.18	-0.18	-0.18	-0.18	-0.18	-0.18
8			-0.18	-0.18	-0.18	-0.18	-0.18	-0.18	-0.18	-0.18	-0.18	-0.18	-0.18	-0.18	-0.18	-0.18	-0.18	-0.18	-0.18	-0.18	-0.18	-0.18	-0.18	-0.18	-0.18
7			-0.18	-0.18	-0.18	-0.18	-0.18	-0.18	-0.18	-0.18	-0.18	-0.18	-0.18	-0.18	-0.18	-0.18	-0.18	-0.18	-0.18	-0.18	-0.18	-0.18	-0.18	-0.18	-0.18
6			-0.18	-0.18	-0.18	-0.18	-0.18	-0.18	-0.18	-0.18	-0.18	-0.18	-0.18	-0.18	-0.18	-0.18	-0.18	-0.18	-0.18	-0.18	-0.18	-0.18	-0.18	-0.18	-0.18
5			-0.18	-0.18	-0.18	-0.18	-0.18	-0.18	-0.18	-0.18	-0.18	-0.18	-0.18	-0.18	-0.18	-0.18	-0.18	-0.18	-0.18	-0.18	-0.18	-0.18	-0.18	-0.18	-0.18
4			-0.18	-0.18	-0.18	-0.18	-0.18	-0.18	-0.18	-0.18	-0.18	-0.18	-0.18	-0.18	-0.18	-0.18	-0.18	-0.18	-0.18	-0.18	-0.18	-0.18	-0.18	-0.18	-0.18
3			-0.18	-0.18	-0.18	-0.18	-0.18	-0.18	-0.18	-0.18	-0.18	-0.18	-0.18	-0.18	-0.18	-0.18	-0.18	-0.18	-0.18	-0.18	-0.18	-0.18	-0.18	-0.18	-0.18
2			-0.18	-0.18	-0.18	-0.18	-0.18	-0.18	-0.18	-0.18	-0.18	-0.18	-0.18	-0.18	-0.18	-0.18	-0.18	-0.18	-0.18	-0.18	-0.18	-0.18	-0.18	-0.18	-0.18
1			-0.18	-0.18	-0.18	-0.18	-0.18	-0.18	-0.18	-0.18	-0.18	-0.18	-0.18	-0.18	-0.18	-0.18	-0.18	-0.18	-0.18	-0.18	-0.18	-0.18	-0.18	-0.18	-0.18

























































TABLE 5. Continued

TIME = 3.5 HOURS

13	1	2	3	4	5	6	7	8	9	10	11	12	13	14	15	16	17	18	19	20	21	22	23	24	25
12		0.27	0.27	0.27	0.27	0.27	0.27	0.27	0.27	0.27	0.27	0.27	0.27	0.27	0.27	0.27	0.27	0.27	0.27	0.27	0.27	0.27	0.27	0.27	0.27
11		0.27	0.27	0.27	0.27	0.27	0.27	0.27	0.27	0.27	0.27	0.27	0.27	0.27	0.27	0.27	0.27	0.27	0.27	0.27	0.27	0.27	0.27	0.27	0.27
10		0.27	0.27	0.27	0.27	0.27	0.27	0.27	0.27	0.27	0.27	0.27	0.27	0.27	0.27	0.27	0.27	0.27	0.27	0.27	0.27	0.27	0.27	0.27	0.27
9		0.27	0.27	0.27	0.27	0.27	0.27	0.27	0.27	0.27	0.27	0.27	0.27	0.27	0.27	0.27	0.27	0.27	0.27	0.27	0.27	0.27	0.27	0.27	0.27
8	0.27	0.27	0.27	0.27	0.27	0.27	0.27	0.27	0.27	0.27	0.27	0.27	0.27	0.27	0.27	0.27	0.27	0.27	0.27	0.27	0.27	0.27	0.27	0.27	0.27
7		0.27	0.27	0.27	0.27	0.27	0.27	0.27	0.27	0.27	0.27	0.27	0.27	0.27	0.27	0.27	0.27	0.27	0.27	0.27	0.27	0.27	0.27	0.27	0.27
6		0.27	0.27	0.27	0.27	0.27	0.27	0.27	0.27	0.27	0.27	0.27	0.27	0.27	0.27	0.27	0.27	0.27	0.27	0.27	0.27	0.27	0.27	0.27	0.27
5		0.27	0.27	0.27	0.27	0.27	0.27	0.27	0.27	0.27	0.27	0.27	0.27	0.27	0.27	0.27	0.27	0.27	0.27	0.27	0.27	0.27	0.27	0.27	0.27
4		0.27	0.27	0.27	0.27	0.27	0.27	0.27	0.27	0.27	0.27	0.27	0.27	0.27	0.27	0.27	0.27	0.27	0.27	0.27	0.27	0.27	0.27	0.27	0.27
3		0.27	0.27	0.27	0.27	0.27	0.27	0.27	0.27	0.27	0.27	0.27	0.27	0.27	0.27	0.27	0.27	0.27	0.27	0.27	0.27	0.27	0.27	0.27	0.27
2		0.27	0.27	0.27	0.27	0.27	0.27	0.27	0.27	0.27	0.27	0.27	0.27	0.27	0.27	0.27	0.27	0.27	0.27	0.27	0.27	0.27	0.27	0.27	0.27
1		0.27	0.27	0.27	0.27	0.27	0.27	0.27	0.27	0.27	0.27	0.27	0.27	0.27	0.27	0.27	0.27	0.27	0.27	0.27	0.27	0.27	0.27	0.27	0.27

TABLE 5. Continued

TIME = 5.0 HOURS

13	1	2	3	4	5	6	7	8	9	10	11	12	13	14	15	16	17	18	19	20	21	22	23	24	25
12			0.30	0.30	0.30	0.30	0.30	0.30	0.30	0.30	0.30	0.30	0.30	0.30	0.30	0.30	0.30	0.30	0.30	0.30	0.30	0.30	0.30	0.30	0.30
11			0.30	0.30	0.30	0.30	0.30	0.30	0.30	0.30	0.30	0.30	0.30	0.30	0.30	0.30	0.30	0.30	0.30	0.30	0.30	0.30	0.30	0.30	0.30
10			0.30	0.30	0.30	0.30	0.30	0.30	0.30	0.30	0.30	0.30	0.30	0.30	0.30	0.30	0.30	0.30	0.30	0.30	0.30	0.30	0.30	0.30	0.30
9			0.30	0.30	0.30	0.30	0.30	0.30	0.30	0.30	0.30	0.30	0.30	0.30	0.30	0.30	0.30	0.30	0.30	0.30	0.30	0.30	0.30	0.30	0.30
8			0.30	0.30	0.30	0.30	0.30	0.30	0.30	0.30	0.30	0.30	0.30	0.30	0.30	0.30	0.30	0.30	0.30	0.30	0.30	0.30	0.30	0.30	0.30
7			0.30	0.30	0.30	0.30	0.30	0.30	0.30	0.30	0.30	0.30	0.30	0.30	0.30	0.30	0.30	0.30	0.30	0.30	0.30	0.30	0.30	0.30	0.30
6			0.30	0.30	0.30	0.30	0.30	0.30	0.30	0.30	0.30	0.30	0.30	0.30	0.30	0.30	0.30	0.30	0.30	0.30	0.30	0.30	0.30	0.30	0.30
5			0.30	0.30	0.30	0.30	0.30	0.30	0.30	0.30	0.30	0.30	0.30	0.30	0.30	0.30	0.30	0.30	0.30	0.30	0.30	0.30	0.30	0.30	0.30
4			0.30	0.30	0.30	0.30	0.30	0.30	0.30	0.30	0.30	0.30	0.30	0.30	0.30	0.30	0.30	0.30	0.30	0.30	0.30	0.30	0.30	0.30	0.30
3			0.30	0.30	0.30	0.30	0.30	0.30	0.30	0.30	0.30	0.30	0.30	0.30	0.30	0.30	0.30	0.30	0.30	0.30	0.30	0.30	0.30	0.30	0.30
2			0.30	0.30	0.30	0.30	0.30	0.30	0.30	0.30	0.30	0.30	0.30	0.30	0.30	0.30	0.30	0.30	0.30	0.30	0.30	0.30	0.30	0.30	0.30
1			0.30	0.30	0.30	0.30	0.30	0.30	0.30	0.30	0.30	0.30	0.30	0.30	0.30	0.30	0.30	0.30	0.30	0.30	0.30	0.30	0.30	0.30	0.30

TABLE 6.  
 U and V Components of Velocity for the Leendertse Implicit Computation  
 $\Delta t = 10$  Secs  
 Other Parameters as in TABLE 4.  
 TIME = 2.5 HOURS

		U FT/SEC																								
		1	2	3	4	5	6	7	8	9	10	11	12	13	14	15	16	17	18	19	20	21	22	23	24	25
12																										
11																										
10																										
9																										
8																										
7																										
6																										
5																										
4																										
3																										
2																										
1																										
13																										
12																										
11																										
10																										
9																										
8																										
7																										
6																										
5																										
4																										
3																										
2																										
1																										

Blank areas - U not calculated or defined







TABLE 8.  
 U and V Components of Velocity for the Implicit-Explicit Computation  
 At = 2 Secs  
 Other Parameters as in TABLE 4.  
 TIME = 2.5 HOURS

		U FT/SEC																								
		1	2	3	4	5	6	7	8	9	10	11	12	13	14	15	16	17	18	19	20	21	22	23	24	25
12																										
11																										
10																										
9																										
8																										
7																										
6																										
5																										
4																										
3																										
2																										
1																										

Blank areas - U not calculated or defined

TABLE 8. Continued

V FT/SEC

13	1	2	3	4	5	6	7	8	9	10	11	12	13	14	15	16	17	18	19	20	21	22	23	24	25
			-0.00	-0.00	-0.00	-0.01	-0.01	-0.01	-0.01	-0.01	-0.01	-0.02	-0.01	-0.02	-0.02	-0.02	-0.01	0.01	0.01	-0.01	-0.02	-0.04			
12			-0.00	-0.00	-0.01	-0.01	-0.01	-0.01	-0.01	-0.02	-0.01	-0.01	-0.01	-0.01	-0.01	-0.01	-0.01	0.01	0.00						
11			-0.00	-0.00	-0.01	-0.01	-0.01	-0.01	-0.01	-0.01	-0.01	-0.01	-0.00	-0.01	-0.01	-0.01	-0.01	-0.01	0.00						
10			-0.00	-0.01	-0.01	-0.01	-0.01	-0.01	-0.01	-0.01	-0.01	-0.00	-0.01	-0.01	-0.01	-0.01	-0.01	-0.01	0.00						
9			-0.00	-0.01	-0.01	-0.01	-0.01	-0.01	-0.01	-0.01	-0.01	-0.00	0.00	0.00	0.00	0.00	0.00	-0.01	-0.02	-0.00	-0.02				
8			-0.00	-0.00	-0.01	-0.01	-0.01	-0.01	-0.01	-0.00	0.00	0.00	0.01	0.01	0.01	0.01	0.01	-0.01	-0.02	-0.02	-0.02	-0.02			
7			-0.00	-0.00	-0.01	-0.01	-0.01	-0.01	-0.00	-0.00	0.00	0.01	0.01	0.01	0.01	0.01	0.01	0.00	-0.01	-0.02	-0.02	0.00			
6			-0.00	-0.00	-0.01	-0.01	-0.01	-0.00	-0.00	-0.00	0.00	0.01	0.01	0.01	0.01	0.01	0.01	0.01	-0.01	-0.02	-0.02	0.00			
5			-0.00	-0.01	-0.01	-0.01	-0.01	-0.00	0.00	0.00	0.01	0.01	0.01	0.01	0.01	0.01	0.01	0.01	0.00	0.00	0.00	0.00	0.00	0.00	0.00
4			0.00	-0.00	-0.00	-0.00	0.00	0.01	0.01	0.01	0.01	0.01	0.02	0.02	0.02	0.02	0.02	0.01	0.01	0.00					
3			-0.00	-0.01	-0.00	-0.01	0.00	0.01	0.01	0.01	0.02	0.02	0.02	0.02	0.02	0.02	0.02	0.02	0.02	0.02	0.00				
2			0.00	0.01	0.01	0.01	0.01	0.00	0.01	0.01	0.01	0.01	0.01	0.01	0.01	0.01	0.01	0.00	0.00	0.00	0.00	0.00			
1																									

Blank areas - V not calculated or defined































TABLE 11. Continued

V FT/SEC

13	1	2	3	4	5	6	7	8	9	10	11	12	13	14	15	16	17	18	19	20	21	22	23	24	25
12			-0.00	-0.00	-0.00	-0.01	-0.01	-0.01	-0.01	-0.01	-0.01	-0.01	-0.01	-0.02	-0.02	-0.02	-0.01	0.00							
11			-0.00	-0.00	-0.01	-0.01	-0.01	-0.01	-0.01	-0.01	-0.02	-0.01	-0.01	-0.01	-0.01	-0.01	-0.01	0.00							
10			0.00	-0.00	-0.01	-0.01	-0.01	-0.01	-0.01	-0.01	-0.01	-0.01	-0.01	-0.01	-0.01	-0.01	-0.01	0.00							
9			-0.00	-0.01	-0.01	-0.01	-0.01	-0.01	-0.01	-0.01	-0.01	-0.00	-0.01	-0.01	-0.01	-0.01	-0.01	-0.01	-0.00						
8			-0.00	-0.00	-0.01	-0.01	-0.01	-0.01	-0.01	-0.00	-0.00	0.00	0.00	0.00	0.00	-0.00	-0.01	-0.02	-0.01	-0.00					
7			-0.00	-0.00	-0.01	-0.01	-0.01	-0.01	-0.01	-0.00	0.00	0.01	0.01	0.01	0.01	0.00	-0.00	-0.01	-0.02	-0.03	-0.03	-0.00			
6			-0.00	-0.00	-0.01	-0.01	-0.01	-0.01	-0.00	0.00	0.00	0.01	0.01	0.01	0.01	0.01	0.01	-0.01	-0.02	-0.03	-0.04	-0.02	0.0		
5			-0.00	-0.00	-0.00	-0.00	-0.00	0.00	0.00	0.01	0.01	0.01	0.02	0.02	0.02	0.01	0.01	-0.00	-0.02	0.0	0.0	0.0	0.0		
4			0.00	0.00	-0.00	-0.00	0.00	0.01	0.01	0.01	0.01	0.02	0.02	0.02	0.02	0.02	0.02	0.01	0.01	0.01				0.0	
3			0.00	0.00	0.01	0.01	0.01	0.01	0.02	0.02	0.02	0.02	0.02	0.02	0.02	0.02	0.02	0.03	0.02	0.03	0.0				
2			-0.00	0.00	0.00	0.00	0.00	0.00	0.00	0.00	0.01	0.01	0.01	0.01	0.01	0.01	0.01	0.00	0.00	0.00	0.0	0.0	0.0		
1																									

## REFERENCES

- Giles, R. V. 1962. Fluid Mechanics and Hydraulics. McGraw Hill, New York. pp. 135-136.
- Hacker, S. 1973. Transport phenomena in estuaries. Ph.D. diss., Louisiana State University, Baton Rouge.
- Hansen, W. 1956. Theorie zur Errechnung des Wasserstandes und der Stromungen in Randmeeren nebst Anwedungen. Tellus 8(3):287-300.
- Leendertse, J. J. 1967. Aspects of a computational model for long-period water wave propagation. Rand Corp., Memorandum RM-5294-PR.
- \_\_\_\_\_, and E. C. Gritton. 1971. A water-quality simulation model for well-mixed estuaries and coastal seas: Vol. II, Computation Procedures, Rand Corp., Memorandum R-708-NYC.
- Sobey, R. J. 1970. Finite-difference schemes compared for wave-deformation characteristics in mathematical modeling of two-dimensional long-wave propagation. U.S. Army Corps of Engineers, Coastal Eng. Res. Center, Tech. Memorandum No. 32.

